ETH
Eidgenössische Technische Hochschule Zürich
Swiss Federal Institute of Technology Zurich

Universität St.Gallen

The Impact of Leverage and Short Selling on Financial Bubbles and Crashes

Master Thesis, Master in Accounting and Finance,
University of St. Gallen,
in Collaboration with the Chair of Entrepreneurial Risks, ETH Zurich

Johannes Christmann

August 23, 2021

Examiners:
Prof. Dr. K. Frauendorfer, University of St. Gallen
Prof. R. Gutsche, Ph.D., University of St. Gallen
External Advisors:
Dr. R. Westphal, Chair of Entrepreneurial Risks, ETH Zurich
Prof. Dr. D. Sornette, Chair of Entrepreneurial Risks, ETH Zurich

Abstract

This thesis investigates the impact of short selling and leverage on financial bubbles. The impact is explored by extending a proven agent-based model of super-exponential financial bubbles with two assets and two types of traders by Kaizoji et al. [62]. Fundamentalists and noise traders invest in a risky and a risk-free asset. Fundamentalists are rational agents that maximize a constant relative risk aversion expected utility with respect to their allocation on the risky asset versus the risk-free asset. The noise traders base their investment decision on social imitation and momentum trading. The model is able to reproduce stylised facts of financial markets such as the fat-tail distribution of returns and volatility clustering. A limitation of the model by Kaizoji et al. [62] is that the agents only have access to their own wealth, which consists of their initial wealth and the wealth generated by their investments. Therefore, the traders are unable to take credit and leverage their position to invest more than their wealth. The number of traders is constant, therefore there is also no influx of new investors. In contrast, financial bubbles are often accompanied by an influx of new investors, credit expansion and excessive leverage. These mechanism are reported to be an important amplifier of financial bubbles.

The focus of the thesis is placed on the extension of the noise trader class to incorporate the ability for them to short sell and leverage. The noise trader is based on the Ising model, a model of ferromagnetism from statistical physics. In the context of the noise trader class, the Ising model describes two competing forces that act on the investment decision: an ordering force, due to social imitation and momentum trading, and a disordering force, due to the traders' individual random behaviour. After a review of the original market model, four different extensions that incorporate leverage and short selling, are outlined and analysed. The first extension is based on the Potts model, a generalization of the Ising model. The other three models are implemented by first defining the microscopic interactions between the traders and then analysing the emerging system properties. The models are able to reproduce some of the stylised facts. However, none of the extensions is able to produce all of them. One of the three models, the ladder model, highlights the potential impact that the combination of leverage, herding and the absence of government intervention can have. The ladder model is linked to Minsky's financial instability hypothesis. Finally, the limitations of the individual models are discussed and directions for further research are given.

Acknowledgements

I would like to express my deepest appreciation to Dr. Rebecca Westphal for her administration and guidance through the process of drafting the thesis. I am especially thankful for her patience, her generous availability and her suggestions.

My sincere thanks goes to Prof. Sornette for giving me the opportunity to write my Master's Thesis at his Chair of Entrepreneurial Risks, ETH Zürich, and also for his feedback and suggestions.

A special thanks to Prof. Dr. Karl Frauendorfer for the support and supervision on part of the University of St. Gallen.

Finally, I want to thank my family, especially Anne and Anya and my parents, for the input and support they gave me and for bearing with me during the whole process.

Contents

List of Figures

List of Tables

Acronyms

ABM Agent-Based Modeling. 13

ACF auto-correlation function. 35, 71, 72, 81

CK constant kappa. 1–3, 30, 32, 35–37, 45–47, 50, 63–66, 71–73, 76–79, 81–83, 85–87, 92

CRRA Constant Relative Risk Aversion. 13, 16, 17

i.i.d. independent and identically distributed. 28

OU Ornstein-Uhlenbeck. 1–3, 28–30, 32, 34–37, 45, 46, 48, 49, 63, 65–67, 71–73, 76–78, 80–83, 85, 86, 88, 89, 92, 94

Chapter 1

Introduction

This thesis investigates the impact of short selling and leverage in the emergence of financial bubbles. The impact is explored by extending a proven agent-based model of super-exponential financial bubbles with two assets and two types of traders by Kaizoji et al. [62]. In the model, fundamentalists and noise traders invest in a risky and a risk-free asset. The model is extended to incorporate the ability for traders to short sell and leverage.

Financial history can be interpreted as a juxtaposition of financial bubbles and crashes. One of the earliest examples for such a crisis can be traced back to Mesopotamia around 3500 BC, where merchants extended credit to farmers, which they were unable to pay back after a bad harvest [49]. The term *bubble* was first used to describe the South Sea Bubble, where the stock price of the British South Sea Company rose considerably in value before collapsing in 1720 [41]. More recent asset bubbles include the Roaring Twenties stock market bubble of 1929, the bubble of 1987 and the Bitcoin cryptocurrency bubble in 2017. Since the 19th century, there has hardly been a decade without a financial bubble of some sorts [98, 66, 107]. The arena in which this perpetual cycle of bubbles and crashes initially starts out in are financial markets. Besides determining prices, sharing risk and reducing transaction costs, financial markets also allocate capital by channeling funds from people or organisations who have an excess to people or organisations who have a shortage. Well-functioning financial markets are engines of growth and due to the flow of funds impact businesses, the production of goods and services, and the economic well-being of countries. Because financial markets are closely intertwined with the real economy, the efficient allocation of capital is of critical importance to a healthy and vibrant overall economy and turmoil in financial markets can cause ripples through the whole economy [87].

Despite the impact that financial bubbles can have on the economy as whole they are a somewhat controversial topic in research. The susceptibility to

a financial bubble and the associated crash imply that there are still open research questions, which is also reflected in the fact that there is no universally agreed upon definition of what constitutes a bubble. The most common definition of financial bubbles describes them as a significant disparity between the asset price and its fundamental value [101, 44, 1]. Kindleberger and Aliber define a bubble as „a generic term for the increases in the prices of securities or currencies in the mania phase of the cycle that cannot be explained by the changes in the economic fundamentals“ [66]. However, in many circumstances the determination of what constitutes the fundamental value of an asset is difficult. Shiller describes bubbles as situations in which the news of a price increase fuels excitement, which is passed on amongst investors in a psychological epidemic [109]. This describes bubbles as an epidemic of speculation. The ambiguous nature shows also in the difficulty of identifying bubbles in real market situations. Often bubbles are only identified after a subsequent crash, which is characterized by a sharp decline in asset prices [50]. An empirical definition of financial bubbles defines market bubbles as the super-exponential growth of an asset price [111]. This definition is also adopted in this thesis .

Financial bubbles also question the applicability of neoclassical financial market theories. The neoclassical financial market theory started with Louis Bacheliers who postulated that asset price dynamics can be modelled with a stochastic process [11]. This insight forms the foundation of the random walk theory, which postulates that asset price returns can be described by a normal distribution, and the asset price itself evolves in time according to a random walk [78]. In combination with the expected utility hypothesis, which describes how rational individuals should behave under uncertainty, the random walk theory forms the foundation of the efficient market hypothesis. Fama [37, p. 383] defines a market as strongly efficient if the „prices always fully reflect all available information“. This implies that a price change is supposed to be associated with a specific exogenous event, which is represented as new information that is incorporated by the market. As a consequence, in informationally efficient markets the price must be impossible to forecast. This randomness is achieved trough the participation of many investors that incorporate all available information immediately to make their trading decisions. Consequently, the more efficient, the more random are the market prices. This is summarised in the the title Samuelsons 1965 hallmark work „Proof that properly anticipated prices fluctuate randomly“ [103]. Besides the efficient market hypothesis, the portfolio selection theory (Makowitz [83]), the capital asset pricing model (Sharpe [108]; Lintner [75]; Mossin [90]), the arbitrage pricing theory and the factors models and their extensions are cornerstones of the neoclassical financial market theory (Fama and French [39]).

Despite or perhaps because of its practical and academic impact, the neoclas-

sical approach faces continued criticism, which is renewed especially after major financial crises such as the Black Monday of 1987 or more recently the Financial Crisis of 2008. While some argue that financial bubbles are consistent with an efficient market [38], others point to the limitations of the neoclassical approach to explain financial bubbles and other market anomalies [20, 33, 57, 77, 109, 9].

The rising criticism primarily focuses on the underlying assumptions of neoclassical market theories. Market participants are assumed to be rational economic agents, „always acting in their own self-interest and making decisions in an optimal fashion by trading off costs and benefits weighted by the statistically correct probabilities and marginal utilities“ [76, p. 1]. Furthermore, the rational market participants are often assumed to be homogeneous and modelled by one representative agent. In this context, homogeneous means that the participants all have the same information and process it identically [71]. From an empirical perspective, the large price fluctuations associated with financial bubbles and crashes cannot be associated with one specific event or new information most of the time [112]. This is an example for a market anomaly that cannot be explained by the efficient market hypothesis alone. In addition, there is evidence that large positive and negative asset price returns occur more often than prescribed by a normal distribution, which is known as „fat tails“ [17]. Fat tails and other statistical properties of financial markets such as volatility clustering are summarised under the umbrella term „stylised facts“ [23, 30, 26, 27].

The criticism and limitations of the neoclassical financial market theory and more generally neoclassical economics fostered the modification of existing theories and the development of new methods and research areas starting in the 1980s.

One tool that has gained significance are *agent based models* (ABM). ABMs can transcend the aforementioned restrictive assumptions. They can model characteristics of financial markets that neoclassical financial market theory often does not account for. They are particularly suited to simulate the actions and interactions of individuals in complex and realistic ways [59] and therefore offer an opportunity to model heterogeneous individuals with respect to the information they process and how they make decisions. The interactions between the individuals in the context of financial markets can include social herding or information cascades [14]. The behaviour of the individuals on a microscopic scale results in non trivial macroscopic properties. These macroscopic properties of the model do not simply correspond to the aggregation of the individual behaviour but are emergent properties only arising due to the interaction of agents [46]. Furthermore, ABMs can be used to investigate out of equilibrium systems [8] and are able to reproduce the stylised facts associated with financial markets [73].

An example for an early agent based model was developed by Kim and Markowitz [64], where two types of traders, re-balancers and portfolio insurers, trade two assets, a stock and cash. The model attempted to investigate the causes of the 1987 Black Monday. Another pioneering model is the Santa Fe Institute artificial stock market. In the market, heterogeneous agents also trade a stock and cash. The agents build an estimation to forecast the future return of the stock and adapt their trading strategy using genetic algorithms [95, 72]. A market model developed by Lux and Marchesi [81, 82] consists of chartists and fundamentalists. The fundamentalists compare the market price to a fair price and sell or buy accordingly. The chartists behaviour depends on the historical price and their peers, meaning they are prone to herding. The trader can switch between the fundamentalist or the chartist strategy. The model is able to produce stylised facts such as volatility clustering. Extensive reviews of some of the agent-based financial market models are provided by Hommes [55], Axtell and Farmer [10], Iori and Porter [59].

Rooted in the tradition of the aforementioned models is the contemporary agent-based model by Kaizoji, Leiss, Saichev and Sornette [62], which is the basis for this thesis. The model also consists of two types of traders, fundamentalists and chartists (or so-called noise trader) that trade a risky and a risk-free asset. The total number of traders is fixed and the traders are not allowed to switch between the types. The fundamentalists maximise a constant relative risk aversion expected utility with respect to the allocation of their wealth to the risk-free and risky asset. The chartists' or noise traders' investment decision depends on social imitation and the momentum of the price of the risky asset. The behaviour of the noise traders is influenced by a time varying herding propensity that controls if the chartists behave randomly or are prone to social imitation and the price momentum. The model is able to reproduce stylised facts such as the fat-tail distribution of returns and volatility clustering. A key trait of the model is that it produces faster-than-exponential price increases, known as super-exponential bubbles.

Since its inception the model has been modified several times. Westphal and Sornette [122] investigate the impact and performance of arbitrageurs on financial bubbles. The model is implemented with a third trader class, the "dragon riders". The dragon riders exploit their ability to diagnose financial bubbles from the endogenous price history to determine optimal entry and exit trading times. In a second paper, Westphal and Sornette [121] analyse the direct market intervention by a policy maker. The policy maker diagnoses bubbles by forming an expectation of the future returns, then invests in burgeoning bubbles and sells countercyclically the overpriced asset to fight market exuberance.

A limitation of the model by Kaizoji et al. [62] is that the agents only have access to their own wealth, which consists of their initial wealth and the

wealth generated by their investments. Therefore, the traders are unable to take credit and leverage their position to invest more than their wealth. The number of traders is constant, therefore there is also no influx of new investors.

While there is no extension of the noise trader class to include leverage and short selling, previous research extended the model of Kaizoji et al. [62] to include multiple risky assets. Damiani [32] couples two Ising models to create a model with two risky assets and one risk free asset. Each Ising model consists of a risky and a risk free asset. The two Ising models are coupled by allowing the noise traders to switch between the two risky assets. Because the two risk free assets are identical, they are counted as one asset. Kopp and Westphal [70, 120] apply the model to Fixed Income markets and replicate the main stylized facts of Fixed Income markets with regards to the emerging dynamics of the yield curves. The model is based on a multi-asset extension. The Ising model describes the transition of the noise traders between a risk free asset and the stock market that contains many assets. A second mechanism is in place to model the decision of the noise traders once they decided to invest in the stock market.

The impact of *short selling and leverage* on the creation and amplification of financial bubbles and crises is debated and the literature associated with this questions is inconclusive. Nonetheless, the opportunity to leverage, defined broadly as using borrowed funds rather than equity to purchase an asset, has been identified as an important component that contributes to the amplification of bubbles. Kindleberger and Aliber [3, p. 21] suggest that during periods of euphoria that are associated with bubbles „an increasing number of investors seek short-term profits from the increases in the prices of real estate and of stocks [...] and an exceptionally large share of these purchases is financed with credit“. They note that each crisis is accompanied by a credit expansion and excessive leverage. This perspective is also shared for historical crisis by Galbraith [43] and Sornette [111]. Several studies find that the likelihood of a bubble increases if credit is available [21, 19] or taking leverage [58] is possible. Allen and Gale [4] argue that investors take into account the limited liability associated with investments financed by credit, which can lead to bubbles. Reinhart and Rogoff [99] attest an increase in credit in the run up to a financial crisis. Caginalp et al. [21] finds that high liquidity increases market bubbles. In addition, Zhou and Li [126] and Zhang and Li [125] find that leverage can contribute to liquidity and the risk of a crisis. Ackert et al. [2] associates margin buying with increasing bubbles. Sornette and Zhou [113] present evidence for foreign capital inflow during the bubble in the US in the year 2000.

Besides leveraging, the practice of short selling is common in financial markets. Short selling refers to „borrowing a financial instrument from another

investor to sell it immediately and close the position in the future by buying and returning the instrument“ [6, p. 1]. Shorting a stock is the mirror position to buying a stock, which one does not own before. Buying a stock can be viewed as a bet on the increase of the stock price while shorting the stock bets on the decrease of the asset price. Therefore, short selling enables investors to bet on decreasing prices. The traditional view on short-selling is that it lowers prices and reduces bubbles [54, 2]. In line with this view, several authors find that short sale constraints can serve as a bubble amplification mechanism [19, 123, 105, 5], because optimistic traders can push up the price while pessimistic trader have no tools to counteract them [53, 84, 123, 56].

In the context of agent-based models, Thurner et al. [116] build a model in which investors can allocate capital to funds, which can invest in assets. The model links the ability of the funds to leverage and the associated margin calls by banks with the fat tail distribution of the asset price fluctuations. Fischer and Riedler [40] purpose a model in which boundedly rational agents can invest in a risky and a risk free asset and also have the ability to leverage, but are limited in their ability to gain and dispose credit. The model can replicate stylised facts and amongst others finds a positive relationship between the target leverage ratio of the traders and price volatility. Given the apparent importance of leverage and short selling in the context of financial bubbles and crisis, this thesis studies both within the scope of the model provided by Kaizoji et al. [62]. The goal of the thesis is to extend the model by Kaizoji to incorporate leverage and short selling and analyse their impact on the creation of financial bubbles.

The numerical simulations of the financial market model are implemented in C++. The results of the simulations are stored in a database using the HDF5 high-performance data library. The analysis of the results is done in Python 3.

1.1 Thesis outline

The thesis is structured as follows. **Chapter 2** reviews the original market model by Kaizoji et al. [62] and others. **Chapter 3** presents the first extension of the model. Specifically, the noise trader class is extended using the Potts model, a generalisation of the Ising model. **Chapter 4** presents a different approach to the extension. Instead of using the tools from statistical physics, three different extensions of the noise trader class are build by defining the states and switching probabilities and studying the resulting properties of the system. This approach is denoted as microscopic. Finally, **Chapter 5** summarises the results and outlines future research directions.

Chapter 2

Original market model

The following chapter presents the financial market model that serves as a basis for further analysis. The original market model was first introduced by Kaizoji et al. [62] and was later extended in several directions [25, 28, 96, 35, 70, 91, 32, 121, 122].

The financial market is modelled as an Agent-Based Modeling (ABM), which constitutes two types of traders, fundamentalists and noise traders, that can trade two types of assets, a risk-free and a risky asset. The risk-free asset represents a zero-coupon government bond with a constant yield and the risky asset represents a stock paying a dividend. An important property of the model is the ability to produce super-exponential financial bubbles, which means that the price of the risky asset exhibits faster-than-exponential growth. Furthermore, the model reproduces several stylized facts of financial markets, for instance volatility clustering and a fat-tail distribution of returns.

The description of the fundamentalists is based on Brock and Hommes [18] and Chiarella et al. [23]. The fundamentalists split their wealth between the risky and risk-free asset to maximize their expected utility from future wealth. The utility is determined by an utility function with Constant Relative Risk Aversion (CRRA). All fundamentalists share the same risk aversion, utility function and information (price, dividend and long-term expectations of return and standard deviation) and, as a consequence, are represented by one agent.

The noise traders are based on the setup in Lux and Marchesi [81]. In contrast to the fundamentalists, an individual noise trader invests her wealth either into the risky asset or into the risk-free asset. Instead of forming expectations on the fundamentals, namely the return and risk of the risky asset, like the fundamentalists, their investment decision is determined by past price momentum and social imitation. An Ising-like structure is em-

ployed to model the social imitation. Like the fundamentalists, the noise traders are also modelled as a single representative noise trader who is endowed with the aggregate wealth of all noise traders and invests into the risky and risk-free asset according to the fraction of noise traders that are invested into either asset.

The price formation process in the market with fundamentalists and noise traders is governed by the market clearing conditions based on Walras' general equilibrium theory [119].

The chapter proceeds with section 2.1, which explains the assets and especially the dividend process in more detail. Sections 2.2 and 2.3 focus on the two types of traders and section 2.4 details the market clearing conditions and the price equation. Section 2.5 presents simulations of the model and their time series.

2.1 Asset and wealth dynamics

There are two assets traded in the market model: a risky asset and a risk-free asset. The risk-free asset represents a zero coupon government bond with a constant rate of return r_f. In the original model, the risk-free rate is defined as the daily risk-free rate of return with the convention of 250 trading days per year. The model assumes that the supply of the risk-free asset is of infinite supply.

The risky asset is modelled after a stock that pays dividends each period. The inherent risk of the stock is associated with the stochastic dividends and the uncertainty of the future price. The dividends are determined each period, in this case each trading day, by a discrete stochastic process:

$$d_t = (1 + r_t^d) d_{t-1} \tag{2.1}$$

$$r_t^d \sim \mathcal{N}(r_d, \sigma_d^2). \tag{2.2}$$

d_t is the dividend of the current period and depends on the previous period d_{t-1} and on a stochastic dividend growth rate r_t^d, which is determined each period. The dividend growth rate is modeled by a normal distribution with expectation value $\mathbf{E}[r_t^d] = r_d$ and standard deviation σ_d. Therefore, the dividend process can be represented by the following equation:

$$d_t = d_0 \prod_{i=1}^{t} (1 + r_i^d). \tag{2.3}$$

The total return of the risky asset r_t^{tot} depends on the dividend yield $\frac{d_t}{P_{t-1}}$ and the return on price r_t:

$$r_t^{tot} = \frac{d_t}{P_{t-1}} + r_t. \tag{2.4}$$

The return of price (or return on capital) is given in the following equation:

$$r_t = \frac{P_t}{P_{t-1}} - 1. \tag{2.5}$$

Equation 2.4 exhibits the two risk factors, the dividends with the stochastic growth factor 2.2 and the uncertainty of the future price. The risk premium is given by the difference between the two returns $r_t^{tot} - r_f$.

The following section describes the wealth of the traders. As mentioned before, the noise traders and the fundamentalists are each modelled as a single representative trader with their respective aggregate portfolios. The portfolios of these two representative traders are determined by the fraction of wealth (W_t^f for the fundamentalist and W_t^n for the noise trader) invested in the risky asset. The fraction of wealth invested in the risky asset is denominated by x_t^f for the fundamentalist and by x_t^n for the noise trader, whereas the fractions invested in the risk-free asset are defined as $(1 - x_t^f)$ and $(1 - x_t^n)$ respectively. The risky fraction is in the interval $x_t^{f,n} \in [0, 1]$.

The wealth equation for the current period depends on the wealth of the previous period:

$$W_t^{f,n} = W_{t-1}^{f,n}[1 + \frac{d_t}{P_{t-1}} + r_t] + W_{t-1}^{f,n}(1 - x_{t-1}^{f,n})(1 + r_f) \tag{2.6}$$

The first part describes the wealth invested in the risky fraction, whereas the second part describes the wealth invested in the risk-free fraction. Equation 2.6 can be rewritten to

$$W_t^{f,n} = W_{t-1}^{f,n}[1 + r_f + x_{t-1}^{f,n}(\frac{d_t}{P_{t-1}} + \frac{P_t}{P_{t-1}} - (1 + r_f)] \tag{2.7}$$

with

$$r_t^{excess} = (\frac{d_t}{P_{t-1}} + \frac{P_t}{P_{t-1}} - (1 + r_f) = (\frac{d_t}{P_{t-1}} + r_t - r_f) \tag{2.8}$$

being the excess return of the risky asset over the risk-free asset. For $r_t^{excess} > 0$ ($r_t^{excess} < 0$) the risky asset is more (less) profitable than the risk-free asset.

2.2 Fundamentalist trader

The fundamentalist traders in the model by Kaizoji et al. [62] are based on Brock and Hommes [18] and Chiarella et al. [23]. They are rational, risk-averse and maximize their expected utility each time period. The model employs an utility function with Constant Relative Risk Aversion (CRRA). Furthermore, the traders only consider a limited time interval, one time step in case of the introduced model, when maximizing their expectation.

All fundamentalists can be modelled by a single representative fundamentalist under the following three assumptions: Each individual maximizes the expectation value the same utility functions. It is furthermore endowed with the same constant risk aversion and it has access to the same public information (price, dividend and long-term expectations of return and standard deviation). The wealth of this representative agent is equal to the sum of the wealth of the individual fundamentalists. Each time period t, the fundamentalists choose the fraction of wealth that they invest in the risky asset by maximizing the expected utility function of their wealth in the future in period $t+1$:

$$x_t^f = \max_{x_t^f} \mathbf{E}_t[U(W_{t+1}^f(x_t^f))]. \tag{2.9}$$

The CRRA utility function is given by the following equation:

$$U(W) = \begin{cases} log(W), & \text{for } \gamma = 1 \\ \frac{W^{1-\gamma}}{1-\gamma}, & \text{for } \gamma \neq 1 \end{cases} \tag{2.10}$$

where the constant risk aversion γ is given by

$$\gamma = -W\frac{U''(W)}{U'(W)}. \tag{2.11}$$

The approximation introduced in [24] leads to the final approximated result

$$x_t^f = \frac{1}{\gamma}\frac{\mathbf{E}_t[r_{t+1}^{excess}]}{\mathrm{Var}[r_{t+1}^{excess}]} \tag{2.12}$$

of the optimization problem in equation 2.9.

The solution in equation 2.12 showcases a trade-off between risk and return, a result associated with modern portfolio theory and mean-variance analysis. Furthermore, the choice for the risky fraction is independent of the

wealth of the fundamentalist, which is a result of the definition of the CRRA utility function.

The expected value of the excess return (equation 2.8) is

$$\mathbf{E}_t[r_{t+1}^{excess}] = \mathbf{E}_t[\frac{d_{t+1}}{P_t} + r_{t+1} - r_f] = \frac{d_t(1+r_d)}{P_t} + \mathbf{E}_t[r_{t+1}] - r_f. \tag{2.13}$$

Kaizoji et al. [62] assumes that the fundamentalists expect a constant rate of return based on the long term behaviour of the stock market

$$\mathbf{E}_t[r_{t+1}] := E_r = cst \tag{2.14}$$

and also a constant variance of the return

$$\mathbf{Var}_t[r_{t+1}] := \sigma_r^2 = cst. \tag{2.15}$$

Kaizoji et al. [62] relates the variance of the return in equation 2.15 to the variance of the excess return in equation 2.12 by assuming that the dividend policy is independent of the market price, following Modigliani and Miller [88, 89], and that $P_t \gg \sqrt{\frac{\mathbf{Var_t}[d_{t+1}]}{\mathbf{Var_t}[r_{t+1}]}}$. This implies in combination with equations 2.8 that the variance of excess return is constant:

$$\mathbf{Var}_t[r_{t+1}^{excess}] := \mathbf{Var}_t[r_{t+1}] + \frac{\mathbf{Var}_t[d_{t+1}]}{P_t^2} \approx \mathbf{Var}_t[r_{t+1}] = \sigma_r^2 = cst. \tag{2.16}$$

As a result, the risky fraction in equation 2.12 is

$$x_f^t = \frac{1}{\gamma}\frac{E_r - r_f + \frac{d_t(1+r_d)}{P_t}}{\sigma_r^2}. \tag{2.17}$$

The terms E_r, r_f and σ_r^2 in equation 2.17 are constants and reflect the expectation of the fundamentalists. r_d is the dividend growth rate that the fundamentalist expects from the asset. In the long run, this is expected to be the primary driver of the asset price. Therefore, the long run price growth of the asset should correspond to the dividend payments. The fundamental value of the stock is the discounted future dividend payments. Besides the constant terms, the risky fraction depends on the dividend-price ratio $\frac{d_t}{P_t}$. The fundamentalists strategy to allocate their funds depends on this ratio. A high dividend-price ratio implies an undervalued stock and is interpreted as a buying signal while a low dividend-price ratio implies an overvalued stock and is interpreted as a sell signal.

2.3 Noise trader

The noise trader class introduced in Kaizoji [62] is based on the work of Lux and Marchesi [81]. In contrast to the fundamentalists, the noise traders are not rational and do not maximize their expected utility but base their investment decision on social imitation and momentum trading strategies. In addition, each noise trader allocates their total wealth to either the risky asset or the risk-free asset, which models a lack of diversification that was among others documented by Kelly [63].

The noise traders are modelled as a single representative agent. The representative noise trader allocates the wealth to the risky and risk-free assets based on the fraction of noise traders that are invested in the respective asset. The fraction of wealth allocated to the risky asset by the representative noise trader is

$$x_t^n = \frac{N_t^+}{N_t^+ + N_t^-} \in [0, 1]. \tag{2.18}$$

Hence, the fraction of wealth allocated to the risk-free asset is given by $(1 - x_t^n)$. N_t^+ are the number of noise traders that are invested in the risky asset at time t, while N_t^- noise traders are invested in the risk-free asset. The total number of noise traders $N_n = N_t^+ + N_t^-$ is constant over time. The definition of the risky fraction in equation 2.18 assumes that the noise traders are homogeneous, meaning that each noise trader is endowed with the same amount of wealth and follows the same trading strategy. Allowing for heterogeneity of the wealth distribution among noise traders has been investigated by Bouchaud and Mézard [16] and Harras et al. [51]. Furthermore, the definition of the risky fraction limits the noise traders to only investing their initial wealth and the wealth generated by their investments. Therefore, the traders are unable to take credit and leverage their position to invest more than their wealth. The number of traders is constant, therefore there is also no influx of new investors.

The decision to invest in the risky or risk-free asset is governed by social imitation and price momentum following strategies. Each trading day, the individual noise trader can choose to switch between the two assets or hold the asset of the previous period. The decision to hold or switch is governed by switching probabilities. As highlighted by Cividino [25], the investment process of the noise traders can be represented as a discrete Markov chain with two possible states that correspond to holding the risky or the risk-free states as depicted in 2.1.

A trader holding the risk-free asset at the beginning of period t decides to switch to the risky asset with probability p_t^- and to hold the risk-free asset

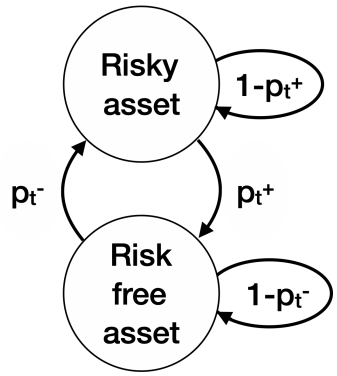

Figure 2.1: Noise trader states

with probability $(1 - p_t^-)$. A trader holding the risky asset at the beginning of period t decides to switch to the risk-free asset with probability p_t^+ and to hold the risky asset with probability $(1 - p_t^+)$.

The probabilities $p_t^{\pm}$, that determine how many noise traders switch between the two assets or states per period, depend on several variables $p_t^{\pm} = p_t^{\pm}(p_{\pm}, \kappa_t, s_t, H_t)$. $p_{\pm}$ is a constant switching probability controlling the average holding time, κ_t is the herding propensity, s_t is the opinion index (also called sentiment) and H_t the price momentum. Before discussing the structure of the switching probabilities, each term is explained individually.

The price momentum term H_t represents the trend following characteristic of noise traders. With the price momentum term, the noise traders evaluate the past time series of the price of the risky asset in order to determine a price trend. This is also called technical analysis. Depending on the value of the price momentum term, the noise traders are more likely or less likely to favour the risky asset. The definition of the momentum term is given by

$$H_t = \theta H_{t-1} + (1-\theta) r_t = \theta H_{t-1} + (1-\theta)\left(\frac{P_t}{P_{t-1}-1}\right), \tag{2.19}$$

and depends on the price momentum of the previous period H_{t-1}, the capital return (see equation 2.5) and a parameter that weights these two contributions θ. $\theta in [0, 1)$ is the memory parameter and determines how far back in time the time series of the price is analysed. $\tau_{memory} = \frac{1}{1-\theta}$ is the characteristic memory time length of the noise traders. For $\theta = 0$ the noise traders only consider the last period $\tau_{memory} = 1$. For $\theta \to 1$, the memory length increases to the entire market history $\tau_{memory} \to \infty$. A value of $\theta = 0.95$ implies that the noise traders look at the last 20 trading days $\tau_{memory} = 20$.

The other factor that influences the decision making of the noise traders are their peers via the social imitation term, called sentiment or opinion index, s_t. The opinion index is based on the work of Lux and Marchesi [81] and defined in the following equation:

$$s_t = \frac{N_t^+ - N_t^-}{N_t^+ + N_t^-} \in [-1, 1]. \tag{2.20}$$

Hence, the sentiment is the difference between the number of traders in the two states divided by the total number of traders and lies within the interval $[-1, 1]$. A positive value of the sentiment represents a bullish opinion and a negative value represents a bearish opinion. The risky fraction and the sentiment are related by

$$s_t = 2x_t^n - 1. \tag{2.21}$$

The structure of the switching probabilities is given by Kaizoji et al. [62] and is introduced in a modified form in the following equations:

$$p_t^+ = \frac{p_+}{2}\left(1 - \kappa_t\left(s_t + H_t\right)\right), \tag{2.22}$$

$$p_t^- = \frac{p_-}{2}\left(1 + \kappa_t\left(s_t + H_t\right)\right). \tag{2.23}$$

As mentioned before, p_t^+ is the probability that a noise trader holding the risky asset switches to the risk-free asset. p_t^- is the probability that a noise trader holding the risk-free asset switches to the risky asset. The momentum term H_t and the social imitation term s_t enter linearly into the equations for the switching probabilities. In contrast to Kaizoji et al. [62] the constant switching probability p is replaced by two constant switching probabilities (p_+ and p_-), one for each switching probability. This implies that the switching probabilities are not symmetric ($p_t^+(p, k_t, s_t, H_t) = p_t^-(p, k_t, -s_t, -H_t)$), but biased, which was suggested by Kohrt [69]. In addition, the constant switching probabilities are found outside of the bracket. The final component of the switching probabilities is the herding propensity κ_t. The herding propensity steers the impact of price momentum and social imitations.

A first step to gain an intuition for the switching probabilities is to set the herding propensity is $\kappa_t = 0$, which means that the probabilities only depend on the constant probabilities and are independent from price momentum and social imitation, $p_t^{\pm} = \frac{p_{\pm}}{2}$. This highlights the potential to introduce a systematic bias towards one of the assets in the switching probabilities. If $p_- > p_+$, there is everything else being equal a bias towards the risky asset

as on average more traders switch to the risky asset than away from it to the risk-free asset. Furthermore, the inverse of $\frac{p_{\pm}}{2}$ can be interpreted as the average holding time of a noise trader of the specific asset. $t_h^+ = \frac{2}{p_+}$ denotes the average holding time of the risky asset and $t_h^- = \frac{2}{p_-}$ denotes the average holding time of the risk-free asset given that there is no herding behaviour ($\kappa_t = 0$).

For $\kappa \neq 0$, the momentum and social imitation terms influence the switching probabilities. A negative herding propensity $\kappa_t < 0$ implies a contrarian trading strategy. In the following work the herding propensity is always assumed to be positive, $\kappa_t > 0$.

To make sure that the switching probabilities are always contained within the interval $[0, 1]$, the switching probabilities distinguish three cases:

$$p_t^{\pm} = \begin{cases} \frac{p_{\pm}}{2}\left(1 \mp \kappa_t \left(s_t + H_t\right)\right), & \text{if } \frac{p_{\pm}}{2}\left(1 \mp \kappa_t \left(s_t + H_t\right)\right) \in [0,1] \\ 0, & \text{if } \frac{p_{\pm}}{2}\left(1 \mp \kappa_t \left(s_t + H_t\right)\right) < 0 \\ 1, & \text{if } \frac{p_{\pm}}{2}\left(1 \mp \kappa_t \left(s_t + H_t\right)\right) > 1. \end{cases} \tag{2.24}$$

Following the definition of the switching probabilities, the time evolution of the number of traders in each state is outlined. An investment decision can be seen as a Bernoulli random variable $\xi(p)$. The investment decision for a trader holding a risky asset is given by

$$\xi(p_{t-1}^+) = \begin{cases} 1, & \text{switch to risk-free with probability } p_{t-1}^+ \\ 0, & \text{hold risky with probability } 1 - p_{t-1}^+, \end{cases} \tag{2.25}$$

while the investment decision for a trader holding a risk-free asset is given by

$$\xi(p_{t-1}^-) = \begin{cases} 1, & \text{switch to risky with probability } p_{t-1}^- \\ 0, & \text{hold risk-free with probability } 1 - p_{t-1}^-. \end{cases} \tag{2.26}$$

The number of traders invested in the risky asset are given by the number of traders that switch to the risky asset and the number of traders that hold the risky asset during period t:

$$N_t^+ = \sum_{n=k}^{N_{t-1}^-} \xi_k(p_{t-1}^-) + \sum_{n=k}^{N_{t+1}^-} [1 - \xi_k(p_{t-1}^+)]. \tag{2.27}$$

The number of traders invested in the risk-free asset are given by the number of traders that switch to the risk-free asset and the number of traders that hold the risk-free asset during period t:

$$N_t^- = \sum_{n=k}^{N_{t-1}^+} \xi_k(p_{t-1}^+) + \sum_{n=k}^{N_{t+1}^-} [1 - \xi_k(p_{t-1}^-)]. \tag{2.28}$$

The definitions for the number of noise traders in the risky state and the risk-free state can be plugged into equations 2.18 and 2.20 to derive the dynamics of the risky fraction and the sentiment.

2.3.1 Relation of the noise trader class and the Ising model

In the following subsection, the link between the Ising model, a model for ferromagnetism employed in statistical physics, and the noise trader class is outlined. Furthermore, the Ising model is of central importance to understand the formation of bubbles in the model as highlighted. The following section is mainly based the analysis of Harras et al. [51], Kaizoji et al. [62], Ollikainen [91], Cividino [25] and Sornette [112].

The Ising model is the simplest model in statistical physics to represent the interaction of elements with a finite number of possible states [112]. The elements are called magnetic moments or spins and are placed on a grid that can be represented by a graph, where the nodes are the spins and the links represent connections between the spins. Each spin can take two values, spin up or down, and interacts only with its nearest neighbors. Each spin tends to align with its neighboring spin to minimize the energy of the system. However, this alignment process of the spins is disturbed by heat energy, which is represented by the temperature. Therefore, there is a competition between order (due to the tendency of the spins to align) and disorder (due the tendency of temperature to orient the spins at random). For the ordered state, the tendency of spins to align outweighs the influence of the temperature, while for the disordered state, the spin orientation is random, because the temperature influence is stronger.

The noise trader class is mapped onto the Ising model by assuming that the noise traders are represented by the spins and can either invest in a risky (up) or a risk-free (down) asset. The interactions of the spins and their tendency to align represents the social imitation between the traders and the temperature represents the individual opinion of their investment choice.

There are several steps to derive the switching probabilities in equations 2.22 and 2.23: choose the appropriate version of the Ising model, set up the correct Hamiltonian (that describes the energy of the system), use the Boltzmann distribution and the detailed balance condition to derive the Glauber

transition rates, linearize the rates and add the constant probability for the holding time.

The Hamiltonian of the fully connected Ising model in an external magnetic field is given by

$$H_N\left(\{s_1,\ldots,s_N\}\right) = -\frac{J}{2N}\sum_{i\neq j=1}^{N} s_i s_j - h\sum_{i=1}^{N} s_i \tag{2.29}$$

and based on Zamponi [124]. There are N spins that each can take on the values $s_i \in \{-1,1\}$ that all interact with one another on fully connected or complete graph. J represents the interaction term between the spins. h defines the external magnetic field. The equilibrium distribution is given by the Boltzmann distribution

$$P_{eq}\left(\{s_1,\ldots,s_N\}\right) = e^{-\beta H_N} \tag{2.30}$$

with $\beta = \frac{1}{k_B T}$ being the inverse temperature. The dynamics of the system are given by the Glauber transition rates [47], which are derived by using the detailed balance condition

$$\frac{p\left(s_i = 1 \to s_i = -1\right)}{p\left(s_i = -1 \to s_i = 1\right)} = \frac{P_{eq}\left(s_i = -1\right)}{P_{eq}\left(s_i = 1\right)} = \frac{e^{-\beta(Jm+h)}}{e^{\beta(Jm+h)}} = \frac{1-\tanh(\beta(Jm+h))}{1+\tanh(\beta(Jm+h))} \tag{2.31}$$

$p\left(s_i = 1 \to s_i = -1\right)$ is the transition probability of a spin flip from 1 to -1 of spin $s_i = 1$ and $P\left(s_i = -1\right)$ is the Boltzmann distribution of a configuration with the spin $s_i = 1$. $P_{eq}\left(s_i = -1\right)$ describes the equilibrium distribution with $s_i = -1$ in the Hamiltonian H_N, whereas $P_{eq}\left(s_i = 1\right)$ describes it for $s_i = 1$ in the Hamiltonian H_N. The ratio of the two can be calculated using the difference of the two Hamiltonians $\frac{P(H_N(s_i=-1))}{P(H_N(s_i=1))} = \frac{e^{-\beta H_N(s_i=-1)}}{e^{-\beta H_N(s_i=+1)}} = e^{-\beta(H_N(s_i=-1)-H_N(s_i=+1))}$, which is

$$\frac{P_{eq}\left(s_i = -1\right)}{P_{eq}\left(s_i = 1\right)} = \frac{e^{-\beta\left(J\left(\frac{\sum_{k\neq i=1}^{N} s_k}{N}\right)+h\right)}}{e^{\beta\left(J\left(\frac{\sum_{k\neq i=1}^{N} s_k}{N}\right)+h\right)}} \tag{2.32}$$

All terms cancel except for the ones involving $s_i = -1$ and $s_i = 1$. Realizing that the average magnetization is given by

$$m = \frac{\sum_{k=1}^{N} s_k}{N}. \tag{2.33}$$

yields $\frac{P_{eq}(s_i=-1)}{P_{eq}(s_i=1)} = \frac{e^{-\beta(Jm+h)}}{e^{\beta(Jm+h)}}$. The last step in equation 2.31 is based on the definition of the tangens hyperbolicus $tanh(x) = \frac{e^x - e^{-x}}{e^x + e^{-x}}$.

The Glauber rates are normalized by multiplying $\frac{1}{2}$, which yields

$$p_G^+(m,h) = \frac{1}{2}[1 - \tanh(\beta(Jm+h))] \tag{2.34}$$

and

$$p_G^-(m,h) = \frac{1}{2}[1 + \tanh(\beta(Jm+h))]. \tag{2.35}$$

In addition, the Glauber rates are linearized, which yields

$$p^+(m,h) = \frac{1}{2}[1 - \beta(Jm+h)] \tag{2.36}$$

and

$$p^-(m,h) = \frac{1}{2}[1 + \beta(Jm+h)]. \tag{2.37}$$

Linear transition rates ensure that a full polarization is possible. While linear rates $p = \frac{1}{2}[1+x] \in [0,1]$ for $x \in [-1,1]$, the non-linear rates with $tanh(x) \in [-0.76, 0.76]$ for $x \in [-1,1]$ can only reach values in the interval $p = \frac{1}{2}[1 + tanh(x)] \in [0.12, 0.88]$.

Furthermore, as Cividino [25] noted, the Glauber transition rates are multiplied by constant switching probabilities $p_\pm$ which leads to

$$p^+(m,h) = \frac{p_+}{2}[1 - \beta(Jm+h)] \tag{2.38}$$

and

$$p^-(m,h) = \frac{p_-}{2}[1 + \beta(Jm+h)]. \tag{2.39}$$

As mentioned before, these constant switching probabilities can be interpreted as the inverse of the holding time of the asset in the absence of the social imitation and momentum:

$$t_h^\pm = \frac{2}{p_\pm} \tag{2.40}$$

For instance, a constant switching probability of $p_{\pm} \approx 0.2$ implies a average holding time of $t_h^{\pm} \approx 10$ time periods. Too short holding periods can lead to unrealistic oscillatory behaviour and a high frequency of opposite polarization of the traders as shown by Cividino [25].

Comparing the final Glauber transition rates in equations 2.38 and 2.39 with the switching probabilities of the original model

$$p_t^+ = \frac{p_+}{2}\left(1 - \kappa_t\left(s_t + H_t\right)\right) \tag{2.41}$$

$$p_t^- = \frac{p_-}{2}\left(1 + \kappa_t\left(s_t + H_t\right)\right), \tag{2.42}$$

highlights how the noise trader class is mapped onto the Ising model.

The inverse of temperature β corresponds to the herding propensity

$$\beta \Leftrightarrow \kappa_t, \tag{2.43}$$

the average magnetization of the spins corresponds to the sentiment or opinion index

$$m \Leftrightarrow s_t, \tag{2.44}$$

and the external magnetic field that is applied to the spins corresponds to the price momentum:

$$h \Leftrightarrow H_t. \tag{2.45}$$

The interaction coupling term J is set to $J = 1$, which implies that all traders interact homogeneously amongst each other.

As mentioned at the beginning of the section, the Ising model undergoes a phase transition between the ordered and a disordered phase. The critical point at which the phase transition occurs can be derived from the self consistency condition [118, 91]:

$$m = tanh(\beta(Jm + h). \tag{2.46}$$

The critical point itself is denoted by the critical temperature T_c, which corresponds to the critical inverse temperature β_c. If the inverse temperature is lower than the critical value $\beta < \beta_c$ ($T > T_c$), disorder reigns. If the inverse temperature is higher than the critical value $\beta > \beta_c$ ($T < T_c$), order

reigns. The critical value of the inverse temperature β_c is found by taking the derivative with respect to m on both sides of equation 2.46. The derivative is evaluated at the points $m = 0$ and $h = 0$:

$$1 = \frac{d}{dm} tanh(\beta(Jm + h)\Big|_{m=0,h=0} = \beta J. \tag{2.47}$$

Therefore, the critical value of the inverse temperature is given by:

$$\beta_c = \frac{1}{J} \tag{2.48}$$

which equals to $\beta_c = 1$ for $J = 1$. Hence, the critical value of the herding propensity is expected to be at $\kappa_c = 1$, with $\kappa_c < 1$ referring to the disordered phase where the noise traders make predominantly random investment decisions and $\kappa_c > 1$ referring to the ordered phase where the noise traders make investment decision predominantly based on social imitation and the price momentum tradings strategies.

2.4 Market clearing and the price equation

This section brings the two assets and the two trader classes together by introducing the market clearing conditions and the price equation. Noise traders and fundamentalists interact through the price equation. As mentioned before, both trader classes are each modelled as a single representative agent, who invests in the risky and the risk-free asset according to respective strategies.

The market clearing conditions are based on Walras' theory of general equilibrium [119] given by the following equation:

$$\Delta D^f_{t-1\to t} + \Delta D^n_{t-1\to t} = 0. \tag{2.49}$$

$\Delta D^f_{t-1\to t}$ and $\Delta D^n_{t-1\to t}$ are the excess demand for the risky asset of the fundamentalists and the noise traders. There is no external supply of the risky asset, hence the excess demands have to balance out.

Describing the excess demands of both trader classes in terms of the risky fraction of the respective class leads to

$$\Delta D^f_{t-1\to t} = W^f_t x^f_t - W^f_{t-1} x^f_{t-1} \frac{P_t}{P_{t-1}}, \tag{2.50}$$

and

$$\Delta D^n_{t-1\to t} = W^n_t x^n_t - W^n_{t-1} x^n_{t-1} \frac{P_t}{P_{t-1}}. \tag{2.51}$$

Employing equation 2.6 for the wealth dynamics of both classes results in

$$\Delta D^f_{t-1\to t} = W^f_t x^f_t \left[1 + r_f + x^f_{t-1}\left(\frac{d_t}{P_{t-1}} + \frac{P_t}{P_{t-1}} - 1 - r_f\right)\right] - W^f_{t-1} x^f_{t-1} \frac{P_t}{P_{t-1}}, \tag{2.52}$$

and

$$\Delta D^n_{t-1\to t} = W^n_t x^n_t \left[1 + r_f + x^n_{t-1}\left(\frac{d_t}{P_{t-1}} + \frac{P_t}{P_{t-1}} - 1 - r_f\right)\right] - W^n_{t-1} x^n_{t-1} \frac{P_t}{P_{t-1}}. \tag{2.53}$$

Employing the final formula of the risky fraction for the fundamentalist (equation 2.17) and imposing the balance condition yield an equation for the price p_t. The derivation is found in Kohrt [69], which simplifies the price equation to a quadratic equation:

$$a_t P_t^2 + b_t P_t + c_t = 0 \tag{2.54}$$

The parameters a_t, b_t and c_t are given by the following equations:

$$a_t = \frac{1}{P_{t-1}}\left[W^n_{t-1} x^n_{t-1}(x^n_t - 1) + W^f_{t-1} x^f_{t-1}\left(\frac{1}{\gamma}\frac{E_r - r_f}{\sigma_r^2} - 1\right)\right], \tag{2.55}$$

$$\begin{aligned} b_t = \frac{1}{\gamma}\frac{W^f_{t-1}}{\sigma_r^2}\left(x^f_{t-1}\frac{d_t(1+r_d)}{P_{t-1}} + (E_r - r_f)\left[x^f_{t-1}\left(\frac{d_t}{P_{t-1}} - 1 - r_f\right) + 1 + r_f\right]\right) \\ + W^n_{t-1} x^n_{t-1}\left[x^n_{t-1}\left(\frac{d_t}{P_{t-1}} - 1 - r_f\right) + 1 + r_f\right], \end{aligned} \tag{2.56}$$

$$c_t = W^f_{t-1}\frac{1}{\gamma}\frac{d_t(1+r_d)}{\sigma_r^2}\left[x^f_{t-1}\left(\frac{d_t}{P_{t-1}} - 1 - r_f\right) + 1 + r_f\right]. \tag{2.57}$$

For $a_t < 0$, $b_t > 0$ and $c_t > 0$, the solution to the quadratic equation 2.54 is

$$P_t = \frac{-b_t - \sqrt{b_t^2 - 4a_t c_t}}{2a_t}. \tag{2.58}$$

2.5 Model dynamics

After the introduction of the assets, traders and the market clearing conditions with the price equation, an exposition of the model dynamics follows. As mentioned, the model evolves in time through discrete intervals, namely trading days. A key role in the dynamical evolution of the market is taken by the herding propensity κ_t of then noise trader class. Therefore, the section first details the role κ_t in the model. Then the parameters chosen for the simulation are outlined. Afterwards the results of the simulation of the model, the time series, are described and analysed.

As mentioned in section 2.3, the herding propensity κ_t weights the impact of the social imitation term (also called sentiment or opinion index) s_t and the momentum term H_t. Kaizoji et al. [62] introduces the herding propensity based on Harras et al. [51] to account for the variations that effect financial markets such as changes in the economic and geopolitical climate. There are two different description of the herding propensity: The first is to model κ_t as constant value $\kappa_t = \kappa = cst.$, which represents a stable environment of the financial market. The second approach is to employ a time-varying stochastic process, which represents the changes in the environment.

Kaizoji et al. [62] uses a discrete Ornstein-Uhlenbeck (OU) stochastic process

$$\kappa_t = \kappa_{t-1} + \eta_\kappa(\mu_\kappa - \kappa_{t-1}) + \sigma_\kappa v_t, \tag{2.59}$$

which characterizes the dynamic regime-switching of financial markets Lux [80]. μ_k is the mean reversion level around which the OU process varies. η_κ represents the mean reversion rate, which describes the velocity with which the OU reverts to the mean reversion level. v_t is a series of standard independent and identically distributed (i.i.d.) random variables with $\mathcal{N}(0,1)$ that realizes a Wiener process. σ_κ is the step size of the Wiener process.

The first two moments of the Ornstein-Uhlenbeck process are given by

$$\mathbf{E}_t[\kappa_t] = \kappa_0 \exp^{-\eta_\kappa t} + \mu_\kappa(1 - \exp^{-\eta_\kappa t}) \tag{2.60}$$

$$\mathbf{Cov}[\kappa_s, \kappa_t] = \frac{\sigma_\kappa^2}{2\eta_\kappa}\left(\exp^{-\eta_\kappa(t-s)} + \exp^{-\eta_\kappa(t+s)}\right) \; s < t. \tag{2.61}$$

In the long run, for $t \to \infty$, the distribution of the process converges to a stationary Gaussian distribution with mean equal to the mean reversion level $\mu_G = \mu_k$ and variance equal to $\sigma_G^2 = \frac{\sigma_\kappa^2}{2\eta_\kappa}$

$$\kappa_t \sim \mathcal{N}(\mu_\kappa, \frac{\sigma_\kappa^2}{2\eta_\kappa}). \tag{2.62}$$

2.5.1 Parameter set

After highlighting the relevance of herding propensity and the OU process, the parameter set used to run the simulations are introduced. Table 2.1 summarizes the choices for the specific values. A more detailed discussion of the choices can be found in Kaizoji et al. [62], Kohrt [69], Ollikainen [91] and Westphal and Sornette [122].

Parameter set		
Assets	$r_f = 4 \times 10^{-5}$	$r_d = 1.6 \times 10^{-4}$
	$P_0 = 1$	$d_0 = 1.6 \times 10^{-4}$
		$\sigma_d = 1.6 \times 10^{-5}$
Fundamentalist	$W_0^f = 10^9$	$E_r = 1.6 \times 10^{-4}$
traders	$\sigma_r^f = 0.02$	$x_0^f = 0.3$
Noise	$W_0^n = 10^9$	$N_n = 1000$
traders	$\theta = 0.95$	$H_0 = 1.6 \times 10^{-4}$
	$p^- = 0.200625$	$p^+ = 0.199375$
	$x_0^n = 0.3$	
Herding	$\kappa_0 = \mu_\kappa$	$\mu_\kappa = 0.98\kappa_c = 0.98$
propensity	$\eta_\kappa \approx 0.11$	$\sigma_\kappa \approx 0.01$

Table 2.1: Parameters for simulation of original market model. The values are based on Westphal and Sornette [122].

The asset parameters are the following: The value of the risk-free rate r_f for the risk-free asset is set to $r_f = 0.004\%$ per time period which accumulates to an annualized risk-free rate of $r_f^{annual} \approx r_f \times 250 = 0.01$ assuming 250 trading days per year. The parameters for the dividend process are determined according to Engsted and Pedersen [36]. The average value of the dividend growth factor r_d is set to $r_d = 0.016\%$, which accumulates to $r_d^{annual} \approx r_d \times 250 = 0.04$. The standard deviation of the growth rate σ_d is equal to $\sigma_d = 0.0016\%$. The small value for σ_d is chosen to emphasize the stochastic aspect of the noise trader strategy and not the dividend structure. The initial dividend value d_0 is set to $d_0 = 0.016\%$, which accumulates to an annual growth rate of $d_0^{annual} \approx d_0 \times 250 = 0.04$. The initial price is set to $P_0 = 1$.

Both traders, the fundamentalists and the noise traders start with an equal amount of wealth, $W_0^f = W_0^n = 10$ Billion. Furthermore, both invest thirty percent of the initial wealth into the risky asset, $x_0^f = x_0^n = 0.3$. The fundamentalists expect, that the average return equals the dividend growth

$E_r = r_d = 0.016\%$. The standard deviation of the return is expected to be $\sigma_r = 0.02$. The initial number of noise traders is set to be $N_n = 1000$. θ is set to be equal to 0.95, which corresponds to a memory length $\tau_{memory} = \frac{1}{1-\theta} = 20$ trading days. Hence, the noise traders consider the prices of the last 20 days to calculate the momentum factor H_t. The initial price momentum is set to the daily average dividend growth rate $H_0 = r_d = 0.016\%$. The constant switching probabilities for the noise traders introduced by Kohrt [69] are set to $p^+ = 0.199375$ and $p^- = 0.200625$, which introduces a bias towards holding the risky asset. Without momentum trading or social imitation, more traders tend to switch to the risky asset. This implies that the frequency of positive price bubbles is higher than the frequency of negative price bubbles, which is also observed in real market data.

As discussed before, the herding propensity is modelled by a constant factor or by the OU stochastic process. When the constant herding propensity is chosen for a simulation, it is set to $\kappa_t = 0.98\kappa_c$, below the critical value of the simulation. This implies that there is no phase transition for the constant herding propensity. The OU stochastic process requires the specification of the mean reversion level μ_κ, the mean reversion rate η_κ and the standard deviation of the Wiener process $\sigma\kappa$. As for the CK simulation, it is useful for the OU process to choose a mean reversion level below the critical value of the herding propensity κ_c. This implies that due to stochastic fluctuations, the model occasionally enters a regime with faster than exponential growth. The mean reversion level is set to $\mu_\kappa = 0.98\kappa_c$. The mean reversion rate η_κ and the standard deviation of the Wiener process $\sigma\kappa$ are set such that the the Gaussian distribution for $t \to \infty$ has a standard deviation of 10% of the critical kappa $\sigma_G = 0.1\kappa_c$ and a deviation of the OU process two standard deviations above the mean reversion level ($\mu_\kappa + 2\sigma_G$), will revert within $\Delta T = 20$ trading days. As mentioned the standard deviation of the limiting Gaussian distribution is $\sigma_G = \frac{\sigma_\kappa}{\sqrt{2\eta_\kappa}}$. In combination with the starting condition,

$$\sigma_\kappa = 0.1\kappa_c\sqrt{2\eta_\kappa}. \tag{2.63}$$

Based on the expectation value of κ 2.60, it is possible to estimate the time needed for the process to revert from a value $\kappa_0 > \kappa_c$ to the mean reversion level μ_κ :

$$\Delta T = \frac{1}{\eta_\kappa}\log\left(\frac{\kappa_0 - \mu_\kappa}{\kappa_c - \mu_\kappa}\right) \tag{2.64}$$

Inverting equation 2.64 yields the following expression for the mean reversion rate

$$\eta_\kappa = \frac{1}{\Delta T} \log\left(\frac{\mu_\kappa + 2 \cdot 0.1\kappa_c - \mu_\kappa}{\kappa_c - \mu_\kappa}\right) = \frac{1}{20} \log\left(\frac{0.2\kappa_c}{0.02\kappa_c}\right) = \frac{1}{20} \log(10) \approx 0.11 \tag{2.65}$$

Plugging the value for η_κ into equation 2.63 yields

$$\sigma_\kappa = 0.1\kappa_c \sqrt{2\eta_\kappa} \approx 0.05. \tag{2.66}$$

The constant risk aversion γ is not externally fixed but calculated internally each time period. Thus, the constant risk aversion is evaluated initially as

$$\gamma = \frac{1}{x_0^f} \frac{E_r - r_f + \frac{d_0(1+r_d)}{P_0}}{\sigma_r^2}. \tag{2.67}$$

As mentioned earlier, one trading day represents one time period in the model. As noted by Sornette [111], the empirical daily standard deviation of realized returns in financial markets is approximately $\sigma_{market} \approx 0.01$. Therefore, as suggested by Ollikainen [91], the model adopts the daily standard deviation of realized returns.

The returns are approximated by a Wiener process with standard deviation at time t equal to $\sigma_t = \sigma_0\sqrt{t}$. Therefore, the standard deviation at two different times t_1 and t_2 of a Wiener process are related by

$$\sigma_{t_2} = \sigma_{t_1} \sqrt{\frac{t_2}{t_1}}. \tag{2.68}$$

From equation 2.68, it is possible to infer the relation of a simulated trading day to a real trading day

$$\frac{t_{\text{sim}}}{t_{\text{market}}} = \frac{\sigma_{\text{sim}}^2}{\sigma_{\text{market}}^2} \tag{2.69}$$

which yields

$$t_{\text{sim}} = \frac{\sigma_{\text{sim}}^2}{0.01^2}. \tag{2.70}$$

Therefore, running a simulation with $T = 5000$ time-steps corresponds to $\frac{T}{20} = 20$ trading years in the model.

2.5.2 Simulation and time series

After reviewing the structure of the original market model and the parameter set throughout the chapter, the following subsection details two simulations of the original market model. The source code of the model was written by Kohrt [69] and later extended by Ollikainen [91] and Westphal [122]. The code is written in the Object Oriented programming paradigm. The majority of the code, including the classes for the traders, the assets and the market, is written in C++. The simulations are stored in a database employing the HDF5 library. The data analysis is done in Python. A pseudo-random number generator with a random seed number is used to obtain reproducible results.

The two simulations are identical with respect to the parameter values chosen except for the herding propensity κ_t. The first simulation is set up using a constant herding propensity and illustrated in figure 2.2 while the second simulation is done using the Ornstein-Uhlenbeck (OU) stochastic process and presented in figure 2.3. The figures show the time evolution of several variables including the price p_t, the return on capital r_t also called price return rate, the price momentum H_t, the dividend price ratio $\frac{d_t}{P_t}$, the switching probabilities of the noise traders $p_t^{\pm}$, the risky fractions for both trader classes $x_t^{n,f}$, the wealth ratio $v_t = \frac{W_t^n}{W_t^f}$ and the herding propensity κ_t. In the following the differences between the two figures are highlighted. The first row in figures 2.2 and 2.3 exhibit the price dynamics for the constant kappa (CK) and the Ornstein-Uhlenbeck OU kappa, which is plotted on a log-linear-scale. The price time series for the CK can be characterized by modest fluctuations around a long term linear growth, which is given by the constant growth factor r_d of the dividend. This is contrasted to the large deviations of the price from this long term growth in figure 2.3 for the OU kappa. There are clearly identifiable price bubbles followed by crashes which manifest trough a sharp increase followed by a sharp decrease in the price P_t at for instance $t \approx 2600$ or $t \approx 4700$.

The presence of endogenous bubbles is the defining difference between the two figures and can also be observed in the return on capital r_t and the price momentum H_t. Both show a relatively uniform oscillatory behaviour for the CK, whilst showing periods of small oscillations followed by periods of large oscillations at the price spikes for the OU kappa simulation. In addition, the interval for r_t and H_t values are roughly twice the range for OU kappa compared to compared to the CK simulation. The dividend price ratio $\frac{d_t}{P_t}$ shows an inverse relationship to the price evolution for CK and OU kappa.

The switching probabilities of the noise trader mirror one another and its sum is constant over time $p_t^+ + p_t^- = \frac{p_+ + p_-}{2} = cst$. The probability to switch

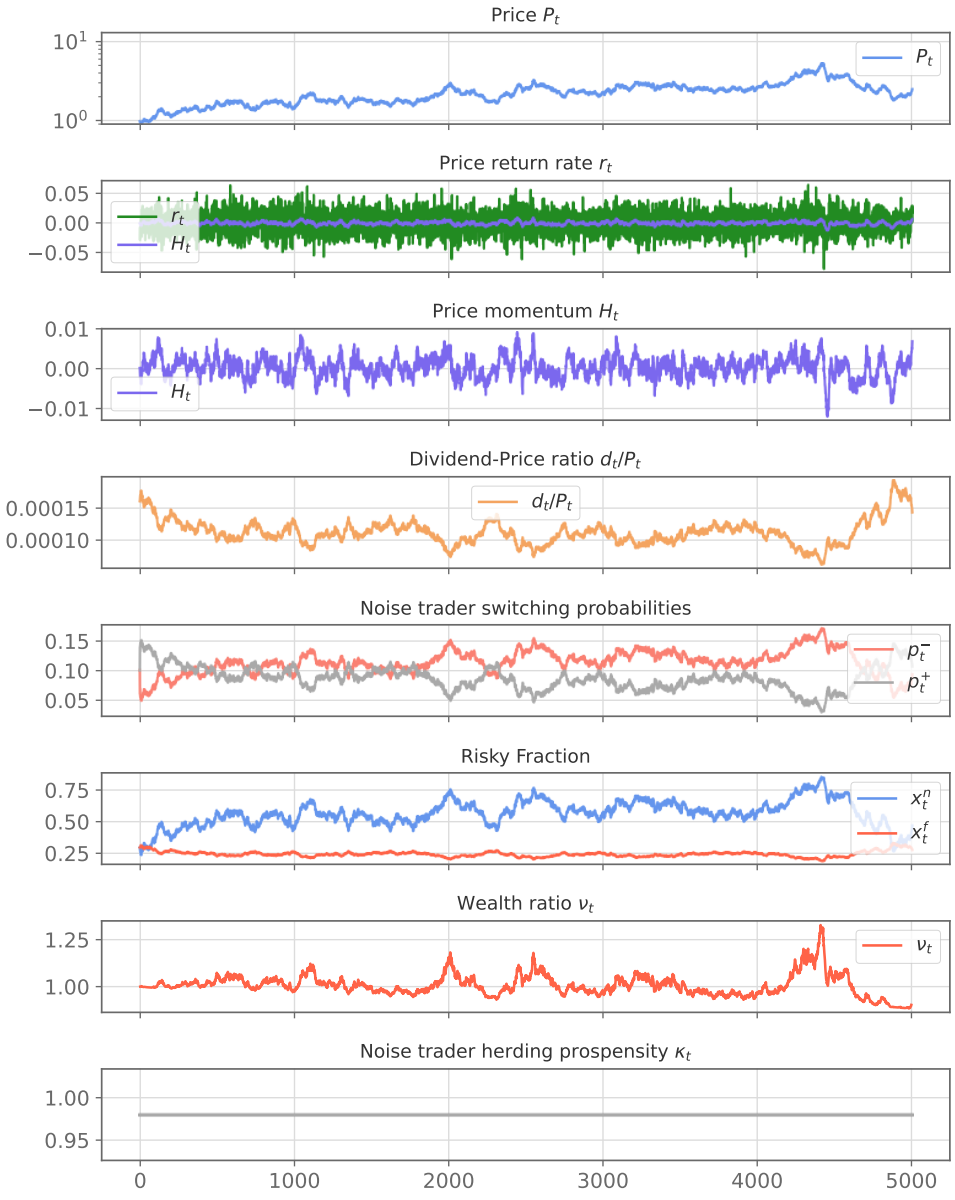

Figure 2.2: Simulation with $\kappa_t = \mu_\kappa = 0.98\kappa_c$. The variables presented in the individual panels are from top panel to bottom: the price p_t, the return on capital r_t, the price momentum H_t, the dividend price ratio $\frac{d_t}{P_t}$, the switching probabilities of the noise traders (from the risky to the risk-free asset p_t^+ and vise versa p_t^-), the risky fractions for both trader classes $x_t^{n,f}$, the wealth ratio $v_t = \frac{W_t^n}{W_t^f}$ and the herding propensity κ_t.

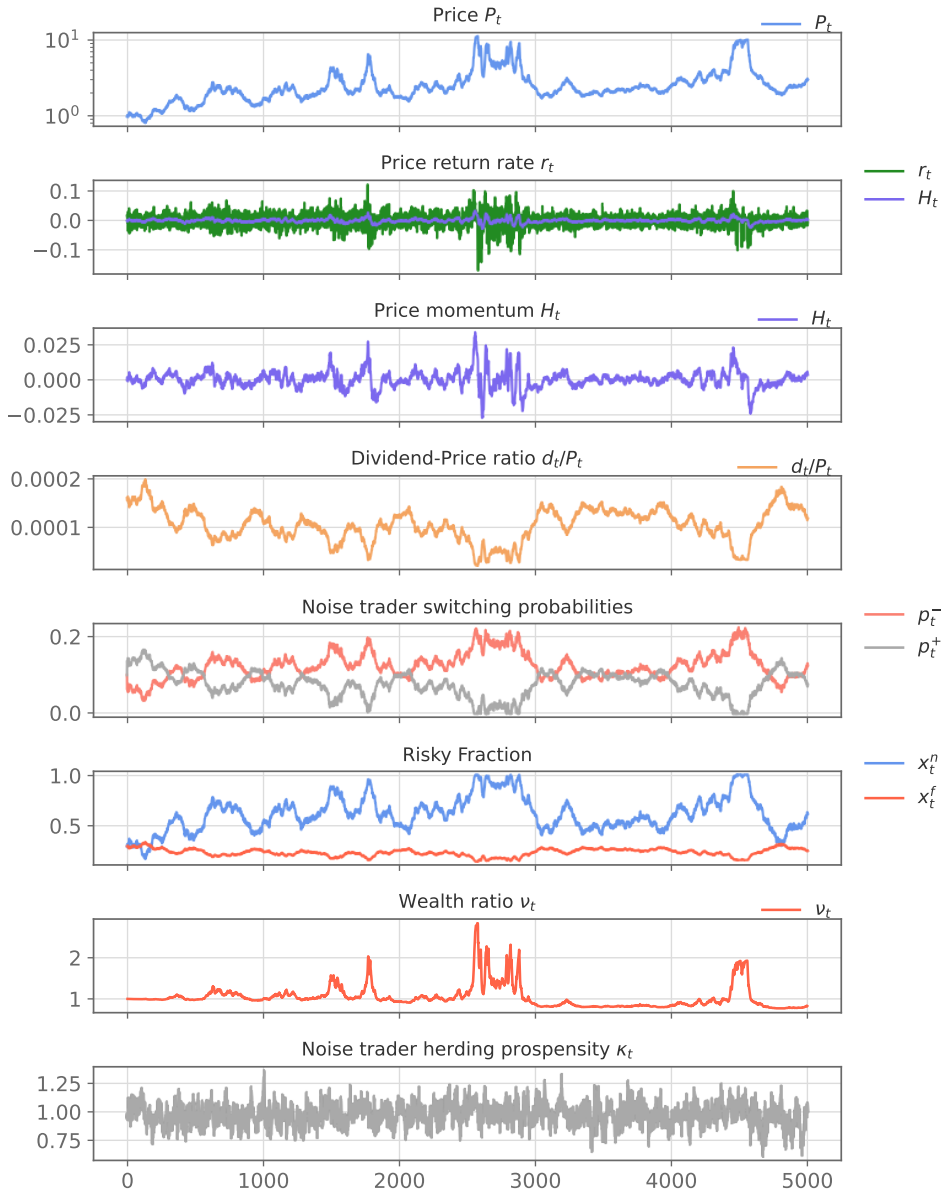

Figure 2.3: Simulation with κ_t as the OU process. The variables presented in the individual panels are from top panel to bottom: the price p_t, the return on capital r_t, the price momentum H_t, the dividend price ratio $\frac{d_t}{P_t}$, the switching probabilities of the noise traders (from the risky to the risk-free asset p_t^+ and vise versa p_t^-), the risky fractions for both trader classes $x_t^{n,f}$, the wealth ratio $v_t = \frac{W_t^n}{W_t^f}$ and the herding propensity κ_t.

from the risk-free to the risky asset p_t^- has a similar trajectory compared to the risky fraction, because a high probability to switch to the risky asset implies a high risky fraction and vice versa. When comparing both simulations, the risky fraction of the noise traders, x_t^n, exhibits larger fluctuations for the OU process. A risky fraction of $x_t^n = 1$ characterizes a full polarization of the noise traders to the risky asset. This can be seen around $t \approx 3600$ in figure 2.3. A polarization to the risk-free asset cannot be seen in the simulation but would correspond to $x_t^n = 0$.

The wealth ratio given by $\nu_t = \frac{W_t^n}{W_t^f}$ defines the total wealth of the noise traders relative to the total wealth of the fundamentalists. The increase in the ratio correlates with the price bubbles. During increases in price, the wealth increases for both investors. While the noise traders tend to invest more in rising prices, the fundamentalists tend to sell off the risky asset when the price increases.

2.5.3 Stylized facts

After the qualitative discussion of the simulation results in the previous section, this section continues with more quantitative aspects. A general practice to assess and validate agent based model of financial markets is to their results to statistical properties of real financial market data, which are often summarized under the umbrella term 'stylized facts'. This section verifies that the model produces volatility clustering and the fat-tail distribution of returns.

Volatility clustering describes the observation that large changes in prices tend to cluster together and is tested for by calculating the auto-correlation function (ACF) of the signed and absolute returns [34]. The ACF for a stochastic process X_t at time τ with a lag l is given by equation 2.71

$$ACF_l\left(X_t\right)(\tau) = \frac{\mathrm{Cov}\left[X_t(\tau)X_t(\tau - l)\right]}{\sqrt{\mathrm{Var}\left[X_t(\tau)\right]\mathrm{Var}\left[X_t(\tau - l)\right]}}. \tag{2.71}$$

where the returns at time τ and at time $(\tau - t)$ are essentially tested for a Pearson correlation.

Figures 2.4 and 2.5 show the ACF for the signed (blue) and absolute (red) returns for the CK simulation (figure 2.4) and the OU kappa simulation (figure 2.5).

The ACF for the CK simulation in figure 2.4 decays quickly to zero for increasing lags l for both the signed and absolute returns. This signals that the returns themselves are little correlated and that there are virtually no ar-

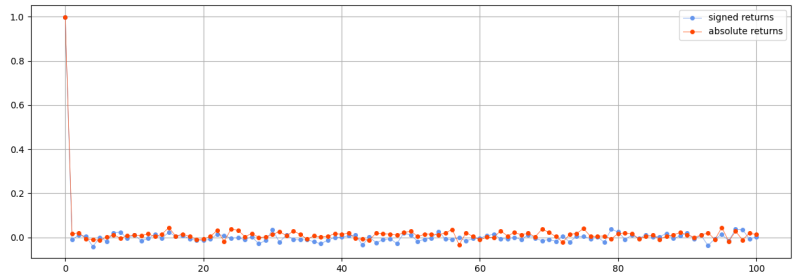

Figure 2.4: ACF for singed (blue) and absolute (red) returns for simulation with constant kappa (CK) with ACF on y-axis and l on x-axis.

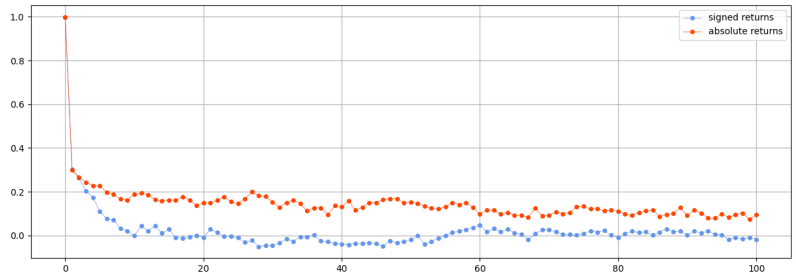

Figure 2.5: ACF for singed (blue) and absolute (red) returns with OU kappa with ACF on y-axis and l on x-axis.

bitrage opportunities in the presence of transaction costs as noted by Kaizoji et al. [62].

The signed returns for the OU kappa simulation in figure 2.5 also decay quickly to zero within $l < 10$. The absolute values of the returns have an auto-correlation function with longer memory. This is also in agreement with Kaizoji et al. [62], Ding et al. [34] and Cont [27] and signals volatility clustering, which was also observed in the visual inspection of figure 2.3.

The fat tail distribution of returns refers to the empirical phenomenon that extreme returns are far more frequent then suggested by the Gaussian distribution [27, 48, 94]. The empirical fat-tail decay of the distribution

$$p(x) \sim x^{-1-\alpha} \tag{2.72}$$

is characterized by the exponent $\alpha \in [2, 4]$.

Figures 2.6 and 2.7 present the fitted parameter for the two simulations. The parameter is $\alpha \approx 4.2$ for the CK simulation and $\alpha \approx 2.0$ for the OU kappa

simulation. This implies that only the simulation with the OU kappa falls within the required range of the parameter.

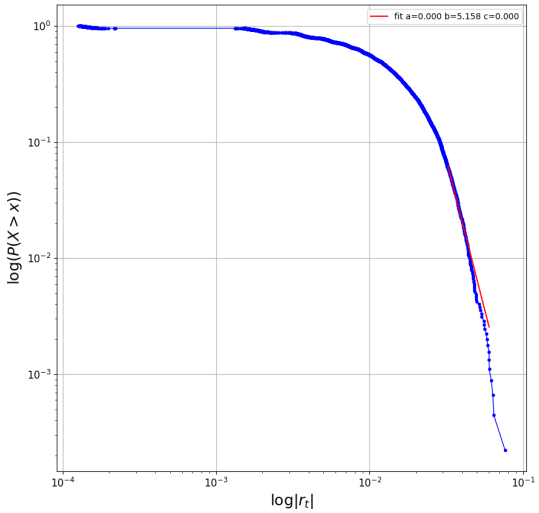

Figure 2.6: Log-log plot of the cumulative distribution function (CDF) of returns for the CK simulation with $\alpha \approx 4.2$.

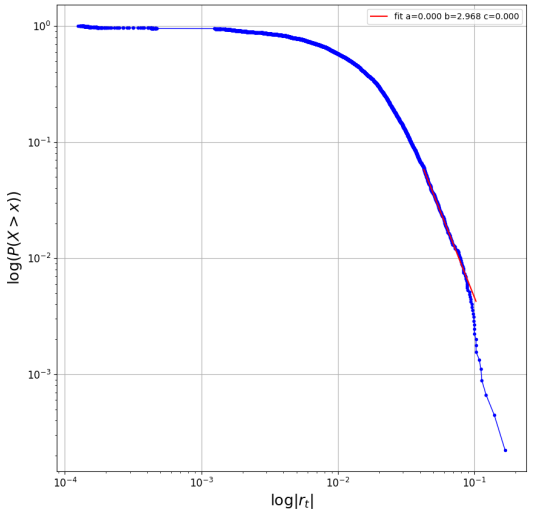

Figure 2.7: Log-log plot of the cumulative distribution function (CDF) of returns for the OU kappa simulation with $\alpha \approx 2.0$.

After introducing the essential aspects of the model with the two trader classes, the market clearing and the model dynamics, the following chapters describes the model extensions.

Chapter 3

Extension of original market model using statistical physics

The previous chapter introduced the original market model with two assets and two trader classes. This chapter focuses on the first extension of the noise trader class. While there are many ways to extend the original model by Kaizoji et al. [62] and its modifications, keeping the essence of the noise trader class imposes some constraints on possible extensions. In this chapter, the goal is to extend the noise trader class to allow for leverage and short selling while preserving the Ising-like structure of social imitation and trend following that governs the polarization of the noise traders and the creation of bubbles.

A natural way to preserve the Ising-like structure of the noise trader class is to base the extension on generalizations of the Ising model from statistical physics. Cividino [25] extended the noise trader class to a multi asset framework by employing the Potts model and the O(n) model amongst others. The following sections outline the Potts and O(n) models and map them from the multi-asset application to the case of one risky asset with leverage and short selling.

3.1 Potts model (for q=4)

In order to describe noise traders that can invest in a risky and risk-free asset but also take a leveraged and a short position in the risky asset, the noise trader class is mapped onto the Potts model. The Potts model allows for spins which can occupy q scalar values $s_i \in \{1, 2, ..., q\}$. In the context of the extension of the noise trader class, the individual spins represent the noise traders and the occupied state represents the investment decision. Hence, an individual noise trader can choose between four different states $s_i \in \{s, rf, r, l\}$, where s represents taking a short position on the risky asset, rf

represents investing in the risk-free asset, r represents investing in the risky asset and l represents taking a leveraged position in the risky asset. The investment decision process of an individual noise trader can be described as a discrete Markov chain, which is depicted in figure 3.1.

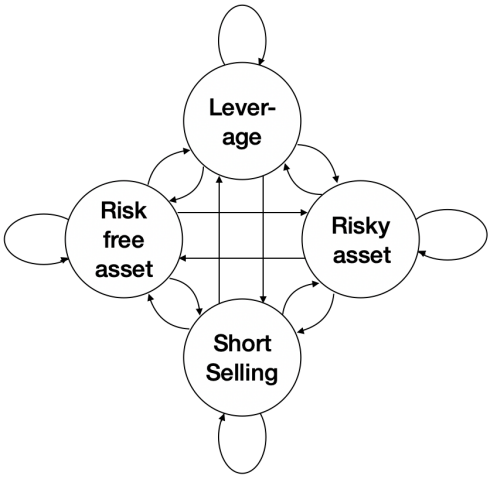

Figure 3.1: Potts model with $q = 4$ states $s_i \in \{s$ = short selling position, rf = risk-free asset, r = risky asset, l = leverage position$\}$.

The derivation of the switching probabilities follows a similar approach to the Ising model (see section 2.3) and is outlined for the general q-state Potts model in Ostilli [93] and Cividino [25]. The main steps are summarized in the following. The fully connected q-state Potts model with an external magnetic field, which acts on the spins, is described by the Hamiltonian

$$H_N\left(\{s_1, \ldots, s_N\}\right) = -\frac{J}{2N}\sum_{i,j=1}^{N}\delta_{s_i,s_j} - \sum_{k=1}^{q}H_k\sum_{i=1}^{N}\delta_{s_i,k}, \tag{3.1}$$

where N presents the number of spins. The individual spin s_i, $i \in \{1, ...N\}$, can take on values $s_i \in \{1, ...q\}$. The interaction among the individual spins is determined by δ_{s_i,s_j}, which equals one if s_i and s_j are in the same state and zero if not. The external magnetic field is described by $H_k\delta_{s_i,k}$, where k corresponds to one of the states of the spins $k \in \{1, ...q\}$. The transition probability of an individual spin to switch from state a to b is given by

$$P_t(a \to b) = \frac{e^{\kappa_t\left(\frac{N_b - N_a}{N} + H_b - H_a\right)}}{\sum_{k=1}^{q} e^{\kappa_t\left(\frac{N_k - N_a}{N} + H_k - H_a\right)}} = \frac{e^{\kappa_t\left(\frac{N_b}{N} + H_b\right)}}{\sum_{k=1}^{q} e^{\kappa_t\left(\frac{N_k}{N} + H_k\right)}}. \tag{3.2}$$

N_a the number of spins in state $a \in \{1, ...q\}$ and N_b the number of spins in state $b \in \{1, ...q\}$. κ_t corresponds to the inverse temperature β (see relation 2.43). H_a and H_k are the external magnetic fields that interact with spins in state a and k. The interaction term of the Hamiltonian is set to $J = 1$. The right side of the equation shows that the transition probability from state a to b is independent of the initial state a.

Comparing these transition probabilities to the original model, it is clear that the sentiment s_t of the original model is replaced by q new sentiments. Each state is associated with a single sentiment defined by

$$s_t^b = \frac{N_b}{N} \text{ with } b \in \{s, rf, r, l\}. \tag{3.3}$$

The transition probabilities can be represented as a matrix as shown in table 3.1.

$P(a \to b)$	s	rf	r	l
s	$P(s \to s)$ $= P(s)$	$P(s \to rf)$ $= P(rf)$	$P(s \to r)$ $= P(r)$	$P(s \to l)$ $= P(l)$
rf	$P(rf \to s)$ $= P(s)$	$P(rf \to rf)$ $= P(rf)$	$P(rf \to r)$ $= P(r)$	$P(rf \to l)$ $= P(l)$
r	$P(r \to s)$ $= P(s)$	$P(r \to rf)$ $= P(rf)$	$P(r \to r)$ $= P(r)$	$P(r \to l)$ $= P(l)$
l	$P(l \to s)$ $= P(s)$	$P(l \to rf)$ $= P(rf)$	$P(l \to r)$ $= P(r)$	$P(l \to l)$ $= P(l)$

Table 3.1: Transition probabilities $P(a \to b)$ for q-state Potts model, where the start states a are on the vertical axis and the end states b are on the horizontal axis.

The independence of the transition probabilities from the initial state a is reflected in the transition probability table, where each column only depends on the respective end state.

Using equation 3.2, the probability of remaining in the same state from one period to the next in the absence of herding behavior $\kappa_t = 0$ is given by $P_t(a \to a)|_{\kappa_t=0} = \frac{1}{q}$. Since $P_t(a \to a)$ is defined as the probability of switching from state a to state a, $(1 - P_t(a \to a))$ defines the probability of switching from state a to any other of the $q - 1$ states. Therefore, the average time that a trader remains in one state in the absence of herding behavior is the inverse of the probability to switch to another state

$$t_h = \frac{1}{1 - P_t\left(a \to a\right)\big|_{\kappa_t = 0}}. \tag{3.4}$$

This implies an inverse proportion between the holding time and the number of states. As an example, for $q = 4$ the holding time equals $t_h = \frac{4}{3}$. If $q = 10$, the holding time equals $t_h = \frac{10}{9}$. The more states there are, the quicker the traders switch between states. The original market model assumed a holding time of 10 periods $t_h = 10$. To remedy the issue of short holding times, Cividino [25] introduces an average holding time t_h, which was also introduced in the original market Ising model, with constant switching probabilities $p_{\pm}$ and the related holding period $t_h^{\pm} = \frac{2}{p_{\pm}}$ to avoid an unrealistically quick switching between the states.

In similar fashion, two constants c and d are introduced to enable an adjustment of the time a trader remains in one state. This allows to increase the probability to remain in state a, $P_t(a \to a)$ while decreasing the probability to switch to any other state $P_t(a \to b)$. The probabilities have to obey the condition

$$P_t(a \to a) + \sum_{b \neq a} P_t(a \to b) = 1. \tag{3.5}$$

$P_t(a \to a)$ is multiplied by the constant c and the probabilities $P_t(a \to b)$ are multiplied by the constant d. If the herding propensity is set to zero $k_t = 0$, this yields $\frac{c}{q} + \frac{d(q-1)}{q} = 1$. In combination with equation 3.1, the constants c and d are given by

$$c = \left(1 - \frac{1}{t_h}\right) q \tag{3.6}$$

$$d = \frac{q - c}{q - 1} = \frac{q - \left(1 - \frac{1}{t_h}\right)}{q - 1} \tag{3.7}$$

This lead the new transition probabilities

$$P_t(a \to a) = \frac{c \cdot e^{\kappa_t\left(\frac{N_a}{N} + H_a\right)}}{\sum_{k=1}^{q} e^{\kappa_t\left(\frac{N_k}{N} + H_k\right)}}, \tag{3.8}$$

$$P_t(a \to b) = \frac{d \cdot e^{\kappa_t\left(\frac{N_b}{N} + H_b\right)}}{\sum_{k=1}^{q} e^{\kappa_t\left(\frac{N_k}{N} + H_k\right)}}, \tag{3.9}$$

For instance, assuming $q = 4$ where $a, b \in \{s, rf, r, l\}$, $t_h = \frac{4}{3}$ leads to $c = d = 1$. The switching probabilities are $P(a \to a)|_{\kappa_t=0} = P(a \to b)|_{\kappa_t=0} = 1/q = 0.25$. However, assuming the holding time of the original market model $t_h = 10$ results in $c = 3.6$ and $d \approx 0.13$. The associated switching probabilities are $P(a \to a)|_{\kappa_t=0} = 0.9$ and $P(a \to b)|_{\kappa_t=0} \approx 0.033$.

In the case of the multi-asset extension, $a, b \in \{1, \dots q\}$ represent the assets that the noise trader can invest in. Furthermore, in the multi-asset extension H_k^t corresponds to the price momentum of asset k. In the leverage and short selling extension, there is only one price momentum H_t for the risky asset. This allows for several ways to define the price momentum factor for the individual states. This point is addressed in more detail in the next chapter in table 4.2. For the Potts model the following definitions are adopted. The risky asset position is associated with a price momentum factor $H_r = H_t - r_f$. When taking the leverage position, the noise trader invests twice the wealth in the risky asset. Hence, the price momentum factor is set to $H_l = 2H_t - r_f$. The risk-free position yields the risk free return r_f and is defined as the opposite of the risky asset factor $H_{rf} = r_f - H_t$. The short position is defined by the opposite of the leveraged position $H_s = r_f - 2H_t$.

Using the transition probabilities of the noise trader class, it is now possible to write down the equations for the evolution of the number of traders in each state. As in the original model, the investment decision is represented by Bernoulli random variables. The discrete time evolution of the noise traders in the different states is given by:

$$N_t^s = \sum_{k=1}^{N_{t-1}^{rf}} \xi_k(p_{t-1}^s) + \sum_{k=1}^{N_{t-1}^{r}} \xi_k(p_{t-1}^s) + \sum_{k=1}^{N_{t-1}^{l}} \xi_k(p_{t-1}^s) + \sum_{k=1}^{N_{t-1}^{s}} [1 - \xi_k(p_{t-1}^{rf}) - \xi_k(p_{t-1}^r) - \xi_k(p_{t-1}^l)], \quad (3.10)$$

$$N_t^{rf} = \sum_{k=1}^{N_{t-1}^{s}} \xi_k(p_{t-1}^{rf}) + \sum_{k=1}^{N_{t-1}^{r}} \xi_k(p_{t-1}^{rf}) + \sum_{k=1}^{N_{t-1}^{l}} \xi_k(p_{t-1}^{rf}) + \sum_{k=1}^{N_{t-1}^{rf}} [1 - \xi_k(p_{t-1}^s) - \xi_k(p_{t-1}^r) - \xi_k(p_{t-1}^l)], \quad (3.11)$$

$$N_t^r = \sum_{n=k}^{N_{t-1}^s} \xi_k(p_{t-1}^r) + \sum_{k=1}^{N_{t-1}^{rf}} \xi_k(p_{t-1}^r) + \sum_{k=1}^{N_{t-1}^l} \xi_k(p_{t-1}^r) + \sum_{k=1}^{N_{t-1}^r} [1 - \xi_k(p_{t-1}^s)\xi_k(p_{t-1}^{rf} - \xi_k(p_{t-1}^l], \quad (3.12)$$

$$N_t^l = \sum_{k=1}^{N_{t-1}^s} \xi_k(p_{t-1}^l) + \sum_{k=1}^{N_{t-1}^{rf}} \xi_k(p_{t-1}^l) + \sum_{k=1}^{N_{t-1}^r} \xi_k(p_{t-1}^l) + \sum_{k=1}^{N_{t-1}^l} [1 - \xi_k(p_{t-1}^s) - \xi_k(p_{t-1}^{rf}) - \xi_k(p_{t-1}^r)]. \quad (3.13)$$

The definition of the risky fraction reflects the values for the polarization of noise traders to the risky asset ($x_t^n = 1$) and the risk-free asset ($x_t^n = 0$) of the original market model and adds the polarization to the leverage ($x_t^n = 2$) and short position ($x_t^n = -1$). The risky fraction is given by

$$x_t^n = \frac{2N_l + N_r - N_s}{N} \in [-1, 2]. \quad (3.14)$$

3.1.1 Model dynamics

After extending the noise trader class to include leverage and short selling using the Potts model, this subsection provides an exposition of its model dynamics. The parameter set of the model is introduced and the time series is described for different simulations.

The parameter set is described in table 3.2. The parameter values for the fundamentalist and the risky and risk-free asset are identical to the original model. Besides investing their total wealth into either the risky or the risk-free asset, each noise trader can double down on their investment by investing twice their respective wealth into one of the two assets. Investing twice their wealth into the risky asset corresponds to the leverage state and investing twice in the risk-free asset to short selling. The probability of one noise trader to initially chose state $k \in \{s, rf, r, l\}$ is given by $p_0^k = 0.25$. The price momentum for state i that the noise trader can occupy is excluded from the simulations $H_k = 0$ for $k \in \{s, rf, r, l\}$ to isolate the impact of the sentiment. The holding time is set to $t_h = 10$.

Parameters		
Assets	$r_f = 4 \times 10^{-5}$	$r_d = 1.6 \times 10^{-4}$
	$P_0 = 1$	$d_0 = 1.6 \times 10^{-4}$
		$\sigma_d = 1.6 \times 10^{-5}$
Fundamentalist	$W_0^f = 10^9$	$E_r = 1.6 \times 10^{-4}$
traders	$\sigma_r^f = 0.02$	
Noise	$W_0^n = 10^9$	$N_n = 1000$
traders	$\theta = 0.95$	$H_0 = 1.6 \times 10^{-4}$
	$q = 4$	$p_0^k = 0.25$ k $\in \{s, rf, r, l\}$
	$t_h = 10$	$H_k = 0$ k $\in \{s, rf, r, l\}$
Herding	$\kappa_0 = \mu_\kappa$	$\mu_\kappa = 0.98\kappa_c$
propensity	$\eta_\kappa \approx 0.11$	$\sigma_\kappa \approx 0.16$

Table 3.2: Parameters for simulating the $q = 4$ state Potts model.

The time series for the two different simulations are presented in figures 3.2 and 3.3. The simulations are identical with respect to the parameter values chosen except for the herding propensity κ_t. The first simulation is set up using a constant herding propensity while the second simulation is done using the Ornstein-Uhlenbeck (OU) stochastic process given by

$$\kappa_t = \kappa_{t-1} + \eta_\kappa(\mu_\kappa - \kappa_{t-1}) + \sigma_\kappa \upsilon_t, \tag{3.15}$$

with mean reversion level $\mu_\kappa = 0.98\kappa_c$. As described in chapter 2.5.3 the critical herding propensity corresponds to the critical inverse temperature β_c. For the mean-field q-state Potts model Ostilli and Mukhamedov [93] derive the theoretical value for critical inverse temperature to be

$$\beta_c = \frac{2(q-1)}{q-2} log(q-1), \tag{3.16}$$

which equals $\beta_c \approx 3.30$ for $q = 4$. Similar to the original model, the mean reversion rate η_κ and the standard deviation of the Wiener process $\sigma\kappa$ are set such that the deviation of the OU process two standard deviations above the mean reversion level ($\mu_\kappa + 2\sigma_G$), will revert within $\Delta T = 20$ trading days. This implies a mean reversion of $\eta_\kappa = \frac{1}{\Delta T} \log\left(\frac{\mu_\kappa + 2 \cdot 0.1\kappa_c - \mu_\kappa}{\kappa_c - \mu_\kappa}\right) = \frac{1}{20} \log\left(\frac{0.2\kappa_c}{0.02\kappa_c}\right) = \frac{1}{20}\log(10) \approx 0.11$. Then $\sigma_\kappa = 0.1\kappa_c\sqrt{2\eta_\kappa} \approx 0.16$.

For the simulation with the constant herding propensity CK, κ_t is set to the mean reversion level $\kappa_t = \mu_\kappa = 0.98\kappa_c$, which is below the critical value of the

simulation. The results for the CK simulation are depicted in figure 3.2. As expected, the there is no phase transition for the constant herding propensity, which is also confirmed when looking at the price time series in the first row and the switching probabilities in the third row. The number of noise traders in each state fluctuate around their mean values of 250. The switching probabilities fluctuate between 0.03 and 0.04, which is in agreement with the expected values based on equation 3.9. There is a steady decline of wealth among the noise trader throughout the simulation compared to the fundamentalists.

Figure 3.3 visualizes the OU simulation. From the two simulations the difference between the OU and CK seems to be marginal. The sentiments in the fourth row of figure 3.3 show similarly small fluctuations compared to the CK simulation. At $T \approx 3000$, there is a noticeable spike in P_t^{rf} and N_{rf}. However, there is no polarization to any state even though the herding propensity enters the critical regime several times. The absence of polarization in the noise trader class can mainly be explained by the small switching probabilities, which are a result of the holding time.

Figure 3.4 visualizes the OU simulation for $t_h = \frac{4}{3}$, which corresponds to the Potts model without the adjustment for the holding time in equation 3.9. A smaller holding time increases the switching probabilities and enables the noise traders to polarize towards one state. For instance, at $T \approx 1000$, they polarize to the risk-free asset and at $T \approx 2200$ to the leverage state. After $T \approx 2200$, the noise traders lost most of their wealth and have only little impact on the price dynamics. It is worth noting that, whenever the noise traders polarize towards on state, there is no gradual polarization but an abrupt one. This is highlighted by the peaks in the row that describes the number of noise traders in each state. An explanation for these discontinuous jumps can be found by looking at the phase transitions for the q-state Potts model in more detail.

The phase transitions for the mean-field q-state Potts model are studied in several papers, for instance in Ostilli and Mukhamedov [93], Lorenzoni and Moro [79], Cuff et al. [31], Kirkpatrick and Wolynes [68] and Thirumalai and Kirkpatrick [115].

Ostilli and Mukhamedov [93] identifies two phase transitions for the mean field Potts model. A first order phase transition at critical value

$$\kappa_c = \frac{2(q-1)}{q-2} log(q-1), \tag{3.17}$$

and a second order phase transition at

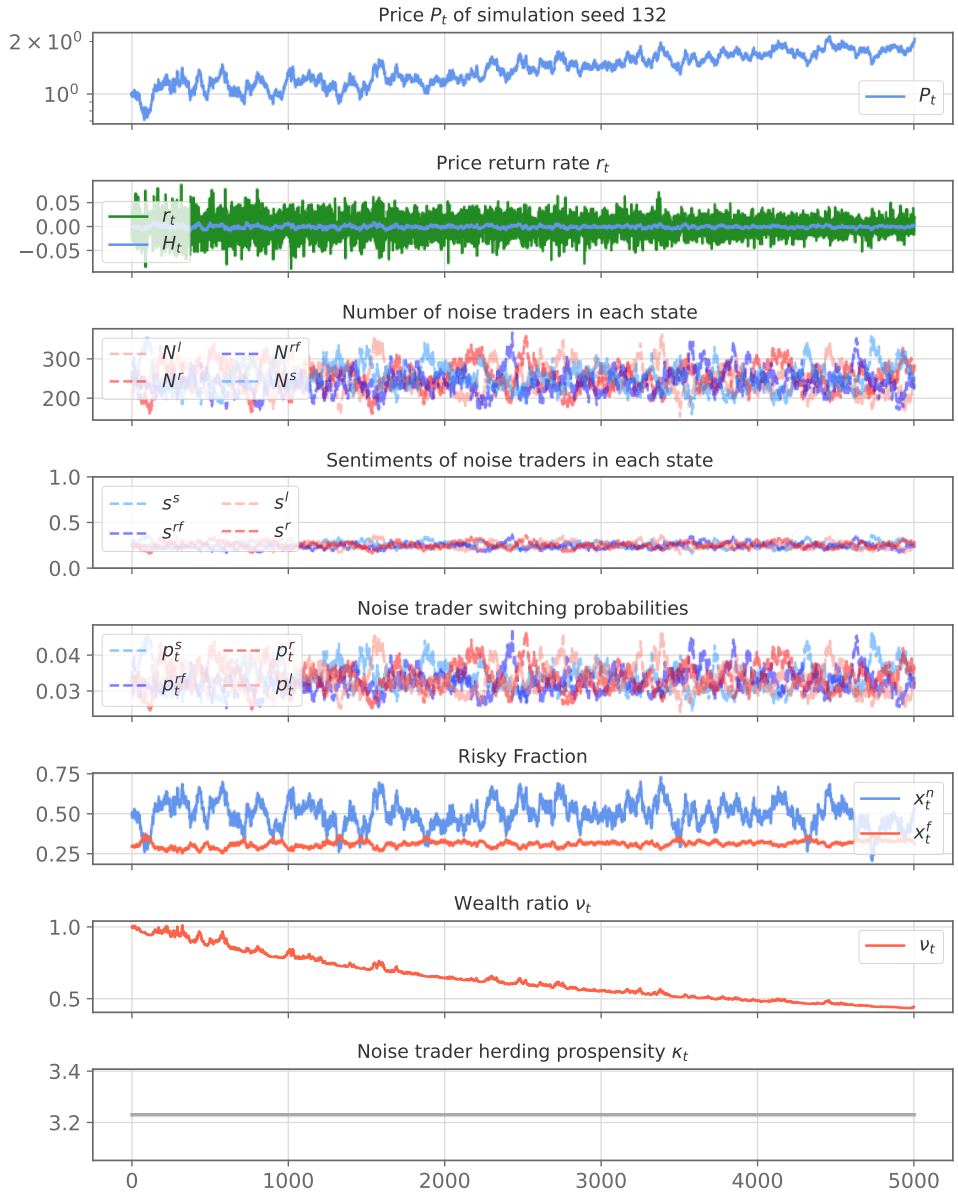

Figure 3.2: Simulation of 4-state Potts model with CK herding propensity. The herding propensity is set to $\kappa_t = 0.98\kappa_c \approx 3.23$, which is below the critical value $\kappa_c \approx 3.30$. The price momentum factors are excluded $H_i = 0$ for $i \in \{s, rf, r, l\}$ to highlight the impact of the sentiment. The holding time is $t_h = 10$. There are no bubbles.

$$\kappa_c = q. \tag{3.18}$$

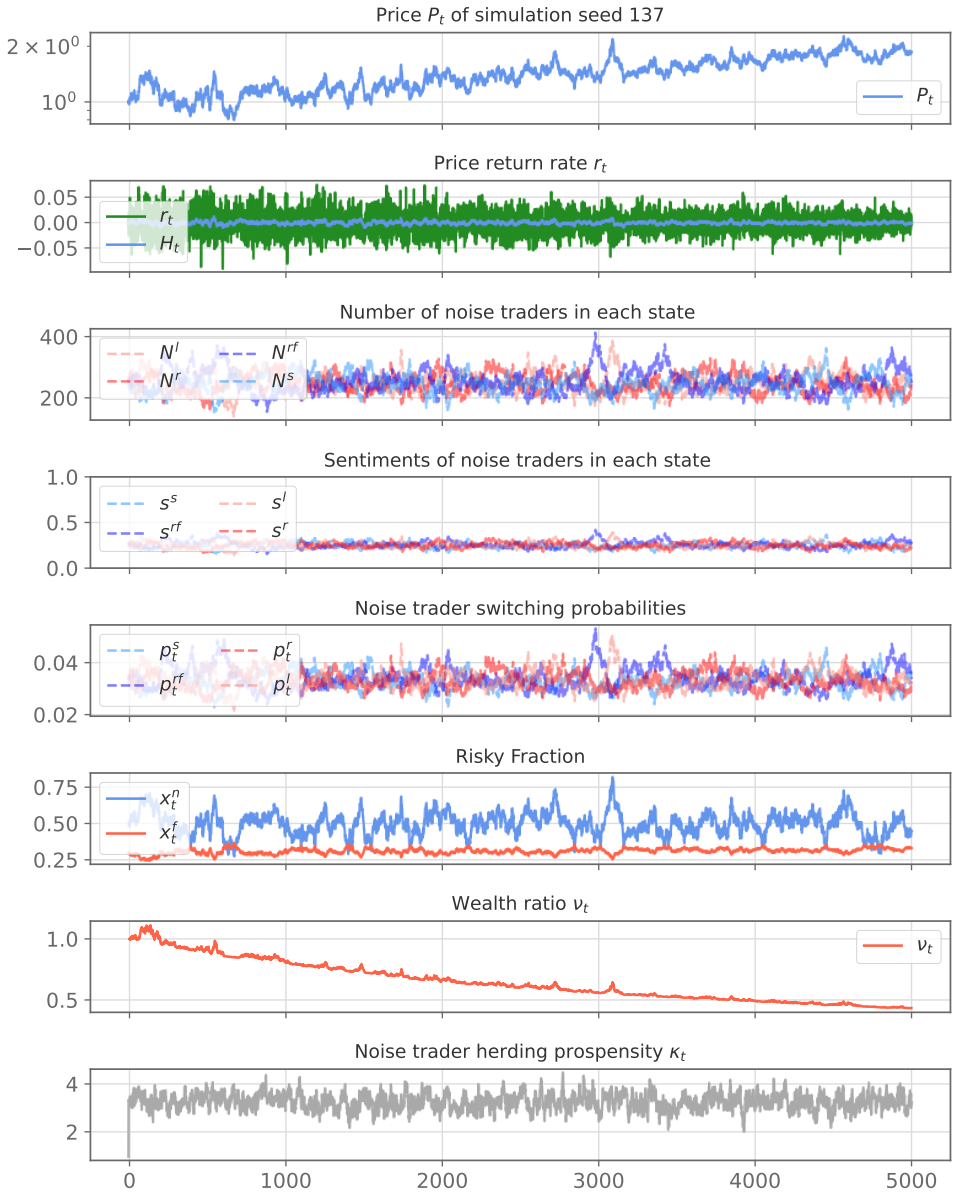

Figure 3.3: Simulation of 4-state Potts model with OU stochastic process for herding propensity. The herding propensity is set to $\kappa_t = 0.98\kappa_c = 3.23$, which is below the critical value $\kappa_c \approx 3.30$. The effects of the price momentum are excluded $H_t = 0$ and $H_i = 0$ for $i \in \{s, rf, r, l\}$. The holding time is $t_h = 10$.

Figure 3.5 shows the bifurcation diagram for the $q = 4$ state mean-field Potts model where the average sentiments ('opinion indexes') of the individual

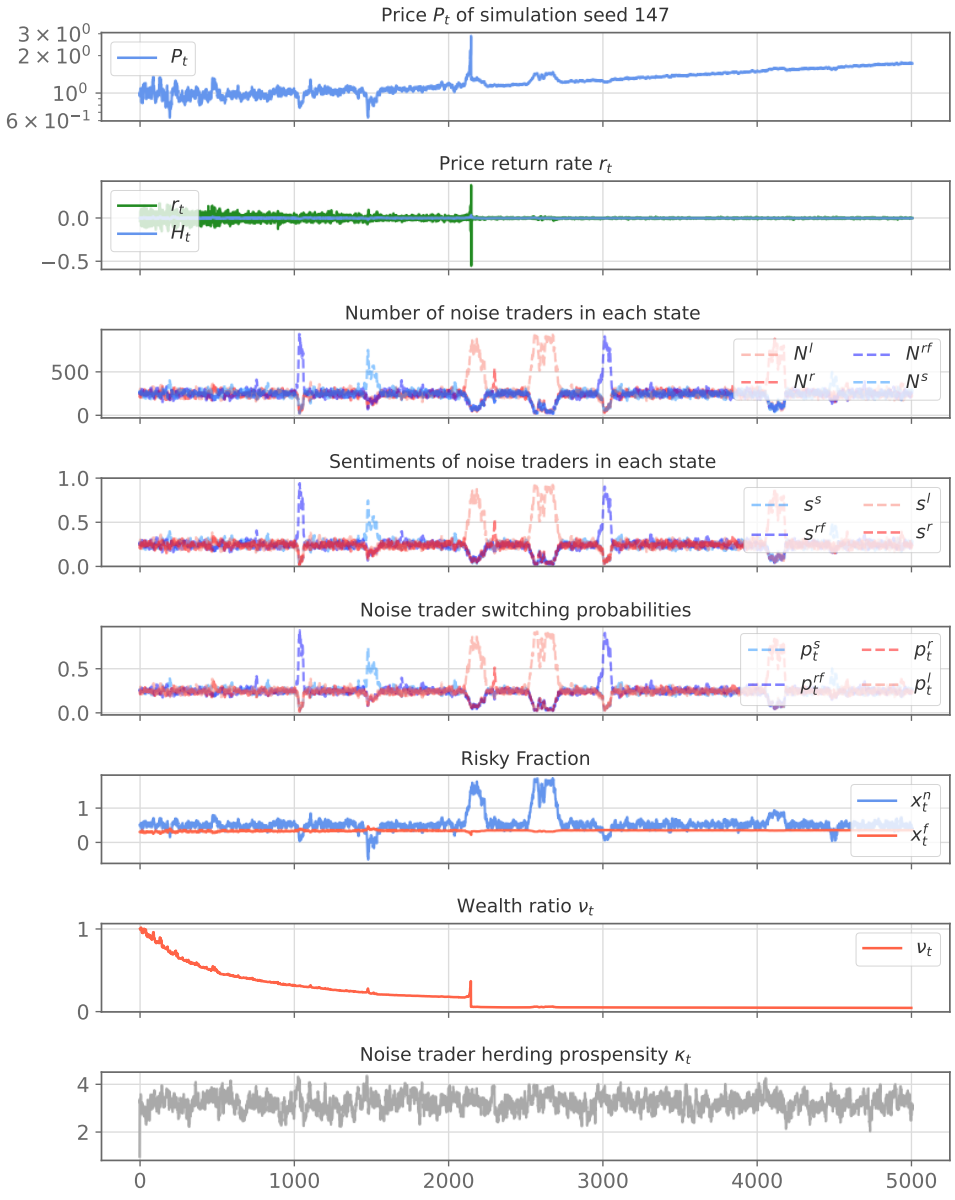

Figure 3.4: Simulation of 4-state Potts model with OU stochastic process for herding propensity. The herding propensity is set to $\kappa_t = 0.98\kappa_c = 3.23$, which is below the critical value $\kappa_c \approx 3.30$. The effects of the price momentum are excluded $H_t = 0$ and $H_i = 0$ for $i \in \{s, rf, r, l\}$. The holding time is $t_h = \frac{4}{3}$.

states s_i with $i \in \{s, rf, r, l\}$ that the noise traders can occupy are plotted for different values of κ. The sentiment of an individual state in the figure is

defined as the time-average over all the simulation's steps $\overline{s_i} = \frac{\sum_{t=1}^{T} s_{it}}{T}$. The diagram is derived by running 1000 CK simulations with different seeds for a list of constant herding propensities in the interval $[0, 5]$. The impact of the price momentum on the switching probabilities for the noise traders is set to zero to decouple the noise trader class from other external factors of the market. The left figure describes the average sentiments for the different constant kappas, while the right figure describes their standard deviations. One can observe two different regimes, a disordered and an ordered regime, that are separated by a phase transition. The figure highlights the discontinuous phase transition at around $\kappa_{c,1st} \approx 3.3$, which is in accordance with the theoretical derivation of the first order phase transition and the associated bifurcation described in Ostilli and Mukhamedov [93]. In that regard, this extension with Potts model differs from the original model, which employs the Ising model and features a 2nd order continuous phase transition at $k_c = 1$.

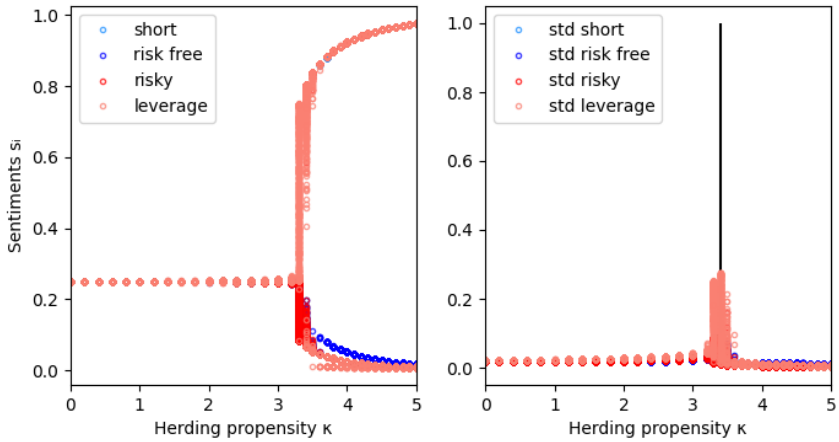

Figure 3.5: Time average and standard deviation of the sentiments s_i with $i \in \{s, rf, r, l\}$ for different constant $\kappa_t = cst$. The first order discontinuous phase transition between the disordered and order state is at $\kappa_{c,1st} \approx 3.30$ and in accordance with theoretical derivations.

Below the critical value $\kappa_{c,1st}$, there is a fixed point with a symmetric and equal distribution of the noise traders among the states with $s_i = \frac{1}{q} = 0.25$ or $N_i = \frac{N}{q}$, where N_i represents the number of noise traders in state i with $i \in \{s, rf, r, l\}$. This is also in accordance with the linear stability analysis done in Cividino [25].

Above the discontinuous phase transition, the noise traders polarize in one of the four possible states. Due to the number of simulations involved, most

of the points are overlapping which makes it more difficult to visualize all four different colors.

The discontinuous phase transition is the reason for the abrupt polarization of the noise traders in figure 3.4. This is also the most important drawback of the Potts model, because a continuous phase transition is needed to describe a continuous and more gradual polarization of the noise trader class towards one state. In addition, in the Potts model all states are directly connected. This implies that the transitions between the states are all equivalent. For instance, a trader can directly switch from the short position to the leverage position. This assumption is questioned in the following chapter.

In conclusion, the $q = 4$ state mean-field Potts model is inadequate to model realistic financial markets due to the nature of the phase transition.

3.2 O(n=4) model

Another possibility to extend the Ising model is to replace the scalar spin values with a vector quantity [25]. The Ising model then becomes the O(n) or n-vector model. In the O(n) or n-vector model, the spins are not represented by scalars but by n-dimensional vectors $\vec{s_i} = (s_{i1}, s_{i2}, ..., s_{in})$. The Hamiltonian for the fully connected O(n) model with an external magnetic field is given by

$$H_N\left(\left\{\vec{S}_1, \ldots, \vec{S}_N\right\}\right) = -\frac{J}{2N}\sum_{i,j=1}^{N}\vec{S}_i \cdot \vec{S}_j - \sum_{i=1}^{N}\vec{h}\cdot\vec{S}_i \tag{3.19}$$

where the spin is a n dimensional vector $\vec{S}_i = (s_{i1}, \ldots, s_{in}) \in \mathbb{S}^{n-1}$ with $||\vec{S}_i|| = 1$.

The transition probabilities to go from state $\vec{A}$ to $\vec{B}$ is given by

$$P(\vec{A} \to \vec{B}) = \frac{e^{\kappa_t}\left(\frac{\sum_i \vec{s}_i \cdot \vec{B}}{N} + \vec{H}\cdot\vec{B}\right)}{\int_{\vec{K}\in\mathbb{S}^{n-1}} e^{\kappa_t\left(\frac{\sum_i \vec{s}_i\cdot\vec{K}}{N} + \vec{H}\cdot\vec{K}\right)}} \tag{3.20}$$

While the O(n) model is useful for the extension to multiple risky assets, it is not as useful for the extension to allow for leverage and short selling. In the multi asset extensions the normalization of the spin vector $||\vec{S}_i|| = 1$ implies that only the total wealth can be invested. Introducing leverage and short selling to the O(n) model requires values for the individual components s_{ij} with $j \in \{1, ...n\}$ to take on q different states as in the Potts model. Therefore, the O(n) model can be a useful tool to model the leverage and short selling

for the multi-asset extension, but does not seem to be promising for the single risky asset case that is investigated in this thesis.

Chapter 4

Extension of original market model from a microscopic perspective

The previous chapter outlined the extension of the original market model using the Potts model and its limitation, which is the discontinuous 1st order phase transition that separates the ordered from the disordered regime. The discontinuous phase transition leads to abrupt polarization of the noise traders and to sharp peaks in the switching probabilities and price time series.

Therefore, this chapter shifts the focus from borrowing concepts from statistical physics to building an extension by formulating the microscopic interactions between the traders and then studying the macroscopic properties of the system. This microscopic perspective entails three steps. Firstly, the state space that the noise traders can occupy is defined. Secondly, the transition rates between the states have to be defined. Together, the state space and the transition rates define the microscopic behavior of the noise trader class. The third step consists of analysing the macroscopic properties that arise from the microscopic interactions of the noise traders.

The microscopic approach was already employed by Damiani [32] and Kopp [70] to extend the original market model to a multi asset case. Damiani [32] extends the market model by coupling different Ising models together at the risky asset as depicted for the three asset case in figure 4.1. The risk-free assets are treated as one asset. The noise traders can switch between the risky assets and also between the risk-free and risky assets. The approach to extend the model to multiple assets by Kopp [70] is depicted in figure 4.2. The Ising model describes the transition of the noise traders between a risky asset and a bond market that contains many bonds. A second mechanism is in place to model the decision of the noise traders once they have decided to invest in the bond market.

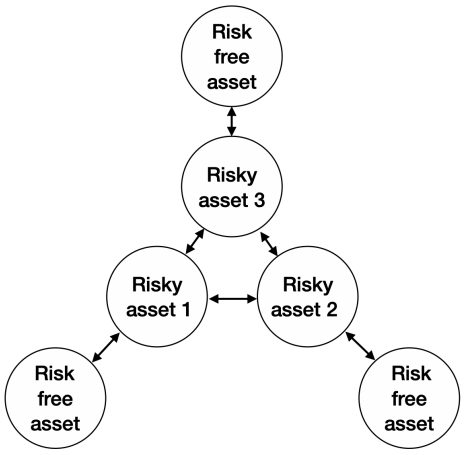

Figure 4.1: Coupled Ising model with 3 risky assets.

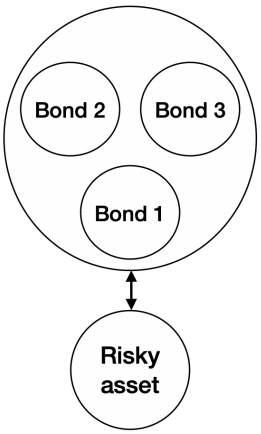

Figure 4.2: Coupled Ising model with risky asset and bond market.

The remainder of the chapter consists of defining the microscopic model of the noise trader by firstly defining the states and secondly the transition probabilities. Then three models that incorporate leverage and short selling differently are presented. For each model, there is a description of the time series and an explanation for the behaviour.

4.1 Definition of states

To include a leverage position and a short position besides the investment into the risk-free and risky asset requires at least four states, similar to the implementation of the Potts model in chapter 3. Therefore, as in the Potts model extension, each noise trader is represented by a spin and can occupy either the short, the risk-free, the risky or the leverage state $s_i \in s, rf, r, l$ and $i \in \{1, ...N\}$. The Potts model enables the noise traders to switch directly between all possible states, which means that the graph of the states is fully connected. This implies that the transitions between the states are all equivalent. For instance, a trader can directly switch from the short position to the leverage position.

However, the four states differ in the exposure to market risk. There is no exposure for the risk-free asset. The risky position and the leverage position are both long positions where the noise trader profits from a price increase, which implies a positive exposure. The risky position exposes the noise trader to risky asset once, while the leverage position exposes the noise trader to the risky asset twice. The short position implies a negative exposure to the market risk of the risky asset, because the noise traders profits from a price decrease. Furthermore, the short and the risk-free position are

associated with a pessimistic market sentiment and the risky and leverage position are associated with a optimistic market position. In general, the market sentiment reflects the attitude of the investors, which is based on a variety of factors [12, 13]. From a behavioural perspective, one can assume that traders first invest their own wealth before borrowing from another entity. Thus, a transition from $x_t^{n_i} = 0$ to $x_t^{n_i} = 2$ can be discarded. Hence, another approach to model the graph of states is to extend the original model by the leverage state on top of the risky state and by the short state below the risk-free state. This 'ladder' structure bears a resemblance to coupling two Ising models together and is visualized in figure 4.3. It is also conceivable to map the transition approach for the multi-asset extension by Kopp [70] onto the extension to include leverage and short selling. Here, the noise trader first decides to invest either into the risk-free asset or the stock market. If the stock market is chosen, a second choice is made to determine among the three alternatives of investing the total wealth into the risky asset, borrowing money to invest twice the amount into the risky asset or borrowing money so take a short position. A visualization of this process is given in figure 4.4.

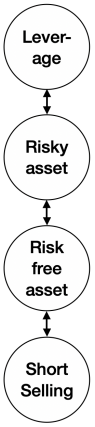

Figure 4.3: Ladder structure with leverage and short position.

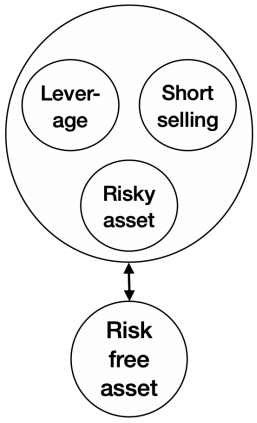

Figure 4.4: Coupled Ising model with stock market and risky asset.

To summarize, three different ways to connect the four different states (short, risk-free, risky and leveraged) are identified: the fully connected graph (figure 3.1), the ladder structure (figure 4.3), and the coupling of the risk-free asset with a market (figure 4.4). With the states defined, it is possible to describe the transition rates between the states.

4.2 Transition rates

The transition rates of the three structures (fully connected, ladder, stock market) can be visualized in a transition matrix or table. For instance, table 4.1 illustrates the allowed transition rates for the ladder structure in figure 4.3. The rows in table 4.1 describe the transition probabilities from state a to all other states. The probabilities of each row (each start state) have to sum up to one with $P_t(a \to a) + \sum_{b \neq a} P_t(a \to b) = 1$.

$P(a \to b)$	s	rf	r	l
s	$P(s \to s)$	$P(s \to rf)$	0	0
rf	$P(rf \to s)$	$P(rf \to rf)$	$P(rf \to r)$	0
r	0	$P(r \to rf)$	$P(r \to r)$	$P(r \to l)$
l	0	0	$P(l \to r)$	$P(l \to l)$

Table 4.1: Transition rates for the ladder structure with leverage and short position.

This section focuses on the features of the transition rates itself. The choices made with respect to the features are of central importance for the dynamics. The features to control are the structure of probabilities, the holding time, the social imitation, the price momentum and other parameters and the herding propensity.

The structure of probabilities describes how the probabilities are normalized and if they are linearized. The original market model with its Ising-like structure suggests to adopt linear switching probabilities which are normalized by the number of states that the traders can occupy (see equation 2.22). The Potts model employs non-linear switching probabilities and they are normalized by the sum of all switching probabilities (see equation 3.2). In addition, the switching probabilities in the original model by Kaizoji et al. [62] are symmetric with no bias $P_t^-(s_t, H_t) = P_t^+(-s_t, -H_t)$. In later extensions, a bias is introduced towards the risky asset [91].

The holding time is represented by the inverse of the probability to switch from state a to any other state for a zero herding propensity and given by $t_h = \frac{1}{1 - P_t(a \to a)|_{\kappa_t = 0}}$. In more general terms, the holding time t_h can be expressed in terms of two constants c and d, which was done in equations 3.6 and 3.7. The individual probabilities are given by $P_t(a \to a)|_{\kappa_t = 0} = \frac{c}{q}$ and $P_t(a \to b)|_{\kappa_t = 0} = \frac{d}{q}$. Usually, c is larger than one while d is smaller than one. The holding time can be the same for all states or can differ between states.

Furthermore, the inverse of the holding time, the constant switching probability $P_t(a \to b)|_{\kappa_t=0}$ can be symmetric, $P_t(a \to b)|_{\kappa_t=0} = P_t(b \to a)|_{\kappa_t=0}$ or asymmetric $P_t(a \to b)|_{\kappa_t=0} \neq P_t(b \to a)|_{\kappa_t=0}$. Asymmetric constant switching probabilities can be implemented to account for behavioral biases. For instance, the notion of risk aversion of prospect theory, which states that people react differently to potential losses compared to potential gains (Kahneman and Tversky [61]), can be accounted for by increasing the constant probabilities from riskier states to less risky states and vice versa, $P_t(r \to l)|_{\kappa_t=0} < P_t(l \to r)|_{\kappa_t=0}$ and $P_t(s \to rf)|_{\kappa_t=0} > P_t(rf \to s)|_{\kappa_t=0}$.

The social imitation represented by the sentiment can be modeled in a variety of ways if the noise trader can occupy more than two states. One can define a global parameter that is the same for all switching probabilities or multiple sentiments for individual switching probabilities. In the following, the different possible definitions are outlined and each definition is motivated and the advantages and disadvantages are highlighted.

The sentiment defined as a single global parameter is given by the form

$$s_t = \frac{N_l + N_r - N_{rf} - N_s}{N} \in [-1, 1], \tag{4.1}$$

where the states with a bullish market contribute positively and the states associated with a bearish market contribute negatively. This definition does not distinguish between investing the total wealth, which is done in the risky and risk free state, and investing twice the total wealth which is done in the leverage and short position. Therefore, the leverage and short position can be counted double to make a distinction $s_t = \frac{2N_l + N_r - N_{rf} - 2N_s}{N} \in [-2, 2]$. Nonetheless using one global parameter with a scalar value is only useful to distinguish two states.

Instead of one global sentiment one can define multiple sentiments. Borrowing from the Ising-like structure of the original model, one approach is to compare the two states involved in the transition probability $P_t(a \to b)$. For the ladder structure, this implies three different sentiments $s_t^{rf,s}$, $s_t^{r,rf}$ and $s_t^{l,r}$. Here, the more pessimistic market opinion is subtracted from the more optimistic one. The sentiments can be normalized by the involved states a and b or by the total number of traders. The two definitions yield

$$s_t^{a,b} = \frac{N_a - N_b}{N_a + N_b} \in [-1, 1], \tag{4.2}$$

with $s_t^{rf,s} = \frac{N_{rf} - N_s}{N_{rf} + N_s}$, $s_t^{r,rf} = \frac{N_r - N_{rf}}{N_r + N_{rf}}$ and $s_t^{l,r} = \frac{N_l - N_r}{N_l + N_r}$ and

$$s_t^{a,b} = \frac{N_a - N_b}{N} \in [-1, 1], \tag{4.3}$$

with $s_t^{rf,s} = \frac{N_{rf} - N_s}{N}$, $s_t^{r,rf} = \frac{N_r - N_{rf}}{N}$ and $s_t^{l,r} = \frac{N_l - N_r}{N}$.

From the perspective of the noise trader, the definitions imply that each trader compares herself with traders of similar sentiment. The definition in equation 4.2 produces more volatile and larger sentiments compared to the other definition in equation 4.3. Again, it would also be possible to weigh leverage and short sales twice to emphasize these two states. In both cases, the overall sentiment can be understood as a (pseudo) vector with three components $s_t = (s_t^{rf,s}, s_t^{r,rf}, s_t^{l,r})$. While the critical herding propensity for definition 4.2 is the same as the original market model $\kappa_c = 1$, the critical herding propensity for definition 4.3 is larger than one and has to be determined numerically $\kappa_c > 1$. Furthermore, if the states are not organized in a ladder structure but for instance are fully connected, there are $\frac{q(q-1)}{2}$ sentiments for q states.

Another way is to compare one state to all the other states. This can be done in absolute terms

$$s_t^a = \frac{N_a - \sum_{b \neq a} N_b}{N_a + \sum_{b \neq a} N_b} \in [-1, 1], \tag{4.4}$$

with for instance sentiment for leverage being calculated as $s_t^l = \frac{N_l - N_s - N_{rf} - N_r}{N_s + N_{rf} + N_r + N_l}$. The state in question can also be weighed by the number of other states $(q-1)$

$$s_t^a = \frac{(q-1)N_a - \sum_{b \neq a} N_b}{(q-1)N_a + \sum_{b \neq a} N_b} \in [-1, 1], \tag{4.5}$$

with for instance sentiment for leverage being calculated as $s_t^l = \frac{3N_l - N_s - N_{rf} - N_r}{3N_s + N_{rf} + N_r + N_l}$. The definition in equation 4.4 has the disadvantage that most of the sentiment values are small and negative. In addition, when the switching probabilities depend on a and b and not only on a, there are only three sentiments required for four states. Therefore, one could compare again the adjacent sentiments, which yields the definitions of equation 4.2 or 4.3.

Finally, there is the possibility to adopt the sentiment used by the mean field Potts model, where each transition probability depends on the sentiment of the final state and is not compared to any other state. The sentiments are given by

$$s_t^b = \frac{N_b}{N} \in [0, 1], \tag{4.6}$$

with $b \in \{s, rf, r, l\}$. Alternatively, the denominator N can be replaced by the two states that the switching probability connects. These sentiments do only range from zero to one.

The price momentum factor is the second factor besides social imitation that is controlled by the herding propensity. Like the sentiment it can also be modeled in a variety of ways if the noise trader can occupy more than two states. The original market model only defines one price momentum factor, which is represented by the external magnetic field H_t in the Ising model (see eq. 2.29). In contrast, there are q external fields H_t^k with $k \in \{1, ...q\}$ in the generalized Potts model (see eq. 3.1).

The associations of the price momenta with the individual states are summarized in table 4.2. Being invested in the risk-free asset is associated with zero risk as the invested wealth is only subject to the risk-free rate r_f. The price momentum factor of the risky asset is the same as the factor in the Ising model. Being invested twice in the risky asset exposes the noise trader to twice the price momentum. The short selling position is associated with the price momentum but opposite sign.

Leverage	$2H_t - r_f$
Risky	H_t
Risk-free	r_f
Short	$-H_t + r_f$

Table 4.2: Definitions of momentum factors for each state.

In general, the traders are exposed to different price momenta depending on the state they are in. However, the choice of the definition of the price momentum factors depends also on the structure of the transition probabilities. As for the sentiment, one can also either compare the price momenta of the states involved in the transition probability $P_t(a \to b)$ or just focus on the price momentum of the final state b.

Comparing the initial and final state yields

$$H_t^{a,b} = H_t^b - H_t^a, \tag{4.7}$$

while focusing on the final state reduces the price momenta to

$$H_t^b. \tag{4.8}$$

In addition, the noise traders do not consider the risk-free rate in their decision about debt, which can be deemed unrealistic. The risk-free rate can be interpreted as the opportunity cost of being in the other states. This is not considered in the original market model, where the noise traders only consider H_t and not r_f in their decision about debt. However, the risk-free rate is usually a fairly small and constant value and adjusting for it does not make a significant difference.

Besides the social imitation and the momentum factor, there are other potential factors that can be incorporated into the model. The transition rates of the noise trader class to the leverage and short selling position is likely to include some form of procyclicality. Therefore, other information and signals generated by the model can be incorporated by the noise trader class to make their buying and selling decisions. A literature search on additional trading signals or other parameters that could influence the switching probabilities yielded two more factors: the price acceleration $\Gamma_{t,f}$ and the trading volume $V_{t,f}$.

The price acceleration $\Gamma_{t,f}$ is defined as the first difference of returns $\Gamma_{t,f} = H_t - H_f$ where t is the current period and f a previous period, for instance $f = t - 1$. Ardila-Alvareza, Forroa and Sornette [7] indicate that the price acceleration reflects the presence of transient positive feedback loops that impact the price formation process. The original market model by Kaizoji et al. [62] is an example of a model, where positive price acceleration leads to super-exponential bubble growth. From the perspective of an individual noise trader, the incorporation of the price acceleration can be justified with the habituation or desensitization phenomena. Habituation or desensitization is defined as the decrease in a response to a constant stimulus (Rankin et al. [97]). The price acceleration represents the change of the price momentum and can create a newly perceived stimulus that can trigger the noise traders to change their behaviour. This means that the Γ-effect can represent the breakdown of the status-quo (Samuelson and Zeckhauser [104], Kahneman et al. [60]). More concretely, when deciding to switch from the risky to the leverage position or from the risk-free to the short position, the acceleration can represent an additional stimulus besides momentum that pushes the noise traders to deviate from the status quo and compensates for the increase in risk associated with the leverage or short position. Therefore, the price acceleration is a valid candidate to be incorporated as a factor that determines the switching probabilities.

The trading volume $V_{t,f}$ is investigated from many different perspectives in the literature. There are several studies that associate bubbles with high trading volume [106, 52, 105]. Kim and Verrecchia link volume to the dispersion of beliefs with regards to public information [65] and Blume et al. [15] to the quality of information. According to Blume et al. [15] traders can use volume in their technical analysis to improve their trading strategy.

Due to the potential to differentiate the leverage and short state from the risk-free and risky state, there were several attempts to incorporate the price acceleration and the trading volume as factors into the transition probabilities. However, preliminary implementations did not provide the desired results. Before utilizing the factors in the a model extension, these factors have to be tested rigorously and in more detail in the original market model. This can provide a thesis topic in its own right (see chapter 5).

The section on the transition rates can be summarized by equation 4.9, which shows the modeling decisions required for the extension to four states:

$$P_t^{a\to b} = P_t^{a\to b}\left(P^{a\to b}, \kappa_t, s_t^{a,b}, H_t^{a,b}, \Gamma_{t,f}^{a,b}, V_{t,f}^{a,b}\right). \tag{4.9}$$

$P_t^{a\to b}$ is the transition probability of a noise trader to switch from state a to state b. $P^{a\to b}$ is the associated constant transition probability. κ_t is the herding propensity. $s_t^{a,b}$ is the sentiment. $H_t^{a,b}$ the price momentum factor, $\Gamma_{t,f}^{a,b}$ the price acceleration and $V_{t,f}^{a,b}$ the trading volume over the time horizon f.

After highlighting the choices that have to be made for the definition of states and the transition rates, three implementations are discussed in the following sections in more detail, namely the ladder model, the three coupled Ising models and the coupled Ising Potts model.

4.3 Ladder model

The ladder model bears the most resemblance to the original market model. The risk-free and the risky state for the noise trader is complemented by the leverage and short position as visualized in figure 4.3, where the leverage position is only connected to the risky state and the short position is only connected to the risk-free state, which is also the example in table 4.1. The model assumes that the noise traders first invest their own wealth before borrowing from another entity. Thus, a transition from the risk-free state to the leverage state is discarded ($x_{t-1}^{n_i} = 0 \nrightarrow x_t^{n_i} = 2$). The restriction to the ladder structure ensures that noise traders leverage more when they are in a transient regime with more wealth during bubbles. During a bubble, a larger fraction of noise traders is invested in the risky asset. The noise

traders switch from the risky asset to the leverage state ($x_{t-1}^{n_i} = 1 \leftrightarrow x_t^{n_i} = 2$) with probability $P_t^{r\to l}$. Hence the number of trades in the leverage state depends on the number of traders with $x_{t-1}^{n_i} = 1$. In addition, the size of the leverage position depends on the amount of their total wealth, because the risky fractions are defined as a fraction of total wealth. A similar reasoning applies to the short position.

The switching probabilities are linear and normalized by $\frac{1}{2}$ and are presented in the following equations

$$\begin{aligned}
P_t^{r\to l} &= \frac{P^{r\to l}}{2}\left(1+\kappa_t\left(s_t^{l,r}+H_t^{l,r}\right)\right)\\
P_t^{l\to r} &= \frac{P^{l\to r}}{2}\left(1-\kappa_t\left(s_t^{l,r}+H_t^{l,r}\right)\right)\\
P_t^{rf\to r} &= \frac{P^{rf\to r}}{2}\left(1+\kappa_t\left(s_t^{l,r}+H_t^{l,r}\right)\right)\\
P_t^{r\to rf} &= \frac{P^{r\to rf}}{2}\left(1-\kappa_t\left(s_t^{l,r}+H_t^{l,r}\right)\right)\\
P_t^{s\to rf} &= \frac{P^{s\to rf}}{2}\left(1+\kappa_t\left(s_t^{l,r}+H_t^{r,s}\right)\right)\\
P_t^{rf\to s} &= \frac{P^{rf\to s}}{2}\left(1-\kappa_t\left(s_t^{l,r}+H_t^{r,s}\right)\right)
\end{aligned} \tag{4.10}$$

The constant switching probabilities are assumed to be symmetric $P^{a\to b} = P^{b\to b}$. The sentiments are defined as a comparison of the two respective states and dividing by their sum with $s_t^{rf,s} = \frac{N_{rf}-N_s}{N_{rf}+N_s}$, $s_t^{r,rf} = \frac{N_r-N_{rf}}{N_r+N_{rf}}$ and $s_t^{l,r} = \frac{N_l-N_r}{N_l+N_r}$. The price momentum factors are defined as

$$H_t^{l,r} = H_t^{r,s} = 2H_t - r_f \tag{4.11}$$

$$H_t^{r,rf} = H_t - r_f \tag{4.12}$$

The definition of the risky fraction reflects the values for the polarization of noise traders to the risky asset ($x_t^n = 1$) and the risk-free asset ($x_t^n = 0$) of the original market model and adds the polarization to the leverage ($x_t^n = 2$) and short position ($x_t^n = -1$). The risky fraction is given by

$$x_t^n = \frac{2N_l + N_r - N_s}{N} \in [-1, 2]. \tag{4.13}$$

The asset and the wealth dynamics, the fundamentalist trader class and the market clearing are defined as in chapter 2.

4.3.1 Simulation and time series

In this section, the parameter set used for the simulations is introduced and the time series are discussed.

The parameter set is summarized in table 4.3. The assets, the fundamentalist trader, the herding propensity and the associated OU stochastic process are initialized with the same values as in the original model. Only the noise trader class parameter values are adjusted.

The noise traders are initialized with equal distribution amongst the four states $N_a = 250$ for $a \in \{s, rf, r, l\}$. The constant switching probabilities are set to $P^{a\to b} = 0.2$ for $a, b \in \{s, rf, r, l\}$, which implies an average holding time of $t_h = 10$.

Parameter set		
Assets	$r_f = 4 \times 10^{-5}$	$r_d = 1.6 \times 10^{-4}$
	$P_0 = 1$	$d_0 = 1.6 \times 10^{-4}$
		$\sigma_d = 1.6 \times 10^{-5}$
Fundamentalist	$W_0^f = 10^9$	$E_r = 1.6 \times 10^{-4}$
traders	$\sigma_r^f = 0.02$	$x_0^f = 0.3$
Noise	$W_0^n = 10^9$	$N_n = 1000$
traders	$\theta = 0.95$	$H_0 = 1.6 \times 10^{-4}$
	$P^{a\to b} = 0.2$	$N_a = 250$
	$x_0^n = 0.5$	
Herding	$\kappa_0 = \mu_\kappa$	$\mu_\kappa = 0.98\kappa_c = 0.98$
propensity	$\eta_\kappa \approx 0.11$	$\sigma_\kappa \approx 0.01$

Table 4.3: Parameters for simulating the three coupled Ising models with parameters $a, b \in \{s, rf, r, l\}$.

The time series are presented for two different simulations, as in the previous chapters. The first simulation is run with the constant herding propensity (CK) and displayed in figure 4.6. The second is done with the OU stochastic process.

The critical value of the OU is the same as for the original market model $\kappa_c = 1$, which is verified in the figure 4.5. The diagram shows a plot of sentiments on the y-axis and kappa on the x-axis. Each sentiment is calculated as the absolute average for a specific constant kappa. Then the sentiment is averaged over a 1000 different seed values leading to the following equation

$$s^{i,j}|_\kappa = \sum_{seeds} \frac{\sum_{t=1}^{T} |s_t^{i,j}|}{T} \text{with } i,j \in \{s, rf, r, l\}. \tag{4.14}$$

The absolute average values are calculated for $s_t^{rf,s}, s_t^{r,rf}, s_t^{l,r}$ with constant kappas in the interval of $[0, 2]$. The plot confirms the phase transition between order and disorder of the ladder model at $k_c = 1$.

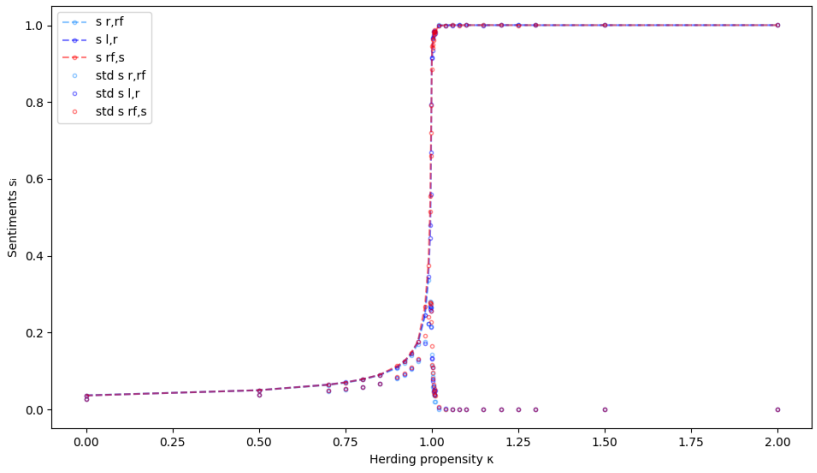

Figure 4.5: Sentiment kappa plot of the ladder model confirming the critical value $\kappa_c = 1.0$. The sentiments $s^{rf,s}$ (red), $s^{r,rf}$ (light blue) and $s^{l,r}$ (blue) and their standard deviations are plotted on the y-axis for different constant kappas on the x-axis.

The first simulation with the constant herding propensity (CK) is presented in figure 4.6. The price time series in the first row fluctuates around the linear upward price trajectory corresponding to the dividend payments. The price returns fluctuate in the interval $[-0.05, 0.05]$, which is similar to the fluctuations of the original market model in absolute values. The next three rows describe the noise trader behaviour in more detail. The noise trader switching probabilities in the fifth row mirror their respective counterpart (e.g. $P_t^{r,rf} \leftrightarrow P_t^{rf,r}$), which is to be expected by the structure of switching probabilities (see eq. 4.10). Their absolute values are also in the range of the original market models switching probabilities. In addition, an increase in the price is accompanied by a switch from more pessimistic states (short and risk-free) to more optimistic states (leverage and risky). The risky fractions in row six show the opposing behaviour of noise traders and fundamentalists. The wealth ratio in row seven slightly decreases over the duration of

the simulation, which implies that the noise trader looses wealth compared to the fundamentalist.

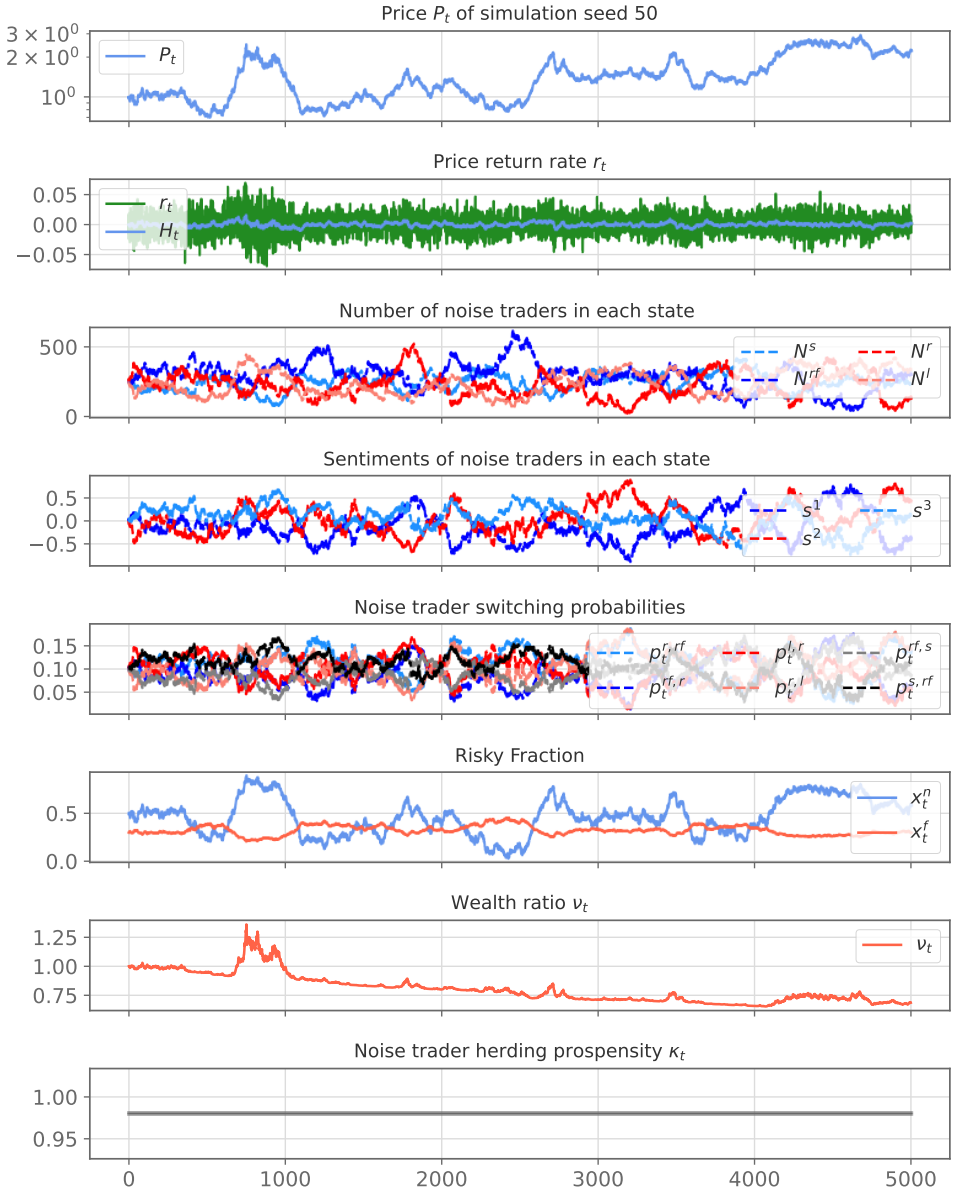

Figure 4.6: Simulation of ladder model with CK herding propensity. The herding propensity is set to $\kappa_t = 0.98\kappa_c = 0.98$, which is below the critical value $\kappa_c = 1.0$.

The second simulation with the OU herding propensity is presented in fig-

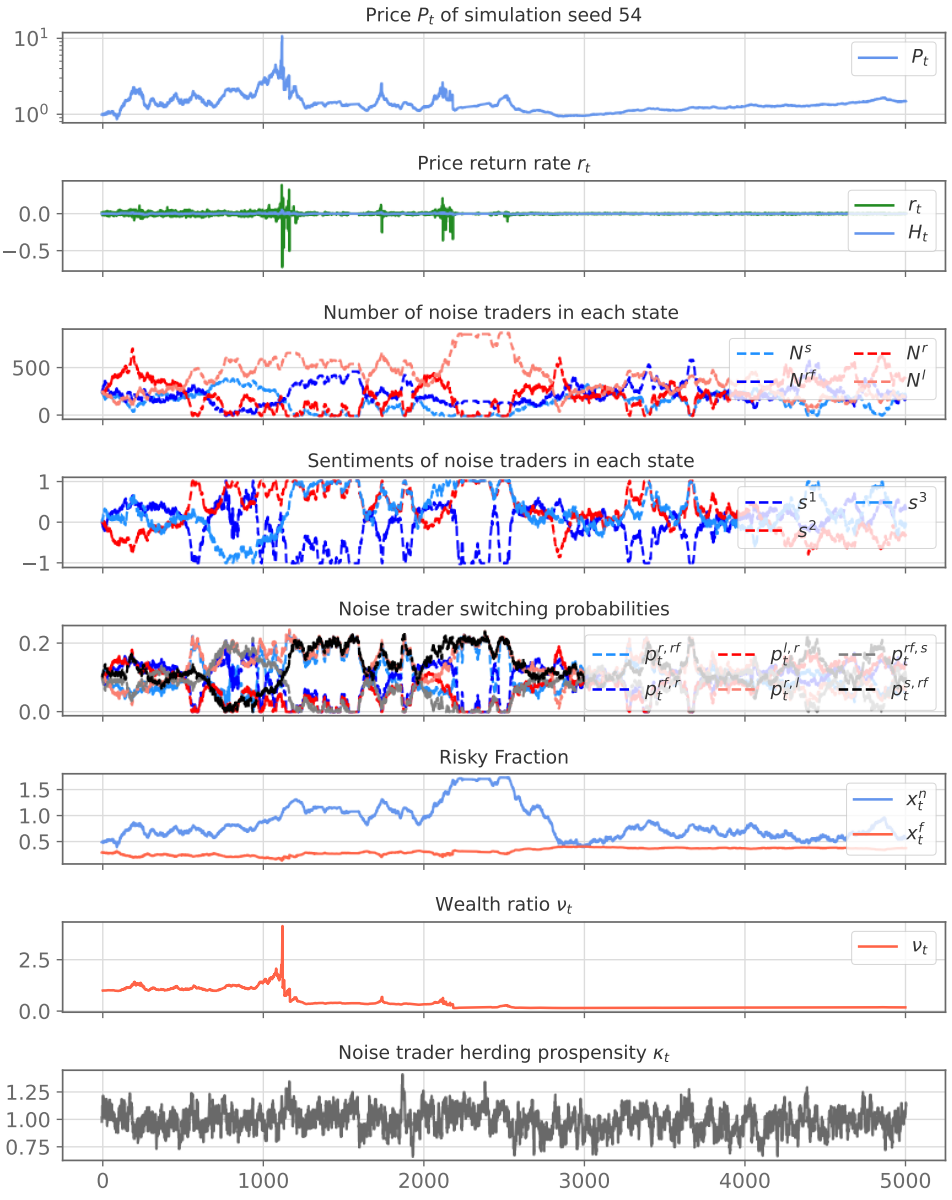

Figure 4.7: Simulation of ladder model with OU stochastic process for the herding propensity with $\mu_\kappa = 0.98$.

ure 4.7. As expected, the OU simulation exhibits more polarizations of the noise trader class compared to the CK simulation, which is reflected in the more volatile sentiments and switching probabilities. The simulation is characterized by a steep price peak at $T \approx 1100$. Before the peak, the simulation shows a behaviour similar to the CK simulation. At around $T \approx 600$, the

noise traders start to polarize towards the risky asset. The resulting price increase results in a sharp price bubble, which immediately bursts. Smaller bubbles with associated crashes can be observed around $T \approx 1700$, $T \approx 2100$ and $T \approx 2500$. The noise traders suffer significant losses and at each crash. Their wealth decreases considerably relative to the fundamentalists. The wealth development of the noise trader and the fundamentalist class in absolute terms is shown in figure 4.8.

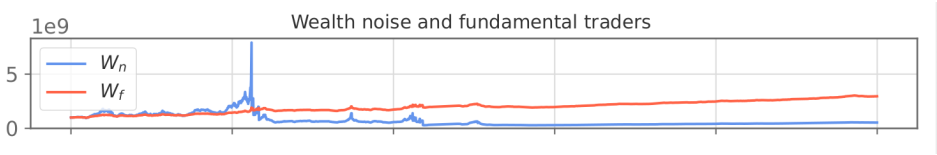

Figure 4.8: Development of absolute wealth of noise traders W_t^n and fundamentalists for simulation of ladder model with OU stochastic process for the herding propensity with $\mu_\kappa = 0.98$.

Because the fundamentalists tend to sell the risky asset when the price increases quickly, their wealth development is largely unaffected by the bubbles and crashes in the simulation. In contrast, figure 4.8 highlights that the noise traders' wealth not only decreases relatively to the fundamentalists but also in absolute terms. Contrary to the original market model, the noise traders struggle to recover from the initial (at around $T \approx 1700$) and the subsequent crashes.

The impact of the two trader classes on the risky asset price depends on their respective wealth W_t^n and W_t^f, which is given in relative terms by $\nu_t = \frac{W_t^n}{W_t^f}$. A large value for ν_t indicates that the noise trader class has a large influence on the price dynamics while a small value indicates that the fundamentalists have a large influence on the price dynamics. Hence, after the crash at $T \approx 1100$, the market is determined by fundamentalists, which materialises in the steady increase of the price, roughly proportional to the dividend growth. Although, the total number of traders in the model is fixed (1000 noise traders and 1000 fundamentalists), the decrease in wealth of the noise traders would be equivalent to the some noise traders "exiting" from a real financial market. After $T \approx 1100$ a large portion of the noise traders have exited, which reduces their impact on the price dynamics visibly and explains the smaller peaks later on. After $T \approx 2500$ the noise traders have no more meaningful impact on the price dynamics. This explains the small price fluctuations around the long term price trend, which is given by the dividend growth factor.

OU simulations over longer periods of time, namely $T = 50000$ and $T = 100000$, reveal that the noise traders are able to increase their wealth in ab-

solute terms after a large crash. However, the fundamentalists consistently outperform the noise traders in the long run and thus the relative wealth of noise traders to the fundamentalists tends to decrease.

The strong influence up to $T \approx 1200$, a fading influence between $T \approx 1200$ and $T \approx 2500$ and virtually no impact after $T \approx 2500$ of the noise traders provides an explanation for why the price is non stationary. A visual inspection and comparison of different intervals of the price time series and the return time series indicates the non stationary nature of the price process. Comparing the original market model simulation with the ladder model, the severity of the losses of the noise traders in the ladder model simulation and their inability to recover to the same degree of wealth as in the original market model may be attributed to their opportunity to take leverage.

Therefore, the following interpretation is formulated. The opportunity to leverage in the ladder model can lead to more severe crashes, which is reflected by the decrease in wealth of the noise traders who are unable to recover from the severity of their losses. The exit of the noise traders from the system is mirrored in the non stationary price and return processes. The exit of the noise traders hints at a key limitation of the ladder model. Both the original market model and the ladder model extension do not account for an intervention by a central bank or by a government. However, real world financial crisis usually incite the intervention of a central bank, which can increase or decrease the interest or use unconventional monetary policies, or of the government, which can use stimulus packages and bail outs [87]. In another application of the market model, Westphal and Sornette [121] demonstrate the usefulness of direct market intervention by a policy maker.

A cautionary tale of an indecisive government response to a financial crisis is found in the Great Depression of 1929. While the Great Depression is not attributed to a single cause or event, the prolonged duration of the Depression termed the Great Contraction by Keynes [42], is in part attributed to a tight monetary policy and a hesitant governmental response [100, 110]. The Great Depression had a large influence on handling subsequent crisis. Roughly eighty years later, the financial crisis of 2008 sparked a number of interventions by central banks and governments around the world. Many governments bailed out financial institutions and employed fiscal stimulus packages that included an increase in government spending and tax cuts as immediate responses [87].

In context of the ladder model, government bailouts and active market interventions would function as mechanisms to reboot the system. More concretely, in the OU simulation of the ladder model, the decrease in wealth of the noise traders and the associated decrease in impact on the market indicates the need for an intervention that restores the wealth of the noise

traders to pre-crisis heights to ensure their continued impact on the price dynamics.

The necessity to incorporate a reboot mechanism in the model hints at a larger question, namely if the model and financial systems in general are intrinsically unstable and require at times a reboot. This notion was formed amongst others by Hyman Minsky in his „Financial Instability Hypothesis“, which gained interest by the public and scholars alike after the financial crisis of 2008.

With his hypothesis, Minsky provides an explanation for an inherently unstable financial system and reasons for its susceptibility to bubbles and crashes. Minsky differentiates between three types of financing: hedge financing, speculative financing and Ponzi financing. Hedge financing implies that the borrowers can cover the interest and principal using the cash flow from their investments. Speculative financing implies that the borrowers can cover the interest using the cash flow from their investments but need to re-borrow to cover the principal. Ponzi financing requires an appreciation of the asset value to refinance the debt. Financial markets and the economy in general are stable if the majority of firms and individuals employ hedge financing. If the majority of the private sector shifts towards speculative or even Ponzi financing, financial markets and the economy become more fragile and a drop in asset prices or another external shock can cause a crash. According to Minsky, financial market go through cycles where periods of stability are succeeded by periods of fragility depending on the prevalent financing type of firms and individuals. The prevalent financing type depends on expectations of firms and individuals. During periods of prolonged economic prosperity, profits and income increase, which makes debt more serviceable. As a response, lending criteria are relaxed and the credit supply is increased, which results in a credit boom. More participants shift from hedge financing to speculative or Ponzi financing in order to generate higher returns. The credit boom propels the growth of asset prices. Hence, periods of economic prosperity and stability can create financial fragility. In summary, Minsky uses the accumulation of debt and the irrational expectations and pro-cyclical behaviours of borrowers and lenders to explain the inherent instability of financial markets [86, 67, 85].

Due to the focus of Minsky's work on the role of financial markets, debt and the irrationality of the market participants, it provides a useful context for the interpretation of the ladder model. One important implication of the financial instability hypothesis is the role of the government and the central bank to reduce financial instability. In his view, the governments task is to control exuberance and excessive speculation by regulation and intervention. The central bank is required to act as a lender of last resort [86, 67]. While Minsky's views are not without criticism, the ladder model highlights the

potential consequences of a lack of government intervention and the dangers of credit accumulation. Minsky work and the ladder model provide a direction for further research, which is outlined in the final chapter.

4.3.2 Stylized facts

The following section describes the stylized facts, volatility clustering and fat tails, for the ladder model.

The volatility clustering is visualized in figures 4.9 and 4.10, which show the ACF for the signed (blue) and absolute (red) returns for the CK simulation (figure 4.9) and the OU kappa simulation (figure 4.10).

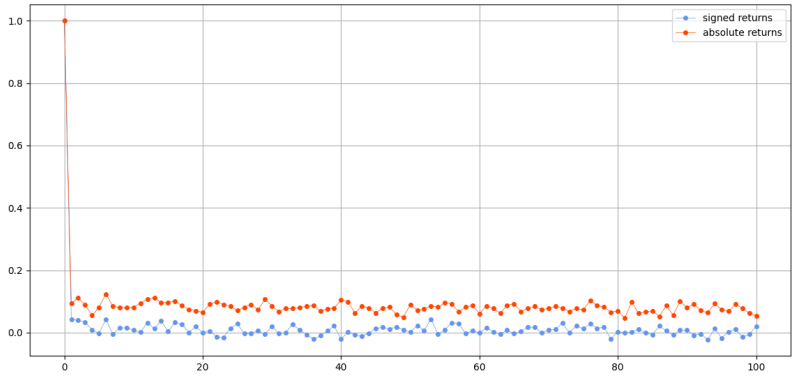

Figure 4.9: ACF for singed (blue) and absolute (red) returns for simulation with constant kappa (CK).

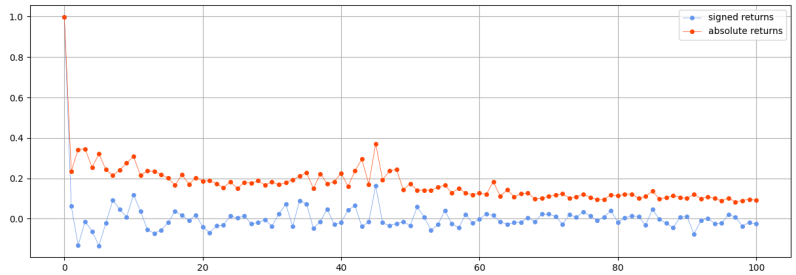

Figure 4.10: ACF for singed (blue) and absolute (red) returns with OU kappa.

The ACF for the CK simulation in figure 4.9 decays quickly to zero for increasing lags l for the signed returns. The absolute returns do not decay to zero but oscillate around $AFC(l)_{absolute} \approx 0.1$. This marks a difference to the original market model, where both the singed and absolute returns are approximately zero for $l > 0$ (see figure 2.4).

The ACF of the signed returns for the OU simulation in figure 4.10 decreases

quickly to zero. However, the fluctuations around zero are more pronounced when compared to the signed returns for the OU simulation of the original market model in figure 2.5. The absolute values of the returns have an autocorrelation function with longer memory. Compared to the original market model and the corresponding absolute returns for the OU simulation in figure 2.5 the ACF exhibits larger fluctuations.

The fat tail distribution of returns for the CK simulation is presented in figure 4.11 and for the OU simulation in figure 4.12. As highlighted in chapter 2 the empirical fat-tail decay of the distribution is characterized by the exponent $-1-\alpha$ with $\alpha \in [2,4]$. The parameter is $\alpha \approx 4.18$ for the CK simulation and $\alpha \approx 0.58$ for the OU kappa simulation. This implies that both simulations do not fall within the required range of the parameter. This conclusion is not surprising, because the bubbles and crashes in the OU simulation are generated by the herding of the noise trader class, which has, as highlighted in the previous section, an insignificant impact on the price dynamics after $T \approx 1200$.

In summary, the ladder model exhibits many similarities to the original market model. The critical herding propensity is the same for the original and the ladder model. For a constant kappa below the critical value, the ladder model display a comparable behaviour to the original model. Nonetheless, the ACF and a visual inspection of the simulation results indicated an increase in volatility. The differences are more pronounced when employing the OU process. The noise traders polarize rapidly, which results in singular price peak after which they have an insignificant impact on the market.

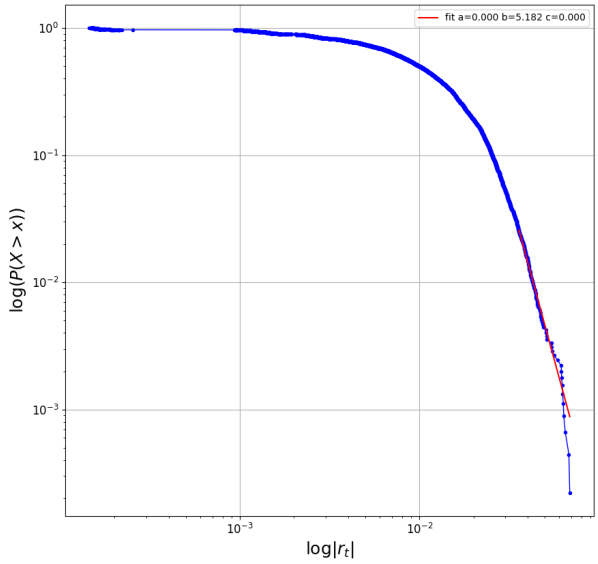

Figure 4.11: Log-log plot of the cumulative distribution function (CDF) of returns for the CK simulation with $\alpha \approx 4.18$.

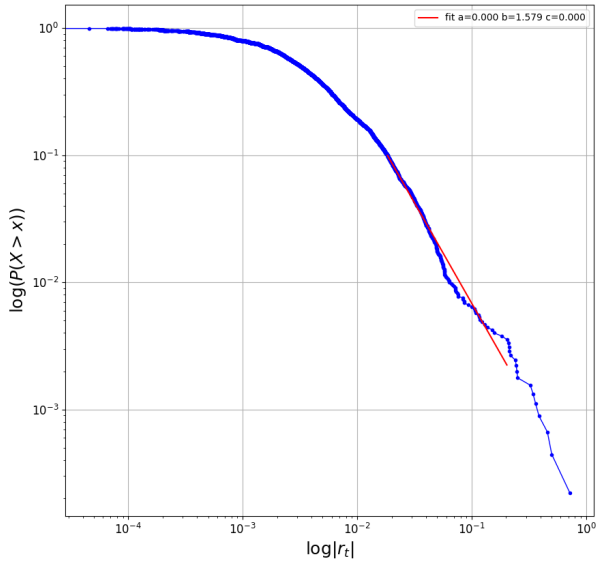

Figure 4.12: Log-log plot of the cumulative distribution function (CDF) of returns for the OU kappa simulation with $\alpha \approx 0.58$.

4.4 Three coupled Ising models

The second model that is investigated consists of three coupled Ising models. The coupling is visualized in figure 4.13 and bears a resemblance to the approach by Damiani [32] visualized in figure 4.1. The first Ising model connects the so-called optimists with the pessimists. The optimists are noise traders that are either invested in the risky or the leveraged position while the pessimists are defined as the noise traders that are invested in either the risk-free asset or the short position. The second Ising model consists of the noise traders in the risky and leverage state. The third Ising model links the risk-free with the short state. Therefore, one can define the following equations:

$$\begin{aligned} N &= N_o + N_p \\ N_o &= N_r + N_l \\ N_p &= N_s + N_{rf}. \end{aligned} \tag{4.15}$$

The total number of noise trader is the sum of the number of optimists N_o and pessimists N_p. The number of optimists equals the sum of noise traders in the leveraged (N_l) and risky state (N_l). The number of pessimists equals the sum of noise traders in the risk-free (N_{rf}) and short (N_s) state.

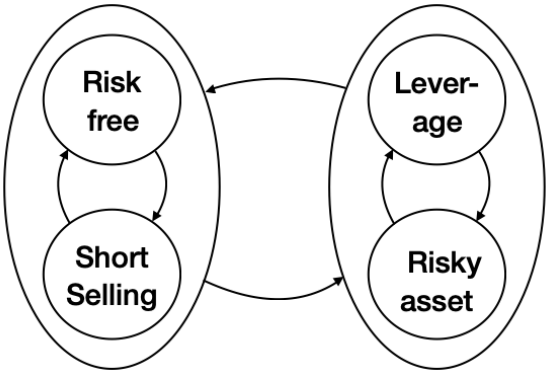

Figure 4.13: Three coupled Ising models.

The investment decision process for the noise trader is structured in three steps. In the first step, the noise traders are allocated to either the optimistic or the pessimistic state of the first Ising model according to the switching probabilities $P_t^{p\to o}$ and $P_t^{o\to p}$. In the second step, the number of traders in the optimistic state of the current period N_o^t are distributed to the risky state and the leverage state according to the distribution of the previous period. This implies

$$N_l^t = x_{t-1}^{l,r} \cdot N_o^t \tag{4.16}$$

$$N_r^t = N_o^t - N_l^t. \tag{4.17}$$

The number of traders in the pessimistic state N_p is treated analogously, which results in the following equations:

$$N_{rf}^t = x_{t-1}^{rf,s} \cdot N_p^t \tag{4.18}$$

$$N_s^t = N_p^t - N_{rf}^t. \tag{4.19}$$

In the third step, the noise traders switch between the risky and leverage state in the second Ising model and between the risk-free and short state in the third Ising model. Essentially, each state of the overarching Ising model that governs the transitions between optimists and pessimists consists of its own Ising model. Hence, the total number of traders in the first model is conserved $N = N_o + N_p$. This is not the case for the second and third Ising model.

The switching probabilities for the first Ising model distinguishing between optimists and pessimists are given by

$$\begin{aligned} P_t^{p\to o} &= \frac{P^{p\to o}}{2}\left(1 + \kappa_t\left(s_t^{o,p} + H_t^{o,p}\right)\right) \\ P_t^{o\to p} &= \frac{P^{o\to p}}{2}\left(1 - \kappa_t\left(s_t^{o,p} + H_t^{o,p}\right)\right) \end{aligned} \tag{4.20}$$

with $s_t^{o,p} = \frac{N_o - N_p}{N_o + N_p}$ and $H_t^{o,p} = H_t$.

The switching probabilities for the second Ising model consisting of the leverage and risky state are given by

$$\begin{aligned} P_t^{r\to l} &= \frac{P^{r\to l}}{2}\left(1 + \kappa_t\left(s_t^{r,l} + H_t^{r,l}\right)\right) \\ P_t^{l\to r} &= \frac{P^{l\to r}}{2}\left(1 - \kappa_t\left(s_t^{l,r} + H_t^{l,r}\right)\right) \end{aligned} \tag{4.21}$$

with $s_t^{l,r} = \frac{N_l - N_r}{N_l + N_r}$ and $H_t^{l,r} = 2H_t - r_f$.

The switching probabilities for the third Ising model consisting of the risk-free and short state are given by

$$\begin{aligned} P_t^{s\to rf} &= \frac{P^{s\to rf}}{2}\left(1+\kappa_t\left(s_t^{rf,s}+H_t^{rf,s}\right)\right) \\ P_t^{rf\to s} &= \frac{P^{rf\to s}}{2}\left(1-\kappa_t\left(s_t^{rf,s}+H_t^{rf,s}\right)\right) \end{aligned} \tag{4.22}$$

with $s_t^{rf,s} = \frac{N_rf - N_s}{N_rf + N_s}$ and $H_t^{rf,s} = 2H_t - r_f$.

The risky fractions are given by

$$\begin{aligned} x_t^{o,p} &= \frac{N_o}{N} \\ x_t^{l,r} &= \frac{N_l}{N_l + N_r} \\ x_t^{rf,s} &= \frac{N_{rf}}{N_{rf} + N_s} \end{aligned} \tag{4.23}$$

where in general $s_t^{a,b} = 2x_t^{a,b} - 1$ for $a, b \in \{o, p, s, rf, r, l\}$. At each time step, first the number of optimists and pessimists are determined. Then the number of traders that switch between the short and the risk-free position as the fractions of the pessimists are determined and the number of traders that switch between the risky and leverage position as the fractions of the optimists are determined. After outlining the model, the next section contains the numerical simulation.

4.4.1 Simulation and time series

In this section, the parameter set used for the simulations is introduced and the time series are discussed.

The parameter set is summarized in table 4.4. The assets, the fundamentalist trader, the herding propensity and the associated OU stochastic process are initialized with the same values as in the original model. Only the noise trader class parameter values are adjusted.

The time series are presented for two different simulations. The first simulation is run with the constant herding propensity (CK) and displayed in figure 4.15. The second is done with the OU stochastic process and visualized in figure 4.16.

Parameter set		
Assets	$r_f = 4 \times 10^{-5}$	$r_d = 1.6 \times 10^{-4}$
	$P_0 = 1$	$d_0 = 1.6 \times 10^{-4}$
		$\sigma_d = 1.6 \times 10^{-5}$
Fundamentalist	$W_0^f = 10^9$	$E_r = 1.6 \times 10^{-4}$
traders	$\sigma_r^f = 0.02$	$x_0^f = 0.3$
Noise	$W_0^n = 10^9$	$N_n = 1000$
traders	$\theta = 0.95$	$H_0 = 1.6 \times 10^{-4}$
	$P^{a \to b} = 0.2$	$N_a = 250$
	$x_0^n = 0.5$	
Herding	$\kappa_0 = \mu_\kappa$	$\mu_\kappa = 0.98\kappa_c$
propensity	$\eta_\kappa \approx 0.11$	$\sigma_\kappa \approx 0.16$

Table 4.4: Parameters for simulating the three coupled Ising models with parameters $a, b \in \{s, rf, r, l\}$.

Since the model consists of three coupled Ising models, the critical value of the OU process is the same for each of the three models and the same as in the original market model. The value of $k_c = 1$ is verified in the figure 4.14. The calculation of the average absolute sentiments is done analogously to the ladder model (see 4.14).

The price time series of the CK simulation output in figure 4.15 displays the characteristic fluctuations around the upwards price trend known from the original market model simulation with the CK in figure 2.2. This is also confirmed by the price return rate in the second row. The noise trader class is described in row three to five. The three Ising models that characterize the behaviour of the noise trader class are color coded. Grey and black describe the Ising model that distinguishes between optimists and pessimists. Red and orange is associated with the Ising model of the optimist state and describes the leverage and risky state. Dark and light blue depict the Ising model of the pessimists consisting of the short and risk-free state.

The number of noise traders in each state are described in row three. As expected from the symmetry of the switching probabilities in equation 4.20, the optimists and pessimists mirror one another around the equal distribution $N_o = N_p = 500$. In addition, the number of noise traders in the short state is mirrored by the number of noise traders in the risk-free state and the number of noise traders in the leverage state is mirrored by the number of noise traders in the risky state. Both fluctuate around the equal distribution of $N_s = N_{rf} = N_r = N_l = 250$, which is also a result of the symmetric switching probabilities (see equations 4.21 and 4.22). The fluctuation around the

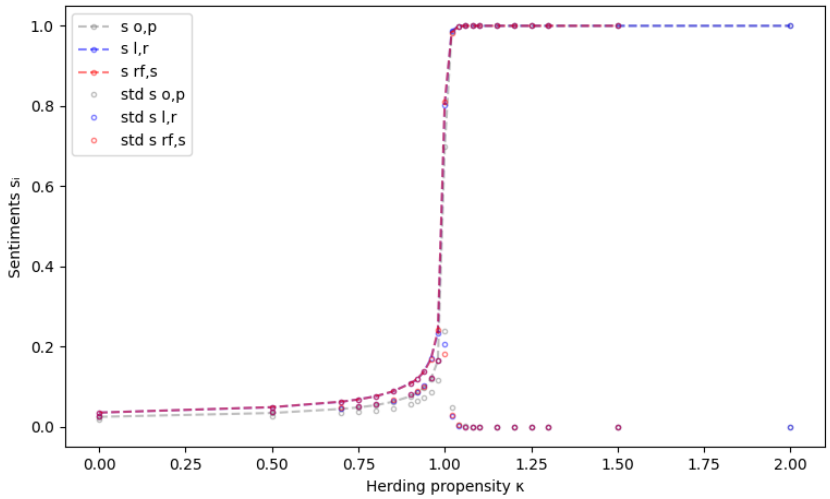

Figure 4.14: Sentiment kappa plot of three coupled Ising models confirming the critical value $\kappa_c = 1.0$. The average absolute sentiments $s^{o,p}$ (grey), $s^{l,r}$ (blue) and $s^{rf,s}$ (red) and their standard deviations are plotted on the y-axis for different constant kappas on the x-axis.

equal distribution of noise traders is also displayed by the sentiments in the fourth row, which all vary around zero. While the sentiment that describes the first Ising model consisting of the optimists and pessimists (colored in gray) is contained in the interval $s_t^{o,p} \in [-0.35, 0.35]$ the other two sentiments ($s_t^{rf,s}$ and $s_t^{l,r}$) routinely reach values outside the interval $[-0.5, 0.5]$. Likewise, the switching probabilities and the risky fractions of the optimist-pessimist Ising model show smaller variations compared to the other two Ising models. The wealth ratio steadily decreases over time from $\nu = 1.0$ to $\nu = 0.5$ indicating the a decrease in wealth for the noise trader class compared to the fundamentalists.

The OU simulation is characterized by two large price peaks and plunges at $T \approx 400$ and $T \approx 600$. This results in the loss of most of the noise traders wealth resulting in the wealth ratio ν decreasing to almost zero in row six. The mirroring of the number of traders observed in the CK simulation can also be observed. However, the number of noise traders time series in row three also highlights multiple polarizations of the noise trader class to one state. The polarizations at for instance $T \approx 800$ and $T \approx 2800$ are accompanied by highly volatile sentiments and switching probabilities. For instance at $T \approx 800$, almost all noise traders are in the optimistic state, with only few pessimists left. This implies that there are only few trader left in the short or risk-free state. A small number of traders implies a more volatile sentiment

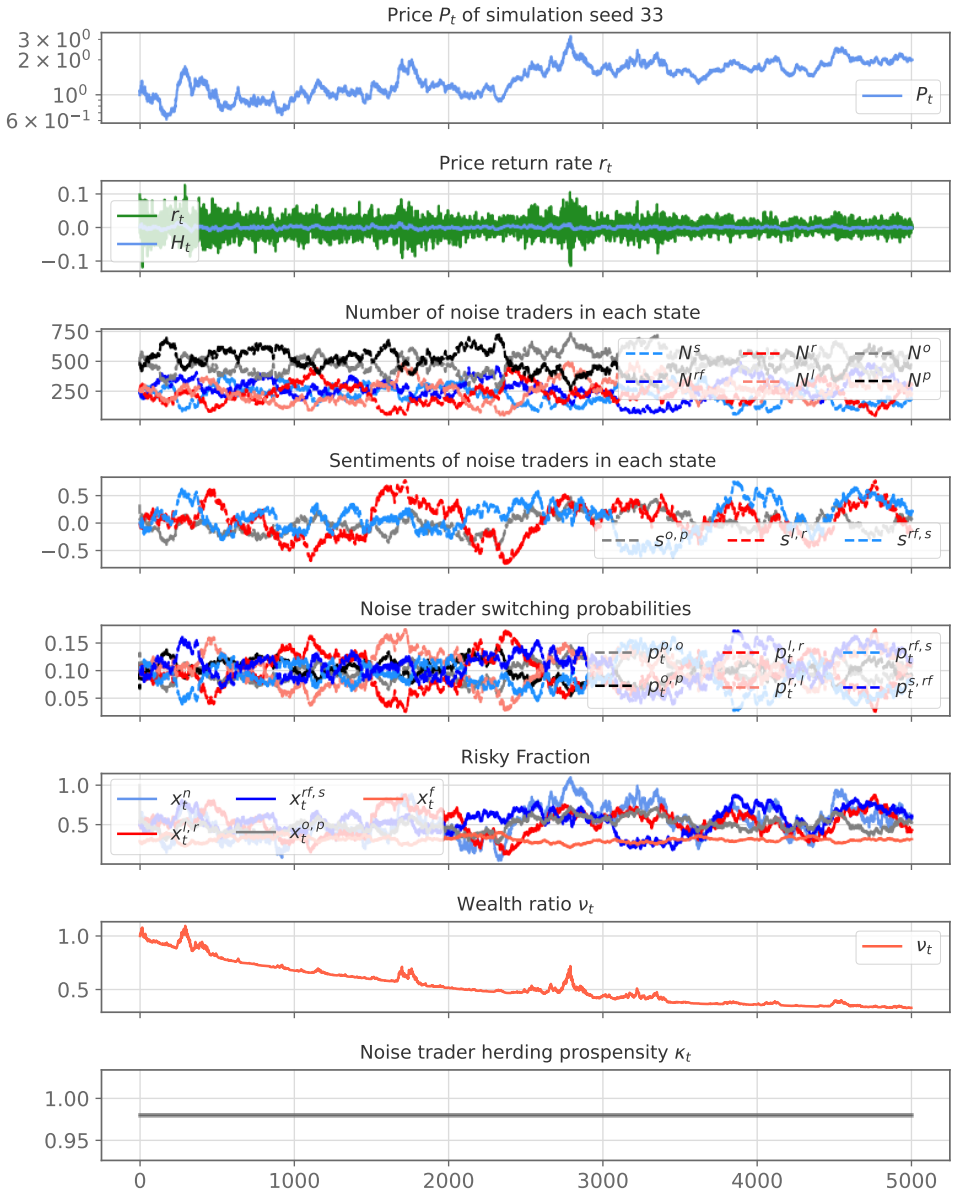

Figure 4.15: Simulation of three coupled Ising models with CK herding propensity. The herding propensity is set to $\kappa_t = 0.98\kappa_c = 0.98$, which is below the critical value $\kappa_c = 1.0$.

$s_t^{rf,s}$, because the switch of one trader has a larger impact. This explains the jump of the $s_t^{rf,s}$ at around $T \approx 900$.

The arguments that concern the ladder model in terms of Minsky's financial instability hypothesis can be applied analogously to the three coupled Ising

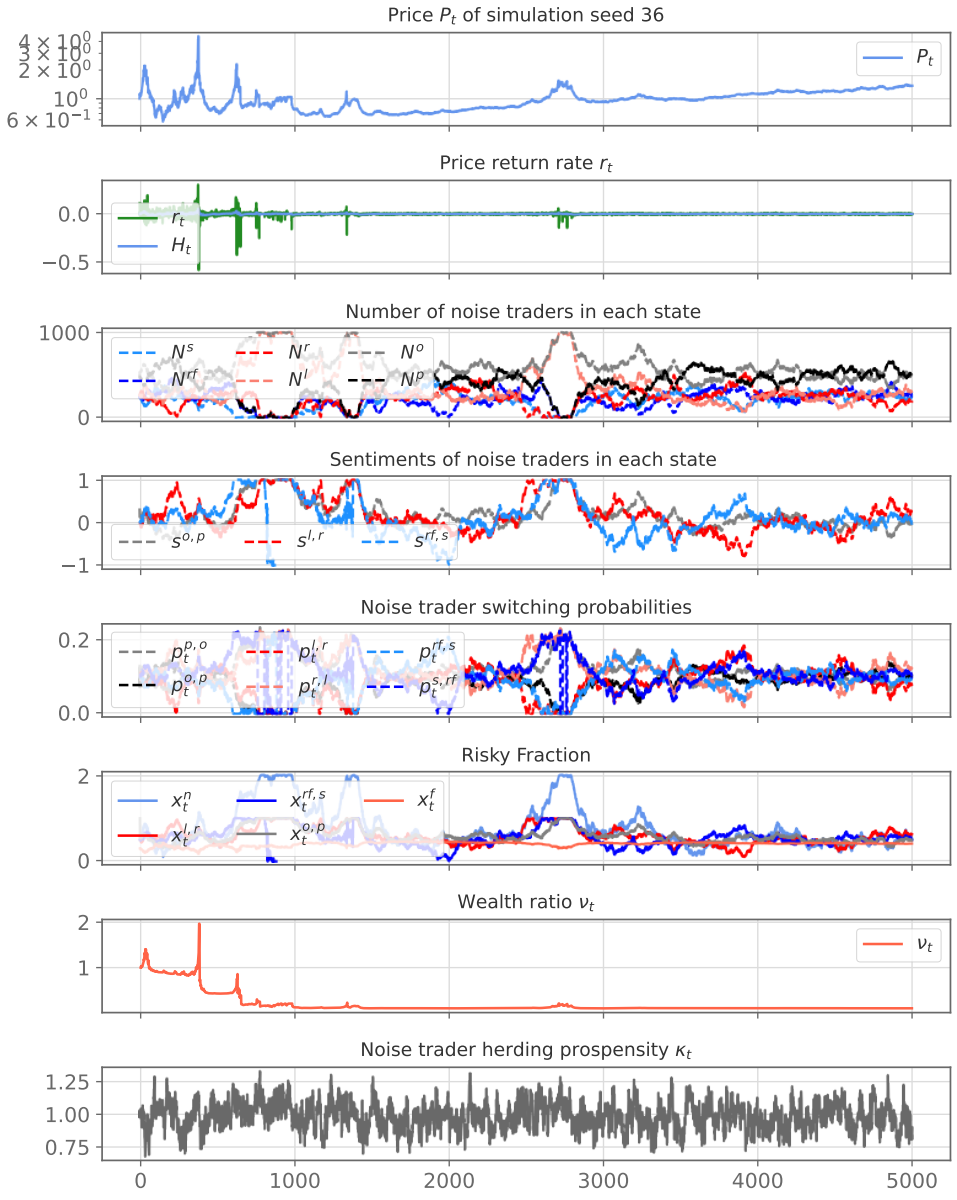

Figure 4.16: Simulation of three coupled Ising models with the OU stochastic process for the herding propensity with $\mu_\kappa = 0.98$.

model OU simulation.

4.4.2 Stylized facts

The following section describes the stylized facts, volatility clustering and fat tails, for the ladder model.

The volatility clustering is visualized in figures 4.17 and 4.18, which show the ACF for the signed (blue) and absolute (red) returns for the CK simulation (figure 4.15) and the OU kappa simulation (figure 4.16).

The ACF for the CK simulation in figure 4.17 behaves similarly to the ACF for the CK simulation of the ladder model in figure 4.9. The ACF decays quickly to zero for increasing lags l for the signed returns. However, the absolute returns do not decay to zero but oscillate around $AFC(l)_{absolute} \approx 0.1$, which differs from the original market model where both the singed and absolute returns are approximately zero for $l > 0$ (see figure 2.4).

The ACF of the signed returns for the OU simulation in figure 4.18 decreases quickly to zero. However, the fluctuations around zero are more pronounced when compared to the signed returns for the CK simulation. The absolute values of the returns have an auto-correlation function with longer memory. Compared to the original market model and the corresponding absolute returns for the OU simulation in figure 2.5, the ACF exhibits larger fluctuations.

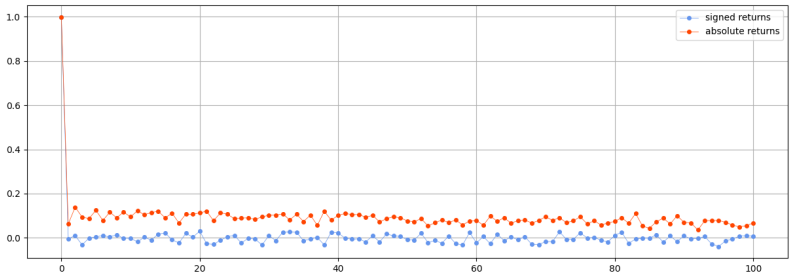

Figure 4.17: ACF for singed (blue) and absolute (red) returns for simulation with constant kappa (CK).

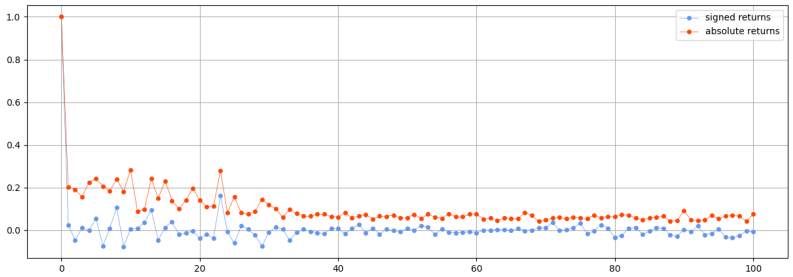

Figure 4.18: ACF for singed (blue) and absolute (red) returns with OU kappa.

The fat tail distribution of returns for the CK simulation is presented in figure 4.19 and for the OU simulation in figure 4.20. As highlighted in chapter 2 the empirical fat-tail decay of the distribution is characterized by the exponent $-1-\alpha$ with $\alpha \in [2,4]$. The parameter is $\alpha \approx 2.48$ for the CK simulation and $\alpha \approx 0.07$ for the OU kappa simulation. This implies that only the simulation with the CK kappa falls within the required range of the parameter.

To conclude, the model consisting of three coupled Ising models produces similar results for the simulation with the constant herding propensity to the original market model. However, for the OU process, the model behave very differently to the original market model. Similarly to the ladder model, the noise traders polarize quite rapidly, which results in a few price peaks after which they do not have a significant impact on the market.

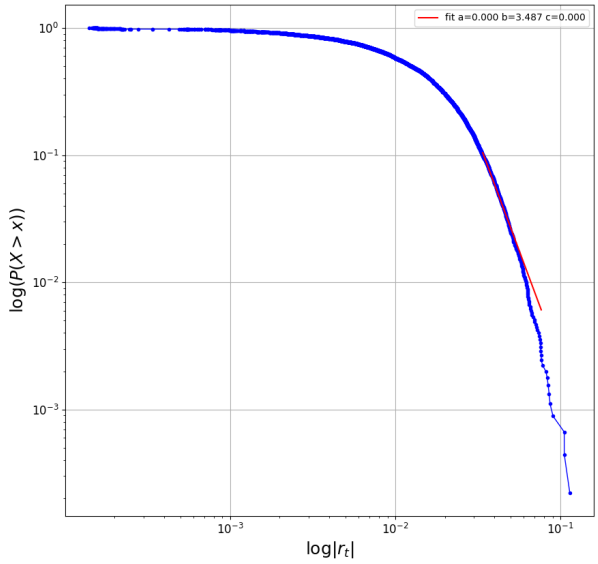

Figure 4.19: Log-log plot of the cumulative distribution function (CDF) of returns for the CK simulation with $\alpha \approx 2.48$.

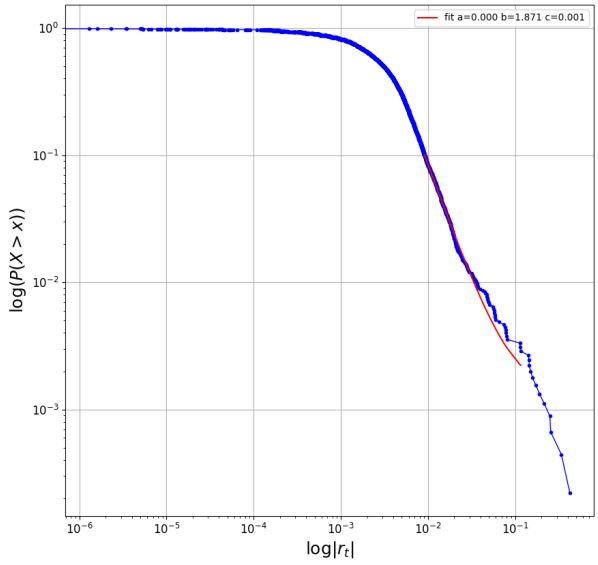

Figure 4.20: Log-log plot of the cumulative distribution function (CDF) of returns for the OU kappa simulation with $\alpha \approx 0.07$.

4.5 Coupled Ising Potts model

The following model consists of an Ising model and a $q = 3$ state Potts model that are coupled. The model distinguishes between a risk-free asset and a stock market. The stock market consists of one risky asset. The noise trader can take a short position, a long position or a leveraged position. The Ising model links the risk-free with the stock market, while the stock market is modelled with the three state Potts model. The coupling of the Ising and Potts model is visualized in figure 4.4 and bears a resemblance to the approach by Kopp [32] visualized in figure 4.2.

The risky fractions of the model are given by

$$\begin{aligned} x_t^n &= \frac{2N_l + N_r - N_s}{N} \\ x_t^{stock,rf} &= \frac{N_{stock}}{N} \\ x_t^i &= \frac{N_i}{N_{stock}}, i \in \{s, r, l\} \end{aligned} \tag{4.24}$$

The investment decision process for the noise trader is structured in three steps. In the first step, the noise traders are allocated to either the risk-free asset or the stock market according to the switching probabilities of the Ising model $P_t^{rf \to stock}$ and $P_t^{stock \to rf}$.

The transition probabilities for the Ising model are defined by

$$\begin{aligned} P_t^{rf \to stock} &= \frac{P^{rf \to stock}}{2} \left(1 + \kappa_t \left(s_t^{rf,stock} + H_t^{rf,stock}\right)\right) \\ P_t^{stock \to rf} &= \frac{P^{stock \to rf}}{2} \left(1 - \kappa_t \left(s_t^{rf,stock} + H_t^{rf,stock}\right)\right) \end{aligned} \tag{4.25}$$

with $s_t^{stock,rf} = \frac{N_{stock} - N_{rf}}{N}$ and $H_t^{stock,rf} = H_t$.

In the second step, the number of traders in the stock market N_{stock} are distributed to the risky, the short and the leverage state according to the distribution of the previous period. This implies

$$N_l^t = x_{t-1}^l \cdot N_{stock}^t \tag{4.26}$$

$$N_r^t = x_{t-1}^r \cdot N_{stock}^t \tag{4.27}$$

$$N_s^t = N_{stock}^t - N_l^t - N_r^t. \tag{4.28}$$

Once the noise traders are distributed to the three states of the stock market they transition according the transition probabilities of the three state Potts model (see also chapter 3 eq. 3.9) which are defined by

$$P_t^{a\to b} = \frac{d \cdot e^{\kappa_t\left(s_t^b + H_t^b\right)}}{\sum_{k\in\{s,r,l\}} e^{\kappa_t\left(s_b + H_t^k\right)}}, \tag{4.29}$$

with $s_t^b = \frac{N_b}{N_{stock}}$, $H_t^l = 2H_t$, $H_t^r = H_t$ and $H_t^s = -2H_t$. The constant d is introduced to represent the holding time as outlined in chapter 3 (see eq. 3.7).

4.5.1 Simulation and time series

In this section, the parameter set used for the simulations is introduced and the time series are discussed on a qualitative level.

Parameter set is summarized in table 4.5. The assets and the fundamentalist trader are initialized with the same values as in the original model. The herding propensity and the associated OU stochastic process of the Ising model are initialized with the same values as in the original model. For the Potts model, the herding propensity is re-scaled based on the critical kappa.

Since the model consists of three coupled Ising models, the critical value of the OU process is the same for each of the three models and the same as in the original market model. The value of $k_c = 1$ is verified in the figure 4.14. The calculation of the average absolute sentiments is done analogously to the ladder model (see 4.14).

Time series are presented for three different simulations. The first simulation is run with the constant herding propensity (CK) and displayed in figure 4.21. The second is done with the OU stochastic process and visualized in figure 4.22. The third simulation (figure 4.23) also employs the OU stochastic process but uses a different holding time for the Potts modell $t_{h,p} = 1.5$.

The critical value of the OU process differs for the two state Ising model and the three state Potts model. As in the previous model, the critical kappa for the Ising model is $k_{c,i} = 1$. The critical kappa for the $q = 3$ state Potts model is $k_{c,p} = 2.77$ (see eq. 3.17).

The price time series of the CK simulation output in figure 4.21 displays larger fluctuations around the upwards price trend at the beginning up to

Parameter set		
Assets	$r_f = 4 \times 10^{-5}$	$r_d = 1.6 \times 10^{-4}$
	$P_0 = 1$	$d_0 = 1.6 \times 10^{-4}$
		$\sigma_d = 1.6 \times 10^{-5}$
Fundamentalist traders	$W_0^f = 10^9$	$E_r = 1.6 \times 10^{-4}$
	$\sigma_r^f = 0.02$	$x_0^f = 0.3$
Noise traders	$W_0^n = 10^9$	$N_n = 1000$
	$\theta = 0.95$	$H_0 = 1.6 \times 10^{-4}$
	$x_0^n = 0.5$	$N_a = 250$
	$t_{h,i} = 10$	$t_{h,p} = 5$
Herding propensity	$\kappa_{0,i} = \mu_{\kappa,i}$	$\mu_{\kappa,i} = 0.98\kappa_{c,i}$
	$\eta_{\kappa,i} \approx 0.11$	$\sigma_{\kappa,i} \approx 0.16$
	$\kappa_{t,p} = \kappa_{t,i} \cdot \kappa_{c,p}$	

Table 4.5: Parameters for simulating the Ising Potts model with parameters $a, b \in \{s, rf, r, l\}$. For the Ising model, the herding propensity is initialised with the values of the original market model. These values are tagged with an i. The herding propensity for the Potts model is the kappa for the Ising model but re-scaled to accommodate the differing critical kappa and denoted by p.

$T \approx 1000$ followed by smaller price fluctuations later on. This is also reflected by the decreasing absolute value of the price return rate in the second row. The number of noise traders in the risk-free asset and in the stock market mirror one another as described by the switching probabilities in equation 4.25. In general, the number of noise traders in each state fluctuates around their expectation value of $N_{rf} = N_{stock} = 500$ and $N_s = N_r = N_l = 166$. The switching probabilities associated with the Ising model ($P_t^{rf,m}$ and $P_t^{m,rf}$) exhibit larger fluctuations compared to the the Potts model switching probabilities (P_t^s, P_t^r and (P_t^l). This difference between the Ising and Potts model is also reflected sentiments in row four. The wealth of the noise trader class halves in the duration of the simulation compared to the fundamentalists.

The OU simulation in figure 4.21 is characterized by a similar price trajectory compared to the CK simulation in figure 4.22. The Ising model exhibits polarizations of the noise trader class from the risk-free asset towards the stock market at $T \approx 2500$ and $T \approx 3100$. Within the stock market, the noise traders almost behave in unison. This can be observed in row three where there are N_s, N_r and N_l exhibits the same behaviour with small deviations from one another at $T \approx 2500$ and $T \approx 3100$. There is little polarization within the stock market. This lack of polarization can be attributed to the

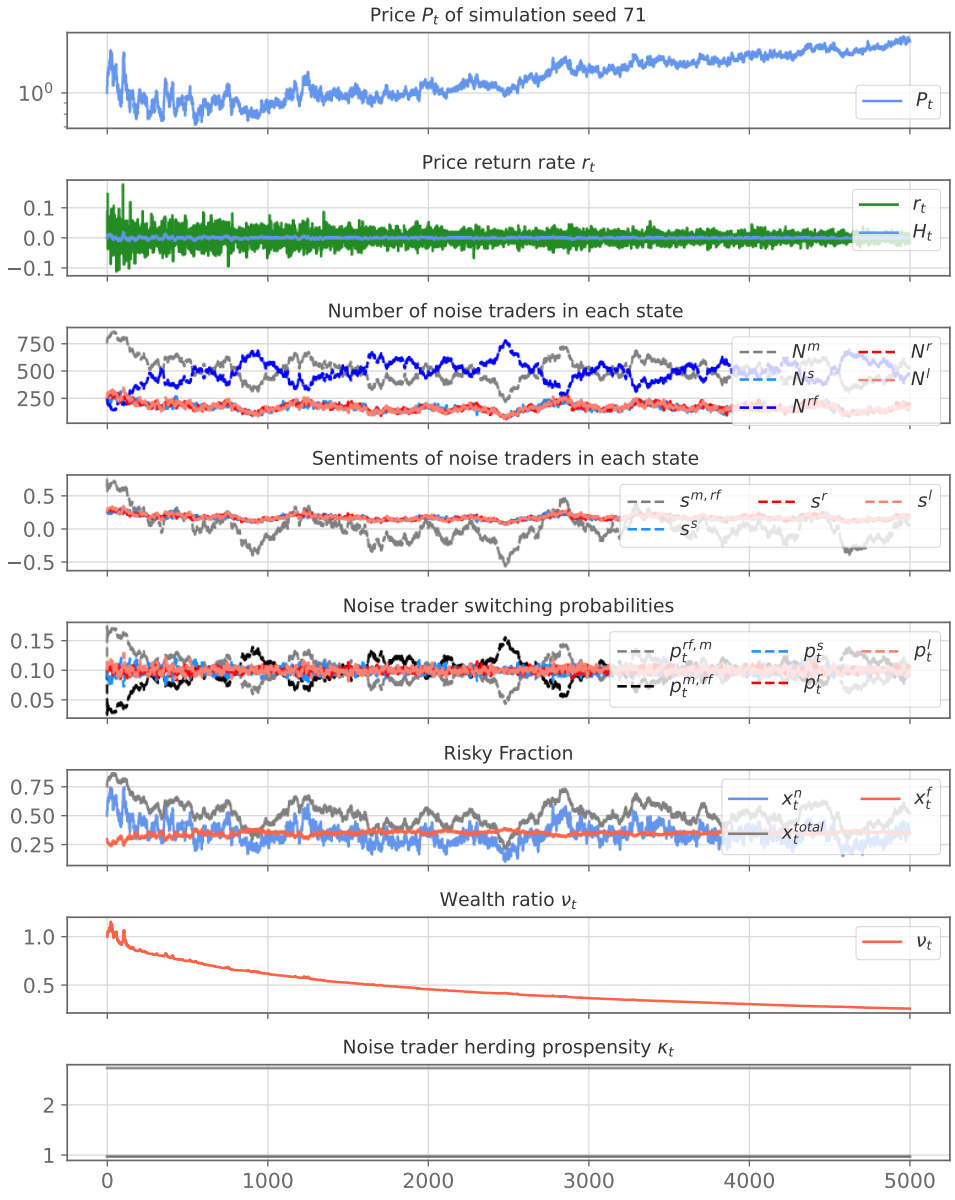

Figure 4.21: Simulation of the coupled Ising Potts model with CK herding propensity.

holding time used for the Potts model $t_{h,p} = 5$. The impact of the holding time can be observed when comparing the second simulation to the third one in figure 4.23.

The first two simulations employ the holding times $t_{h,i} = 10$ for the Ising model and $t_{h,p} = 5$ for the Potts model, which result in switching proba-

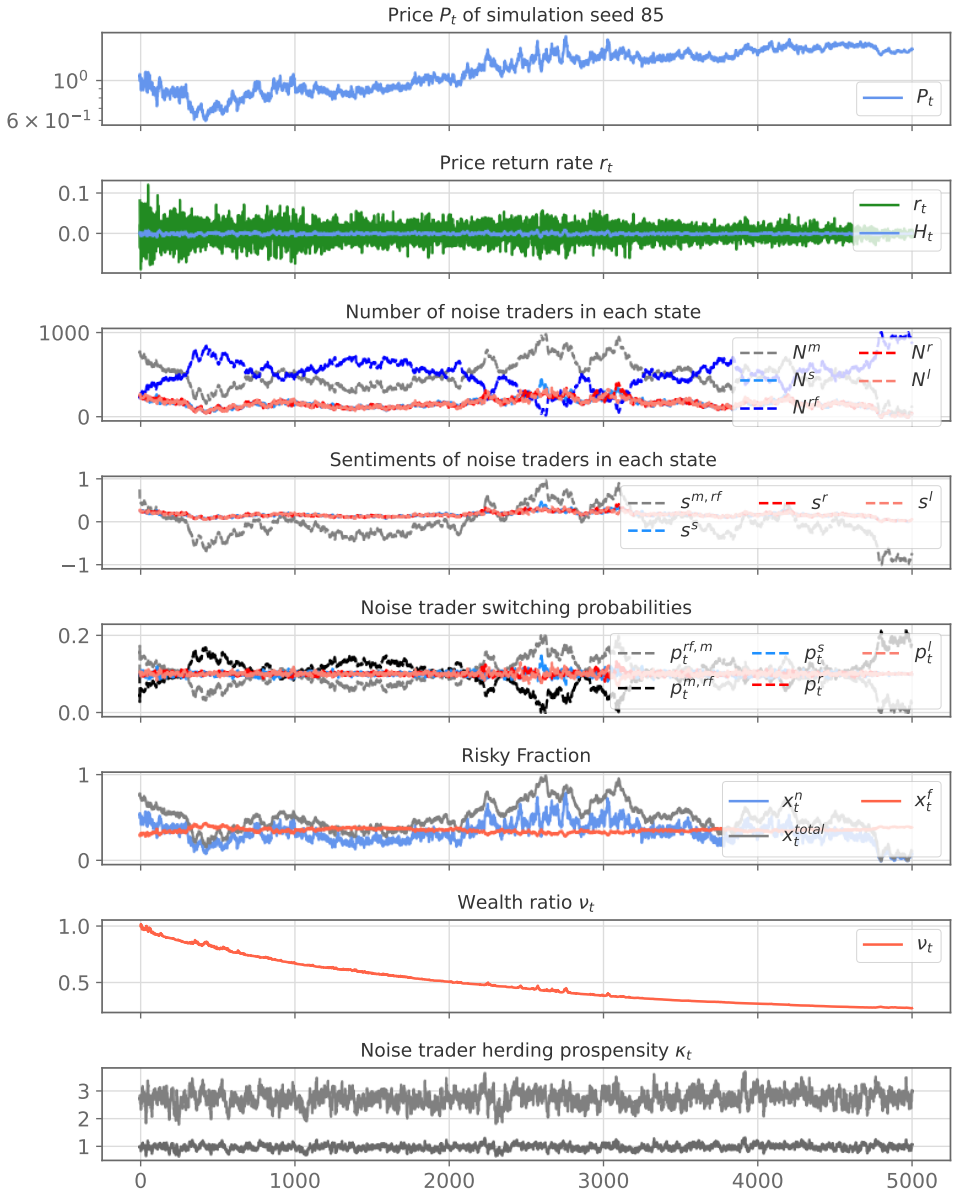

Figure 4.22: Simulation of the coupled Ising Potts model with OU herding propensity.

bilities equal to $P_t^{a\to b}|_{\kappa_t=0}= 0.1$ in the absence of herding for both the Ising model and the Potts model. The third simulation changes the holding time of the Potts model to $t_{h,p} = 1.5$, which corresponds to $d = 1$ in equation 4.29 and $P_t^{a\to b}|_{\kappa_t=0}= \frac{1}{3}$. The switching probabilities for the short, risky and leverage state are significantly larger compared to figure 4.22 and allow for

polarizations in the Potts model as can be observed at $T \approx 100$ or $T \approx 1000$. However, the polarizations are not gradually but abrupt and result in the noise traders losing most of their wealth and impact on the price dynamics.

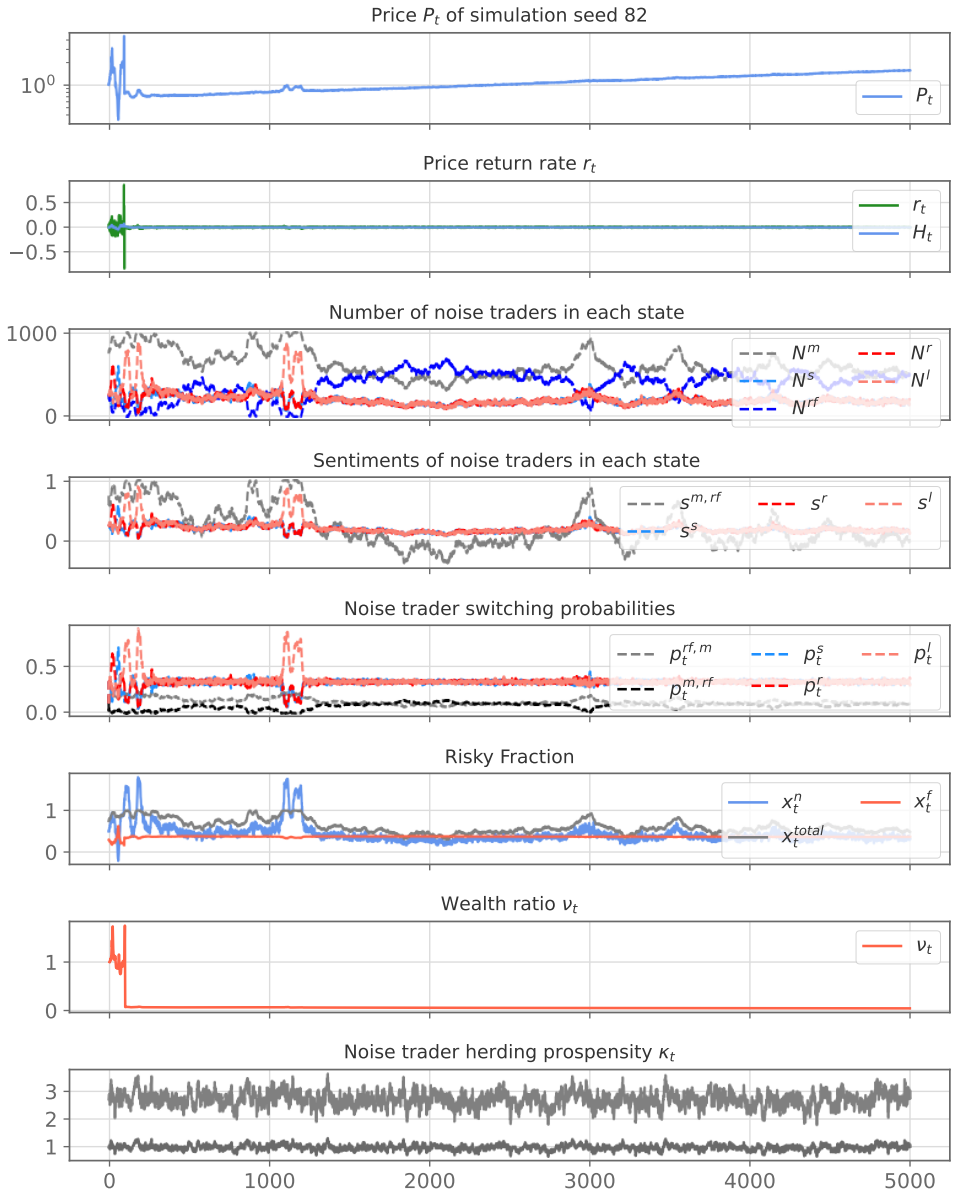

Figure 4.23: Simulation of the coupled Ising Potts model with OU herding propensity with $t_{h,p} = 1.5$ and $d = 1$.

The three state Potts model suffers from the same problem associated with the four state Potts model outlined in chapter 3, namely the discontinuous phase transition. As a result, the Ising Potts model is unable to produce realistic price time series.

The chapter outlined three extensions of the original market model. Each model is a different incarnation of the underlying idea to formulate the microscopic interactions between the traders first and to study the resulting macroscopic properties of these interactions second. This microscopic approach permits to test many different variations on what states the traders can occupy and how these states are connected. However, this flexibility in model design comes with the challenge to explain the results without an established methodology to compare the results to. This lack of established theory is the major drawback of the microscopic approach.

Chapter 5

Conclusion and Outlook

The present work is based on the agent based model of a financial market first outlined by Kaizoji et al. [62]. The model is able to produce faster-than-exponentially growing bubbles and several stylized facts of financial markets. The goal of the present work has been to extend and apply this ABM to incorporate the ability of the traders to short sell or leverage a position.

Chapter 2 reviewed the original market model. The focus has been on the understanding of the noise trader class and its constraint defined by the risky fraction to only be able to invest the accumulated wealth. Chapter 3 outlined the general q state mean field Potts model and applied it to the noise trader class to extend the two states of the original model to $q = 4$. The implementation of the Potts model was unable to produce realistic market simulations. The main drawback of the Potts model is the abrupt polarization of the noise traders. The abrupt polarization reflects the underlying nature of the phase transition of the $q = 4$ state mean field Potts model, which is characterized as of first order and discontinuous. The other candidate from statistical physics, the O(n) model or n-vector model, was found to be only useful for a multi-asset extension.

Chapter 4 shifts the focus from borrowing concepts from statistical physics to building an extension by formulating the microscopic interactions between the traders and then studying the macroscopic properties of the system. The microscopic interactions are based on behavioural observations of traders. The key levers in building the model are the definition of the states and their connections, the structure of transition probabilities, the holding time, the sentiment and the price momentum and other price related factors such as trading volume and price acceleration. The first model discussed is the ladder model, which arranges the states like a ladder starting from the lowest stair, the short state, over the risk-free and the risky state, to the highest stair, the leverage state. A qualitative inspection of simulation shows

promising behaviour for the CK process below the critical kappa. In the OU simulation, the noise traders suffer significant losses in absolute terms and also relative to the fundamentalists during crashes. Hence, the opportunity to leverage in the ladder model can lead to more severe crashes, which is reflected by the decrease in wealth of the noise traders who are unable to recover from the severity of their losses. Due to the focus of Hyman Minsky's work on the role of financial markets, debt and the irrationality of the market participants, his financial instability hypothesis provides a useful context for the interpretation of the ladder model. Considering the financial instability hypothesis, the OU simulation highlights the potential impact that a combination of leverage, herding behaviour and the absence of government intervention can have on financial markets. The ladder model exhibits volatility clustering but no clear indication for fat tails over the simulation horizon, which can be viewed as a result of the non stationarity of the price process of the OU simulation. The second model couples three Ising models. The first Ising model consists of optimists and pessimists. The second Ising model describes the optimists which can occupy the leverage and the risky state. The third Ising model describes pessimists which can occupy the risk-free and the short state. Similarly to the ladder model, the noise traders polarize quite rapidly, which results in a few price peaks after which they do not have a significant impact on the market. There is no clear indication of fat tails but the model exhibits volatility clustering. The three coupled Ising models admit also the interpretation through the lens of Minsky's work. The third model couples an Ising model and a Potts model. The Ising model describes the interaction of the risk-free asset and the stock market. The $q = 3$ state mean field Potts model describes the stock market consisting of a leverage, a risky and a short state. The three state Potts model suffers from the same problem associated with the four state Potts model outlined in chapter 3, namely the discontinuous phase transition. As a result, the Ising Potts model is unable to produce realistic price time series. Chapter 4 also demonstrates the limitations of the microscopic approach. While this approach permits great flexibility in model design, it is challenging to explain the results without an established methodology to compare the results to. There are many further directions to take with the extended market models, which are summarized in the following.

5.1 Further directions of research

The analysis of the Potts model in chapter 3 and 4 of this thesis was restricted to the mean field case, which is associated with a 1st order phase transition for $q > 2$ and assumes an infinite number of trader, which can be questioned. In real financial markets, the number of traders trading a stock is finite and typically is in the thousands. A way to avoid the 1st order phase transition

is to discard the mean field assumption and use other network topologies for the noise traders. For instance, the Potts model exhibits a continuous phase transition for complex networks with a power law exponent $\gamma \leq 3$ for $q \geq 3$ or on a complete graph in a microcanoncial ensemble [93]. More information is also provided in [114, 74, 92, 102, 29]. However, dropping the mean field assumption implies that the noise traders cannot be aggregated to one representative agent and have to be modelled individually, which is computationally expensive.

Minsky's financial instability hypothesis in connection with the findings of the ladder model provide another opportunity for further research. So far the model does not incorporate a reboot mechanism in terms of a government or a central bank. The model offers the opportunity to further investigate the question if financial markets are intrinsically unstable and require reboots. This can be done by including the government or central bank as entities and study their impact and the impact of different policies on the system. Furthermore, the impact of leverage on the price time series can be quantified using for instance the draw-down epsilon delta method [45] to compare the bubbles of the original market model and a model that incorporates leverage, or by investigating the non stationary nature of the price process in more detail.

There are additional opportunities to couple Ising models to extend a two state model to four states. For instance, instead of the ladder connection of the states, the short state could be connected only to the risky and the leverage state and the risk-free asset could be connected only to the risky asset. Furthermore, to avoid the discontinuous phase transition of the Potts model in the model that couples an Ising model to a Potts model, the Potts model could be replaced by three Ising models connecting the three states of the Potts model. However, these approaches are only constructing additional combinations.

A more promising alternative is to further investigate the behaviour of investors and derive other models from that. Specifically, the behavioural reasons and signals for deciding to leverage or short sell are challenging to determine. In this context, one group of modeling tools that might be interesting to work with are multinomial choice models with correlations among alternatives such as the Nested Logit model and Mixed Logit models [117].

In context of the noise trader class, additional parameters besides the sentiment and the price momentum could be included to create heterogeneous trading strategies amongst the noise traders. An interesting aspect to investigate would be how a trader using acceleration $\Gamma_{t,f}$ and volume $V_{t,f}$ in addition to momentum would perform compared to the fundamentalists and the standard noise traders.

Finally, the original model and the extensions in this thesis all used either a

constant herding propensity or the OU stochastic process. There are other processes the herding propensity κ_t can follow, for instance the Lévy flight, a random walk in which the step lengths have a Lévy distribution, which exhibits a set of random short movements connected by infrequent longer ones [22].

Bibliography

[1] Dilip Abreu and Markus K Brunnermeier. Bubbles and crashes. *Econometrica*, 71(1):173–204, 2003.

[2] Lucy F Ackert, Narat Charupat, Bryan K Church, and Richard Deaves. Margin, short selling, and lotteries in experimental asset markets. *Southern Economic Journal*, pages 419–436, 2006.

[3] Robert Z Aliber and Charles P Kindleberger. *Manias, panics, and crashes: A history of financial crises*. Springer, 2017.

[4] Franklin Allen and Douglas Gale. Bubbles and crises. *The economic journal*, 110(460):236–255, 2000.

[5] Franklin Allen, Stephen Morris, and Andrew Postlewaite. Finite bubbles with short sale constraints and asymmetric information. *Journal of Economic Theory*, 61(2):206–229, 1993.

[6] Mikhail Anufriev and Jan Tuinstra. The impact of short-selling constraints on financial market stability in a heterogeneous agents model. *Journal of Economic Dynamics and Control*, 37(8):1523–1543, 2013.

[7] Diego Ardila-Alvarez, Zalan Forro, and Didier Sornette. The acceleration effect and gamma factor in asset pricing. *Physica A: Statistical Mechanics and its Applications*, 569:125367, 2021.

[8] W Brian Arthur. Out-of-equilibrium economics and agent-based modeling. *Handbook of computational economics*, 2:1551–1564, 2006.

[9] Doron Avramov and Tarun Chordia. Asset pricing models and financial market anomalies. *The Review of Financial Studies*, 19(3):1001–1040, 2006.

[10] R Axtell and J Doyne Farmer. Agent-based modeling in economics and finance: Past, present, and future, 2017.

[11] Louis Bachelier. Théorie de la spéculation. In *Annales scientifiques de l'École normale supérieure*, volume 17, pages 21–86, 1900.

[12] Malcolm Baker and Jeffrey Wurgler. Investor sentiment in the stock market. *Journal of economic perspectives*, 21(2):129–152, 2007.

[13] Nicholas Barberis, Andrei Shleifer, and Robert W Vishny. *A model of investor sentiment*. Princeton University Press, 2005.

[14] Sushil Bikhchandani, David Hirshleifer, and Ivo Welch. A theory of fads, fashion, custom, and cultural change as informational cascades. *Journal of political Economy*, 100(5):992–1026, 1992.

[15] Lawrence Blume, David Easley, and Maureen O'hara. Market statistics and technical analysis: The role of volume. *The journal of finance*, 49(1):153–181, 1994.

[16] Jean-Philippe Bouchaud and Marc Mézard. Wealth condensation in a simple model of economy. *Physica A: Statistical Mechanics and its Applications*, 282(3-4):536–545, 2000.

[17] Jean-Philippe Bouchaud and Marc Potters. *Theory of financial risk and derivative pricing: from statistical physics to risk management*. Cambridge university press, 2003.

[18] William A Brock, Cars H Hommes, et al. Rational animal spirits. 1999.

[19] Markus K Brunnermeier and Martin Oehmke. Bubbles, financial crises, and systemic risk. *Handbook of the Economics of Finance*, 2:1221–1288, 2013.

[20] Willem H Buiter. The macroeconomics of dr pangloss a critical survey of the new classical macroeconomics. *The Economic Journal*, 90(357):34–50, 1980.

[21] Gunduz Caginalp, David Porter, and Vernon Smith. Financial bubbles: Excess cash, momentum, and incomplete information. *The Journal of Psychology and Financial Markets*, 2(2):80–99, 2001.

[22] Alexei V Chechkin, Ralf Metzler, Joseph Klafter, Vsevolod Yu Gonchar, et al. Introduction to the theory of lévy flights. *Anomalous transport*, 129, 2008.

[23] Carl Chiarella, Roberto Dieci, and Xue-Zhong He. Heterogeneity, market mechanisms, and asset price dynamics. pages 277–344, 2009.

[24] Carl Chiarella and Xue-Zhong He. Asset price and wealth dynamics under heterogeneous expectations. *Quantitative Finance*, 1:509–526, 2001.

[25] Davide Cividino. A statistical physics approach to financial bubbles: Ising-like modeling of social imitation in an agent-based multi-asset market. 2020.

[26] Rama Cont. Empirical properties of asset returns: stylized facts and statistical issues. *Quantitative finance*, 1(2):223, 2001.

[27] Rama Cont. Volatility clustering in financial markets: empirical facts and agent-based models. In *Long memory in economics*, pages 289–309. Springer, 2007.

[28] Jean-Remy Conti. Long-term behavior of an artificial market, composed of fundamentalists and noise traders. 2018.

[29] Marius Costeniuc, Richard S Ellis, and Hugo Touchette. Complete analysis of phase transitions and ensemble equivalence for the curie–weiss–potts model. *Journal of Mathematical Physics*, 46(6):063301, 2005.

[30] Matthieu Cristelli, Luciano Pietronero, and Andrea Zaccaria. Critical overview of agent-based models for economics. *arXiv preprint arXiv:1101.1847*, 2011.

[31] Paul Cuff, Jian Ding, Oren Louidor, Eyal Lubetzky, Yuval Peres, and Allan Sly. Glauber dynamics for the mean-field potts model. *Journal of Statistical Physics*, 149(3):432–477, 2012.

[32] Emily Damiani. Equilibrium model of fundamentalist and noise traders in a multi-asset framework. 2019.

[33] Domenico delli Gatti, Giorgio Fagiolo, Mauro Gallegati, Matteo Richiardi, and Alberto Russo. *Agent-based models in economics: A Toolkit*. Cambridge University Press, 2018.

[34] Zhuanxin Ding, Clive WJ Granger, and Robert F Engle. A long memory property of stock market returns and a new model. *Journal of empirical finance*, 1(1):83–106, 1993.

[35] Sayuli Drouard. Effects of controlling or exploiting financial bubbles on market dynamics, in the framework of an agent-based model. 2020.

[36] Tom Engsted and Thomas Q Pedersen. The dividend–price ratio does predict dividend growth: International evidence. *Journal of Empirical Finance*, 17(4):585–605, 2010.

[37] Eugene F Fama. Session topic: stock market price behavior. *The Journal of Finance*, 25(2):383–417, 1970.

[38] Eugene F Fama. Two pillars of asset pricing. *American Economic Review*, 104(6):1467–85, 2014.

[39] Eugene F Fama and Kenneth R French. *Multifactor explanations of asset pricing anomalies*. University of Chicago Press, 2021.

[40] Thomas Fischer and Jesper Riedler. Prices, debt and market structure in an agent-based model of the financial market. *Journal of Economic Dynamics and Control*, 48:95–120, 2014.

[41] Rik GP Frehen, William N Goetzmann, and K Geert Rouwenhorst. New evidence on the first financial bubble. *Journal of Financial Economics*, 108(3):585–607, 2013.

[42] Milton Friedman and Anna Jacobson Schwartz. *The great contraction, 1929-1933*. Princeton University Press, 2012.

[43] John Kenneth Galbraith. The great crash 1929, a mariner book, 1997.

[44] Peter M Garber. Famous first bubbles. *Journal of Economic perspectives*, 4(2):35–54, 1990.

[45] Jan-Christian Gerlach, Guilherme Demos, and Didier Sornette. Dissection of bitcoin's multiscale bubble history from january 2012 to february 2018. *Royal Society open science*, 6(7):180643, 2019.

[46] Nigel Gilbert. *Agent-based models*, volume 153. Sage Publications, 2019.

[47] Roy J Glauber. Time-dependent statistics of the ising model. *Journal of mathematical physics*, 4(2):294–307, 1963.

[48] Parameswaran Gopikrishnan, Martin Meyer, LA Nunes Amaral, and H Eugene Stanley. Inverse cubic law for the distribution of stock price variations. *The European Physical Journal B-Condensed Matter and Complex Systems*, 3(2):139–140, 1998.

[49] David Graeber. *Debt: The first 5000 years*. Penguin UK, 2012.

[50] A Greenspan. *Remarks on "Economic Volatility" at the "Rethinking Stabilization Policy". In: Symposium Sponsored by the Federal Reserve Bank of Kansas City, Jackson Hole, Wyoming, August 29–31, 2002.* 2002.

[51] Georges Harras, Claudio J Tessone, and Didier Sornette. Noise-induced volatility of collective dynamics. *Physical Review E*, 85(1):011150, 2012.

[52] Milton Harris and Artur Raviv. Differences of opinion make a horse race. *The Review of Financial Studies*, 6(3):473–506, 1993.

[53] J Michael Harrison and David M Kreps. Speculative investor behavior in a stock market with heterogeneous expectations. *The Quarterly Journal of Economics*, 92(2):323–336, 1978.

[54] Ernan Haruvy and Charles N Noussair. The effect of short selling on bubbles and crashes in experimental spot asset markets. *The Journal of Finance*, 61(3):1119–1157, 2006.

[55] Cars H Hommes. Heterogeneous agent models in economics and finance. *Handbook of computational economics*, 2:1109–1186, 2006.

[56] Harrison Hong and Jeremy C Stein. Disagreement and the stock market. *Journal of Economic perspectives*, 21(2):109–128, 2007.

[57] Kevin D Hoover. Macroeconomics, history of from 1933 to present. 2015.

[58] Ji-Ping Huang. Fluctuation phenomena: Leverage could be positive and negative. In *Experimental Econophysics*, pages 45–62. Springer, 2015.

[59] Giulia Iori and James Porter. Agent-based modelling for financial markets. 2012.

[60] Daniel Kahneman, Jack L Knetsch, and Richard H Thaler. Anomalies: The endowment effect, loss aversion, and status quo bias. *Journal of Economic perspectives*, 5(1):193–206, 1991.

[61] Daniel Kahneman and Amos Tversky. Prospect theory: An analysis of decision under risk. In *Handbook of the fundamentals of financial decision making: Part I*, pages 99–127. World Scientific, 2013.

[62] Taisei Kaizoji, Matthias Leiss, Alexander Saichev, and Didier Sornette. Super-exponential endogenous bubbles in an equilibrium model of fundamentalist and chartist traders. *Journal of Economic Behavior & Organization*, 112:289–310, 2015.

[63] Morgan Kelly. All their eggs in one basket: Portfolio diversification of us households. *Journal of Economic Behavior & Organization*, 27(1):87–96, 1995.

[64] Gew-rae Kim and Harry M Markowitz. Investment rules, margin, and market volatility. *Journal of Portfolio Management*, 16(1):45, 1989.

[65] Oliver Kim and Robert E Verrecchia. Market reaction to anticipated announcements. *Journal of Financial Economics*, 30(2):273–309, 1991.

[66] Charles P Kindleberger and Robert Z Aliber. *Manias, panics and crashes: a history of financial crises*. Palgrave Macmillan, 2011.

[67] John King. Hyman minsky and the financial instability hypothesis. In *The Oxford Handbook of Post-Keynesian Economics, Volume 1*. 2013.

[68] TR Kirkpatrick and PG Wolynes. Stable and metastable states in mean-field potts and structural glasses. *Physical Review B*, 36(16):8552, 1987.

[69] Ralf Kohrt. The market impact of exploiting financial bubbles. 2016.

[70] Antoine Kopp. Equilibrium model of a fixed income market with fundamentalist and chartist traders. 2020.

[71] David M Kreps et al. *A course in microeconomic theory*. Princeton university press, 1990.

[72] Blake LeBaron. Building the santa fe artificial stock market. *Physica A*, pages 1–20, 2002.

[73] Blake LeBaron. Agent-based financial markets: Matching stylized facts with style. *Post Walrasian Macroeconomics: Beyond the DSGE Model*, pages 221–235, 2006.

[74] Ching Hua Lee and Andrew Lucas. Simple model for multiple-choice collective decision making. *Physical Review E*, 90(5):052804, 2014.

[75] John Lintner. The valuation of risk assets and the selection of risky investments in stock portfolios and capital budgets. In *Stochastic optimization models in finance*, pages 131–155. Elsevier, 1975.

[76] Andrew W Lo. Reconciling efficient markets with behavioral finance: the adaptive markets hypothesis. *Journal of investment consulting*, 7(2):21–44, 2005.

[77] Andrew W Lo. *The adaptive markets hypothesis*. Princeton University Press, 2019.

[78] Otto Loistl. *Kapitalmarkttheorie*, volume 3. Oldenbourg München, 1994.

[79] Paolo Lorenzoni and Antonio Moro. Exact analysis of phase transitions in mean-field potts models. *Physical Review E*, 100(2):022103, 2019.

[80] Thomas Lux. Herd behaviour, bubbles and crashes. *The economic journal*, 105(431):881–896, 1995.

[81] Thomas Lux and Michele Marchesi. Scaling and criticality in a stochastic multi-agent model of a financial market. *Nature*, 397(6719):498–500, 1999.

[82] Thomas Lux and Michele Marchesi. Volatility clustering in financial markets: a microsimulation of interacting agents. *International journal of theoretical and applied finance*, 3(04):675–702, 2000.

[83] Harry Markowitz. The utility of wealth. *Journal of political Economy*, 60(2):151–158, 1952.

[84] Edward M Miller. Risk, uncertainty, and divergence of opinion. *The Journal of finance*, 32(4):1151–1168, 1977.

[85] Hyman P Minsky and Henry Kaufman. *Stabilizing an unstable economy*, volume 1. McGraw-Hill New York, 2008.

[86] Hyman P Minsky Ph D. The financial-instability hypothesis: capitalist processes and the behavior of the economy. 1982.

[87] Frederic S Mishkin. *The economics of money, banking, and financial markets*. Pearson education, 2007.

[88] Franco Modigliani and Merton H Miller. The cost of capital, corporation finance and the theory of investment. *The American economic review*, 48(3):261–297, 1958.

[89] Franco Modigliani and Merton H Miller. Corporate income taxes and the cost of capital: a correction. *The American economic review*, 53(3):433–443, 1963.

[90] Jan Mossin. Equilibrium in a capital asset market. *Econometrica: Journal of the econometric society*, pages 768–783, 1966.

[91] Madis Ollikainen. Multiple market regimes in an equilibrium model of fundamentalist and noise traders. *Master's thesis, ETH Zürich*, 2016.

[92] M Ostilli. Mean-field models with short-range correlations. *EPL (Europhysics Letters)*, 97(5):50008, 2012.

[93] M Ostilli and F Mukhamedov. Continuous-and discrete-time glauber dynamics. first-and second-order phase transitions in mean-field potts models. *EPL (Europhysics Letters)*, 101(6):60008, 2013.

[94] Adrian Pagan. The econometrics of financial markets. *Journal of empirical finance*, 3(1):15–102, 1996.

[95] RG Palmer, W Brian Arthur, John H Holland, and Blake LeBaron. An artificial stock market. *Artificial Life and Robotics*, 3(1):27–31, 1999.

[96] Daniel Philipp. Influence of lppl traders on financial markets. 2015.

[97] Catharine H Rankin, Thomas Abrams, Robert J Barry, Seema Bhatnagar, David F Clayton, John Colombo, Gianluca Coppola, Mark A Geyer, David L Glanzman, Stephen Marsland, et al. Habituation revisited: an updated and revised description of the behavioral characteristics of habituation. *Neurobiology of learning and memory*, 92(2):135–138, 2009.

[98] Carmen M Reinhart and Kenneth S Rogoff. This time is different. 2009.

[99] Carmen M Reinhart and Kenneth S Rogoff. From financial crash to debt crisis. *American Economic Review*, 101(5):1676–1706, 2011.

[100] Lionel Robbins and Murray Weidenbaum. *The great depression*. Routledge, 2017.

[101] J Barkley Rosser. *From Catastrophe to Chaos: A General Theory of Economic Discontinuities: Mathematics, Microeconomics and Finance*, volume 1. Springer Science & Business Media, 2000.

[102] UA Rozikov. Gibbs measures of potts model on cayley trees: a survey and applications. *arXiv preprint arXiv:2103.07391*, 2021.

[103] Paul A Samuelson. Proof that properly anticipated prices fluctuate randomly. In *The world scientific handbook of futures markets*, pages 25–38. World Scientific, 2016.

[104] William Samuelson and Richard Zeckhauser. Status quo bias in decision making. *Journal of risk and uncertainty*, 1(1):7–59, 1988.

[105] Jose A Scheinkman and Wei Xiong. Overconfidence and speculative bubbles. *Journal of political Economy*, 111(6):1183–1220, 2003.

[106] Anna Scherbina and Bernd Schlusche. Asset price bubbles: a survey. *Quantitative Finance*, 14(4):589–604, 2014.

[107] Moritz Schularick and Alan M Taylor. Credit booms gone bust: Monetary policy, leverage cycles, and financial crises, 1870-2008. *American Economic Review*, 102(2):1029–61, 2012.

[108] William F Sharpe. Capital asset prices: A theory of market equilibrium under conditions of risk. *The journal of finance*, 19(3):425–442, 1964.

[109] Robert J Shiller. *Irrational exuberance*. Princeton university press, 2015.

[110] Robert Skidelsky. The great depression: Keynes's perspective. In *The interwar depression in an international context*, pages 99–112. Oldenbourg Wissenschaftsverlag, 2009.

[111] Didier Sornette. *Why stock markets crash*. Princeton university press, 2009.

[112] Didier Sornette. Physics and financial economics (1776–2014): puzzles, ising and agent-based models. *Reports on progress in physics*, 77(6):062001, 2014.

[113] Didier Sornette and Wei-Xing Zhou. Evidence of fueling of the 2000 new economy bubble by foreign capital inflow: implications for the future of the us economy and its stock market. *Physica A: Statistical Mechanics and its Applications*, 332:412–440, 2004.

[114] Ryo Tamura, Shu Tanaka, and Naoki Kawashima. Phase transition in potts model with invisible states. *Progress of theoretical physics*, 124(2):381–388, 2010.

[115] D Thirumalai and TR Kirkpatrick. Mean-field potts glass model: Initial-condition effects on dynamics and properties of metastable states. *Physical Review B*, 38(7):4881, 1988.

[116] Stefan Thurner, J Doyne Farmer, and John Geanakoplos. Leverage causes fat tails and clustered volatility. *Quantitative Finance*, 12(5):695–707, 2012.

[117] Kenneth E Train. *Discrete choice methods with simulation*. Cambridge university press, 2009.

[118] Franz Utermohlen. Mean field theory solution of the ising model, 2018.

[119] L Walras. Eléments d'economie politique pure ou théorie de la richesse sociale (paris: R. pichon and r. durand-auzias/lausanne: F. rouge). *Transl. as Elements of Pure Economics*, 1926.

[120] Rebecca Westphal. *Agent-based models to understand, exploit and prevent financial bubbles*. PhD thesis, ETH Zurich, 2021.

[121] Rebecca Westphal and Didier Sornette. How market intervention can prevent bubbles and crashes. *Swiss Finance Institute Research Paper*, (12-74), 2020.

[122] Rebecca Westphal and Didier Sornette. Market impact and performance of arbitrageurs of financial bubbles in an agent-based model. *Journal of Economic Behavior & Organization*, 171:1–23, 2020.

[123] Wei Xiong. Bubbles, crises, and heterogeneous beliefs. Technical report, National Bureau of Economic Research, 2013.

[124] Francesco Zamponi. Mean field theory of spin glasses. *arXiv preprint arXiv:1008.4844*, 2010.

[125] Ting Zhang and Honggang Li. Buying on margin, selling short in an agent-based market model. *Physica A: Statistical Mechanics and its Applications*, 392(18):4075–4082, 2013.

[126] Xuan Zhou and Honggang Li. Buying on margin and short selling in an artificial double auction market. *Computational Economics*, 54(4):1473–1489, 2019.

Eidgenössische Technische Hochschule Zürich
Swiss Federal Institute of Technology Zurich

Declaration of originality

The signed declaration of originality is a component of every semester paper, Bachelor's thesis, Master's thesis and any other degree paper undertaken during the course of studies, including the respective electronic versions.

Lecturers may also require a declaration of originality for other written papers compiled for their courses.

I hereby confirm that I am the sole author of the written work here enclosed and that I have compiled it in my own words. Parts excepted are corrections of form and content by the supervisor.

Title of work (in block letters):

Authored by (in block letters):
For papers written by groups the names of all authors are required.

Name(s):	**First name(s):**

With my signature I confirm that

- I have committed none of the forms of plagiarism described in the 'Citation etiquette' information sheet.
- I have documented all methods, data and processes truthfully.
- I have not manipulated any data.
- I have mentioned all persons who were significant facilitators of the work.

I am aware that the work may be screened electronically for plagiarism.

Place, date	**Signature(s)**

For papers written by groups the names of all authors are required. Their signatures collectively guarantee the entire content of the written paper.